# FUNCTIONAL ANALYSIS OF *pax2/5/8* GENES AND THEIR GENETIC INTERACTIONS IN ZEBRAFISH EAR DEVELOPMENT

A Dissertation

by

SU JIN KWAK

Submitted to the Office of Graduate Studies of
Texas A&M University
in partial fulfillment of the requirements for the degree of

DOCTOR OF PHILOSOPHY

May 2006

Major Subject: Biology

# FUNCTIONAL ANALYSIS OF *pax2/5/8* GENES AND THEIR GENETIC INTERACTIONS IN ZEBRAFISH EAR DEVELOPMENT

A Dissertation

by

SU JIN KWAK

Submitted to the Office of Graduate Studies of
Texas A&M University
in partial fulfillment of the requirements for the degree of

DOCTOR OF PHILOSOPHY

Approved by:

| | |
|---|---|
| Chair of Committee, | Bruce B. Riley |
| Committee Members, | Arne C. Lekven |
| | Mark Zoran |
| | Sumana Datta |
| Head of Department, | Vincent Cassone |

May 2006

Major Subject: Biology

# ABSTRACT

Functional Analysis of *pax2/5/8* Genes and Their Genetic Interactions

in Zebrafish Ear Development. (May 2006)

Su Jin Kwak, B.S., KAIST;

M.S., Seoul National University

Chair of Advisory Committee: Dr. Bruce B. Riley

The vertebrate inner ear is a sensory organ responsible for auditory and vestibular function. Since its complex structure and cell types arise from a simply structured group of ectodermal cells, called the otic placode, the development of the inner ear has been a popular subject in embryology and developmental biology for decades. To date, many regulatory molecules and their functions have been identified in inner ear development showing considerable conservation among vertebrates. In vertebrates, Fgfs (fibroblast growth factors) from surrounding tissues are the main otic inducer and regulate various otic genes' expression. Under the control of Fgf signals, *pax2/5/8* genes are expressed in the otic region in the critical stages of otic development suggesting their function in otic development. In order to understand the function of *pax2/5/8* genes and their interactions in the developing ear, we utilize zebrafish as a model system. Among zebrafish *pax2/5/8* genes, *pax8* is the earliest gene expressed in the preotic region while *pax2a* and *pax2b* are expressed slightly later. We found that *pax8* is initially required for normal otic induction. Subsequently, *pax8*, *pax2a* and *pax2b* function redundantly to

maintain otic fate. After otic placodes are induced by an Fgf signaling network, expression of Fgf3, one of otic inducers in zebrafish, persists in the hindbrain rhombomere 4. To investigate the function of the persistant Fgf3 expression, we examined a mutant with expanded Fgf3 expression in the hindbrain. Together with *fgf3* knockdown results, we discovered that Fgf3 has later roles in specifying the antero-posterior (A-P) axis in the otic vesicle and regulating hair cell formation. We further identified *pax5* as one of the genes regulated by the hindbrain Fgf3 activity, and *pax5* function to be required for utricular hair cell survival.

# ACKNOWLEDGMENTS

I would like to express my gratitude to all those without whom this dissertation would not have been possible. First, I am greatly indebted to my advisor, Dr. Bruce Riley, who is my mentor and a role model as a scientist and a teacher. His patience and encouragement have carried me through difficult times and his tremendous effort to teach me and insightful advice have made all my research possible. I am deeply grateful to my committee members. Dr. Arne Lekven has been always willing to discuss my questions in molecular biology. Dr. Mark Zoran has taught me neurobiology and provided instrumental advice for the *pax5* project. Dr. Sumana Datta has given insightful comments on my research. I also thank Dr. Louise Abbott for her corrections and comments on my dissertation.

I have been so blessed to have great lab members. I would like to express sincere gratitude to them. Dr. Bryan Phillips and Min-Yung Chiang have helped me learn all lab work from the beginning. Elly Sweet and Bonny Butler, with their dedication in the lab, active discussions with me, and their sweet hearts, made my time in the lab very pleasant. I am appreciative of Dr. Hye-Joo Kwon for her mentoring and discussions. I thank Shruti Vemarju for her instrumental collaboration in the *pax5* project. I also thank Reeha Dhason for her support in all lab and fish work and Mahesh Padanad for balancing feminine moods in our lab. I would like to extend my thanks to all zebrafish lab members for their collaboration.

I am deeply grateful to my parents and family who trust me and have provided endless support. Especially, I would like to give special thanks to my husband, Iksu Jun for his love and considerate support to complete this work.

Above all, I greatly thank my God for giving me all opportunities and precious people and allowing me to know Him more through his creatures.

# TABLE OF CONTENTS

# LIST OF FIGURES

# LIST OF TABLES

# CHAPTER I

# INTRODUCTION

Vertebrate inner ear development is a highly dynamic process. The delicate inner ear structure, which is required for maintaining balance and hearing, derives from the otic placode, a group of ectodermal cells in the edge of the neural plate. Thus the study of inner ear development from the naïve ectoderm to diverse cell types and the complicate structure will help to understand various cellular and molecular events in embryonic development. In addition to its embryological importance, understanding inner ear development is critical to many human diseases. Using forward and reverse genetics, many molecules regulating inner ear development have been identified, but their functions in ear development and downstream molecular mechanisms are not understood. The expression of *Paired box* (*Pax*) *2/5/8* genes is detected in the comparable regions of developing inner ears in all vertebrates suggesting their conserved function in ear development. Therefore, investigating *Pax2/5/8* gene function will help to dissect conserved molecular mechanisms in vertebrate inner ear development. This study focuses on analyzing *pax2/5/8* gene function in inner ear development and their interactions with the Fgf, otic inducing signal.

---

This dissertation follows the style and format of *Development.*

## OVERT MORPHOLOGY OF THE INNER EAR

The vertebrate inner ear is a sensory organ consisting of interconnected chambers for vestibular and auditory function (reviewed in Haddon and Lewis, 1996; Torres and Giraldez, 1998; Riley and Phillips, 2003). The number and the spatial arrangement of ear chambers vary to some degree among vertebrate species. The teleost inner ear has 6 chambers. The utricle, saccule, and lagena are aligned along the anterior-posterior axis, but the utricle is located more dorsally than the other two chambers. Three semicircular canals are the dorsalmost structures. The avian inner ear has one more chamber, the cochlea. The mammal inner ear has 6 chambers, but instead of the lagena, it has a cochlea posterior to the saccule (Fig. 1). In all vertebrates, three semicircular canals sense rotational acceleration, and the utricle senses gravity and linear acceleration. The cochlea is the primary auditory endorgan in the avian and mammalian ear. In the amphibian and fish ears, the lagena and saccule function as auditory endorgans but these are the vestibular endorgans in other organisms. The sensory epithelium in each chamber is the place for sensing and transmitting vestibular and auditory stimuli. Each sensory epithelium is composed of hair cells, support cells, and neurons which innervate hair cells (Fig. 2). The hair cell, as its name indicates, protrudes ciliary bundles into the lumen of the ear and mechanical deflection of these ciliary bundles stimulates the hair cell. In fish, hair cells in the utricle, the saccule and the lagena are associated with dense calcium carbonate crystals, otoliths (Fig. 2B). Otoliths transmit acceleration force, gravity, or sound vibrations to hair cells. Hair cells in the semicircular canals project

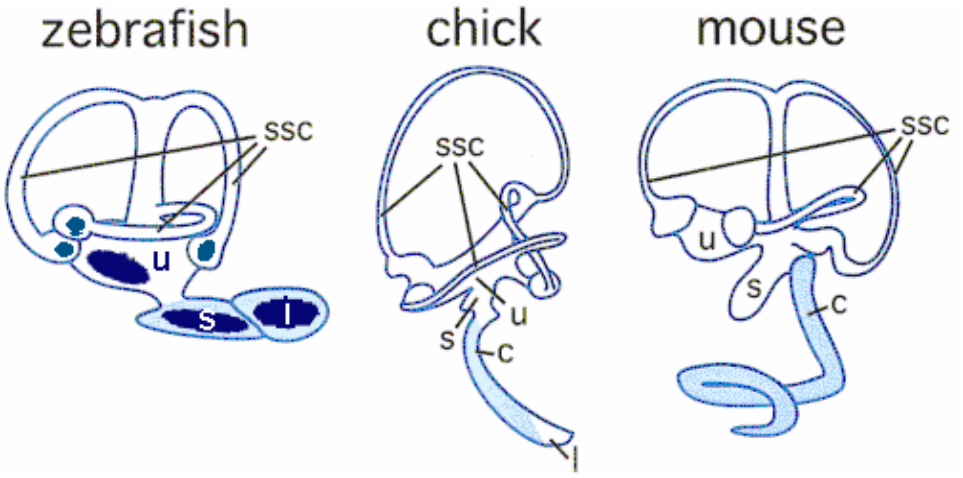


**Fig. 1**. Diagrams of the structure of vertebrate inner ears. Dark blue areas indicate sensory patches in each chamber of the zebrafish inner ear. Chambers colored in blue are auditory chambers; all others are vestibular chambers. u: utricle, s: saccule, l: lagena, c: cochlea, ssc: semicircular canals. (adapted and modified from Riley and Phillips, 2003).

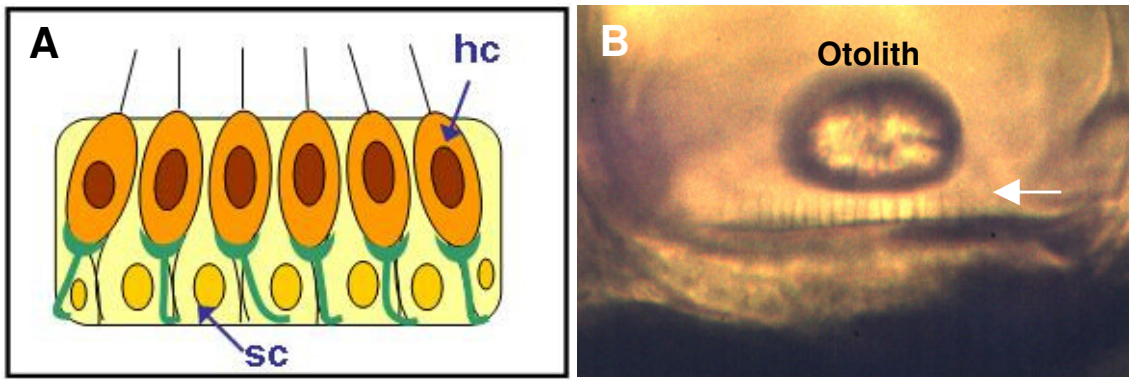


**Fig. 2**. Structure of the sensory epithelium in the inner ear. (A) Diagram showing the arrangement of three components, hair cells (hc), support cells (sc), and innervating neurons (green). (B) DIC image of the utricular macula at 72 hpf. Lateral view. Utricular, saccular and lagenar hair cells are associated with otoliths. White arrow indicates cilia of utricular hair cells.

extremely long cilia for sensing fluid motions in the canal. All chambers are filled with a fluid, called endolymph. This fluid contains ions balanced for hair cell function and flows through the endolymphatic duct in the medial wall of the inner ear helping maintain the proper volume.

The VIIIth cranial nerve, named vestibuloacoustic ganglion (VAG) or statoacoustic ganglion (SAG), is a group of bipolar neurons which transmits signals from all vestibular and auditory hair cells to the hindbrain. This is located between the ventromedial wall of the ear and the ventral part of the neural tube.

## DEVELOPMENT OF THE INNER EAR

The inner ear of all vertebrates develops from a thickened ectoderm, the otic placode, located laterally to the hindbrain. This group of cells is detectable in mid-somitogenesis stages, in zebrafish, from 14 hpf (hour post fertilization) (Fig. 3A). After formation, the placode is transformed into a hollow vesicle (Fig. 3B). In birds and mammals, this transformation occurs by invagination of the placode, changing from a flat sheet to a cup and then a vesicle. A completely closed vesicle pinches off and sinks in the mesenchyme under the surface ectoderm. However, the zebrafish otic vesicle forms by cavitation. In this process, the nuclei of otic cells move outward to the placode surface.

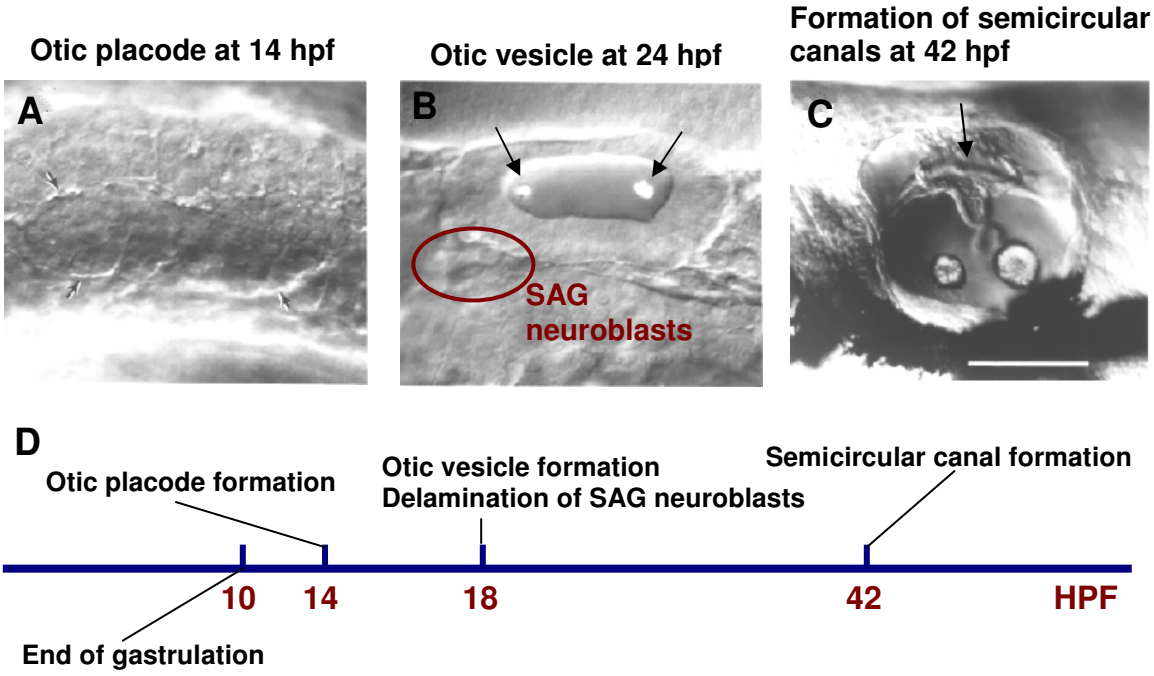


**Fig. 3**. Overview of otic development in zebrafish. (A) a DIC image of the otic placode at 14 hpf, lateral view. Arrows indicate the surface of the otic placode. (B) A DIC image of the otic vesicle at 24 hpf. Two otoliths (arrows) are formed first in the anterior (utricular) and the posterior (saccular) region of the otic vesicle. SAG neuroblasts are specified and delaminated (circle) from 22 hpf to 42 hpf. (C) A DIC image of the otic vesicle at 42 hpf. Protrusions of the vesicle wall (arrow) for semicircular canal formation initiate from 42 hpf (figures were retrieved from Zebrafish Information Network (ZFIN), Structure description: ear, the Zebrafish International Resource Center, University of Oregon, Eugene, available http://zfin.org/zf_info/anatomy/dict/ear/ear.html , accessed Jan. 2006). (D) A diagram to show major developmental stages of the inner ear with respect to time (hours post fertilization, HPF).

In addition, in the center of the placode, actin is localized and cells lose cell-cell adhesion to make a thin slit-like lumen (Haddon and Lewis, 1996). The otic vesicle expands rapidly by increasing both the number and the size of otic cells. A complex structure begins to form by extensive folding of the otic epithelium. For example, zebrafish otic vesicles form protrusions from the lateral, anterior and posterior epithelium from 42 hpf. These protrusions elongate into the lumen and finally fuse in the center of the lumen to form empty spaces between semicircular canals and other chambers (Fig. 3C).

## OTIC INDUCTION AND IDENTIFIED OTIC INDUCERS

Studies of how naïve surface ectoderm is induced to form the otic placode (otic induction) have been conducted extensively since the 1920's. Analogous to those of Spemann organizer, classical embryological experiments were performed to identify which cells are competent to form the otic placode and the tissues that induce it. Experiments performed in various species have demonstrated that (1) initially, all embryonic ectoderm is competent to form the otic placode, and this competence is gradually restricted to the otic region; (2) the otic cell fate is determined by mid-somitogensis; (3) the activity of periotic tissues to re-specify foreign ectoderm to the otic tissue persists by mid-to late-somitogensis, and the hindbrain and mesoderm underneath

the otic region are sources of inducing signals (reviewed in Baker and Bronner-Fraser, 2001; Normaly and Grainger, 2002; Riley and Phillips, 2003).

Since the early 1990's, the identity of the inducing signal from the hindbrain and mesoderm has been unveiled in various species. Fgf signaling has been identified as an otic inducing signaling in all examined species. For example, knocking down Fgf3 function with antisense oligonucleotides or antibodies blocks formation of the otic vesicle in chick explants, while the application of Fgf2 to chick ectoderm explants induces otic vesicle formation in the absence of the hindbrain (Represa et al., 1991). Misexpression of Fgfs using viral vectors can induce an otic placode in the head and trunk ectoderm of chick embryos (Vendrill et al., 2000). In addition, application of beads soaked with Fgf2 and Fgf3 in the trunk region of *Xenopus* embryos induces the formation of ectopic otic vesicles in *Xenopus* embryos (Lombardo et al., 1998). Recent studies have identified that multiple *Fgf* genes function redundantly to induce otic cells. For example, Fgf3 and Fgf8 act as redundant otic inducers in zebrafish (Phillips, et al., 2001; Maroon et al., 2002; Leger and Brand, 2002). Knockdown of either Fgf3 or Fgf8 produces malformed otic vesicles, but blocking both Fgf3 and Fgf8 function prevents expression of early otic markers and the formation of otic placodes. Gene knockdown studies are supported by the finding that zebrafish embryos treated with the Fgf inhibitor SU5402 fail to form otic placodes (Maroon et al., 2002; Leger and Brand, 2002). In the mouse, Fgf3 from the neuroectoderm and Fgf10 from the mesenchyme underlying the otic region are redundantly required for otic induction (Wright and Mansour, 2003). Fgf8, which is expressed in a much broader region including endoderm, mesenchyme

and the preotic region, is also reported to regulate otic induction. Since reducing Fgf8 function in an Fgf3 null background reduces Fgf10 expression in the mesenchyme and subsequently blocks otic induction. This suggests that Fgf8 is involved in otic induction by initiating or maintaining Fgf10 expression, which functions together with Fgf3 to induce the placode (Ladher et al., 2005).

The involvement of other signals in otic induction has been postulated, but they appear to function indirectly by regulating Fgf signaling. Fgf19 in chick mesoderm explants induces some otic marker expression only with neural tissue or beads soaked with Wnt8c. Based on these data, it was proposed that Fgf19 in mesoderm induces *Wnt8c* in neural tissue and both Fgf19 and Wnt8c cooperate in otic induction (Ladher et al., 2000). However, it was also observed that exogenous Wnt8c induces *Fgf3* whose activity in otic induction was already shown in chick explants (Represa et al., 1991; Ladher et al., 2000; Vendrell et al., 2000). Thus, it is likely that Fgf3 induced by Wnt8c regulates otic marker expression together with Fgf19. Supporting this idea, the relationship between Wnts and Fgfs was clearly identified in zebrafish. Phillips and colleagues showed that Wnt8 ORF2 activity is required for the timely expression of *fgf3* and *fgf8* genes in the hindbrain, which regulate actual induction in the adjacent ectoderm (Phillips et al., 2004).

Perturbation of retinoic acid signaling affects otic induction, but this is a secondary consequence of aberrant hindbrain development. Blocking of retinoic acid (RA) signaling in mice induces ectopic otic vesicles (White et al., 2000; Dupe et al., 1999). In contrast, the application of RA to zebrafish embryos results in the formation

of ectopic otic vesicles (Phillips et al., 2001). Despite opposite results, in both cases, hindbrain segments expressing Fgfs are expanded and ectopic otic vesicles form lateral to the enlarged hindbrain segments. Moreover, ectopic formation of otic vesicles is suppressed by blocking Fgf signaling (Phillips et al., 2001). These data imply that Fgfs are the major otic inducer and other signaling molecules are direct or indirect regulators of Fgf activity.

## TRANSCRIPTION FACTORS EXPRESSED IN THE OTIC INDUCTION STAGE

Numerous transcription factors are expressed in the preotic region and regulate otic development. Among many transcription factors, functions of *Pax* (*paired box*), *Six* (*sine oculis*), *Eya* (*eyes absent*), and *Dach* (*dachshund*) genes have been studied to identify whether a well-known gene interaction for eye development, Pax-Six-Eya-Dach regulatory network, is conserved in ear development. In *Drosophila* eye development, *eyeless* (*Pax6*) turns on the expression of *eyes absent* (*eya*) and *sine oculis* (*six*). The expression of *dachshund* (*dach*) requires *eya* and *six* functions as upstream activators. Eya makes direct protein-protein interactions with Six and Dach respectively and these protein complexes are required to upregulate and to maintain expression of each gene and to regulate downstream target genes (Reviewed in Desplan, 1997; Wasersik and

Mass, 2000). A similar gene network has been discovered in vertebrate eye development and muscle development (Heanue et al., 1999) suggesting the conservation of this regulatory network in various organ systems. Interestingly, members of *Pax-Six-Eya-Dach* gene families are also expressed in the otic region. *Pax8* and *Pax2* are expressed in the otic region from early otic induction stages in all vertebrates. *Eya1* in mouse, *Xenopus,* and zebrafish, and *Eya2* in chick are expressed in the preplacodal region after *Pax8* expression but before *Pax2* expression (Sahly et al., 1999; David et al., 2001; Heanue et al., 2002; Streit, 2002). *Six4* is also expressed in the preplacodal region. However, *Dach* genes are not expressed in the otic region until the otic vesicle stage (Hammond et al., 2002) and their expression in the ear is not dependent on the *Pax2* or *Eya1* function. Therefore, it appears that *Pax-Six-Eya-Dach* gene network functions in a modified manner in ear development.

Together with *Eya* and *Six*, several *Distalless* (*dlx*) genes are expressed in the preplacodal region. *Dlx* genes are located in the vertebrate genome as linked pairs, (reviewed in Kraus and Lufkin, 1999) and one pair of *dlx* genes appear to function together in otic development. In mouse, *Dlx5* and *Dlx6* double knockout mutants produce small and poorly differentiated otic vesicles (Robledo et al., 2002). Otic defects in double knockout mutants are more severe than those in a single *Dlx5* or *Dlx6* gene knockout mutants. Similarly, knocking down *dlx3b* and *dlx4b* function synergistically inhibits otic induction in zebrafish (Solomon and Fritz, 2002).

Recently, *hearsay* (*hsy*), a mutant with very tiny or no otic vesicles, was identified as a null mutant for *foxi1* gene in zebrafish (Solomon et al., 2003). A forkhead

class transcription factor, *foxi1* is initially expressed in the antero-ventral region (prospective epidermis) of the embryo in early gastrulation stages. By late gastrulation stages, ventral expression is down regulated and *foxi1* expression remains in two discrete patches which are the lateral edges of the expression domain. This expression region encompasses the expression domain of *pax8*, the earliest otic gene, and *hsy* lacks *pax8* expression in the otic region indicating *foxi1* as an upstream regulator for *pax8*. Expression of other otic genes is significantly reduced and delayed and this failure of early otic induction causes ear defects in *hsy* mutants (Solomon et al., 2003).

## OTIC VESICLE DIFFERENTIATION

From the beginning of the otic vesicle stage, otic cells differentiate into various cell types. Even before the otic vesicle forms, some sets of genes are expressed differentially in the anterior-posterior (A-P), dorso-ventral (D-V), and medio-lateral (M-L) axes of the otic placode. In zebrafish, *nkx5.1* and *pax5* are expressed in the anterior portion of the otic vesicle from 17 hpf (Pfeffer et al., 1998; Adamska et al., 2000). Zebrafish *pax2a* is initially expressed in the entire otic placode, but it becomes restricted to the ventro-medial region of the otic vesicle when the otic vesicle begins to form. Signals from the hindbrain have been speculated to contribute to axis determination in the otic vesicle. Chick *Pax2*, a homologue of *pax2a* in zebrafish, is also expressed in the medial wall of

the otic vesicle responding to the hindbrain signal. Rotating the otic vesicle 180 degrees respecifies *Pax2* expression to the region abutting the hindbrain (Hutson et al., 1999). Ablation of hindbrain tissue causes *Pax2* to be expressed throughout the entire vesicle rather than being restricted to the medial part of the otic vesicle (Hutson et al., 1999). These data suggest that signals from the hindbrain contribute to specify the medio-lateral axis in the embryos.

The floor plate and the notochord are located medially and ventrally to the otic vesicle. A secreting signaling molecule, Shh is expressed in the floor plate and the notochord, providing axial information to otic cells. *Shh* knockout mice show the perturbation of D-V and M-L axes (Riccomangno et al., 2002). This mutant shows the expansion of dorsal markers and reduction or ablation of ventral markers in the otic vesicle. Shh signaling in zebrafish is reported to regulate A-P axis patterning but not D-V and M-L axes as mouse Shh. *Smoothened* mutants, whose Shh signaling is blocked, have normal D-V and M-L patterning but show mirror image duplication of some anterior fates (Hammond et al., 2003). Overexpression of *shh* causes duplicated expression of some posterior markers in the anterior region. Since Shh appears to be uniformly expressed along the A-P axis, it is unclear why A-P patterning is altered in zebrafish (Hammond et al., 2003).

Retinoic acid (RA) also contributes to the M-L axis patterning. Blocking retinoic acid signaling causes malformed and lateralized otic vesicles (Niederreither et al., 2000). RA expression in the ventral otic vesicle suggests RA may regulate gene expression in the vesicle wall directly, but the effect of hindbrain defects in RA mutants needs to be

carefully examined to determine whether abnormal hindbrain development disturbs M-L axis patterning in the otic vesicle.

## HAIR CELL FORMATION

Formation of sensory epithelia is coupled to morphogenesis of corresponding chamber walls in amniotes, but in fish, sensory epithelia form much earlier before any discernable morphogenesis of nonsensory epithelia. Among six sensory epithelia of the zebrafish inner ear, the sensory epithelium in the utricle (utricular macula) in the antero-ventral region and the sensory epithelium in the saccule (saccular macula) in the posterior and more medial region develop first. Sensory epithelia in semicircular canals (anterior crista, lateral crista and posterior crista) are visible after 60 hpf, but the lateral crista is formed slightly later than the other two. The lagenar macula forms much later, after day 10. Sensory epithelia contain two cell types, hair cells and support cells which originate from a common pool of precursors, the equivalence group. Cell lineage analysis using retroviral infection in chick showed that both types of cells emerge from a common precursor cell (Fekete et al., 1998). Alternative cell fates in the equivalence group are determined by Delta-Notch signaling in a process called lateral inhibition. Delta proteins, tethered ligands that inhibit differentiation, are expressed in all cells in the equivalence group at a low level. Within the equivalence group, homogeneously

expressed *delta* genes are upregulated only in a subset of cells (hair cells) activating Notch (receptor) signaling in neighboring cells. Activated Notch signaling suppresses hair cell fate therefore, neighboring cells become support cells. By this mechanism, hair cells and supporting cells are arranged in a regularly spaced pattern. Direct evidence for lateral inhibition in hair cell formation has been presented in zebrafish. Mind-bomb (*mib*) is an ubiquitin ligase which is required for protein trafficking and turnover at the cell surface (Itoh et al., 2003). Although the exact mechanism is not clear, this process is essential for Delta-Notch signaling. Mutation of *mib* gene blocks all Delta-Notch signaling so that excessive hair cells are produced without any support cells (Haddon et al., 1998a, b). A dominant negative mutation of *deltaA* (*dlA*) gene causes milder effects on hair cell formation, but it also produces more hair cells at the expense of support cells (Riley et al., 1999).

A group of basic helix–loop-helix (bHLH) transcription factors, which are homologous to the *Drosophila atonal* gene, are also involved in hair cell formation. They are expressed in the equivalence group and later are upregulated in the new forming hair cell. Disruption of *atonal homologue 1* (*atoh1*) gene function inhibits formation of hair cells and support cells in mouse, while ectopic expression of *atoh1* in mouse nonsensory epithelia of the ear induces both hair cells and support cells (Woods et al., 2004). Two *atonal* homologs (*atoh1a* and *atoh1b*) are found in zebrafish. Knocking down either of these genes partially inhibits hair cell formation, while knocking down both gene functions blocks all hair cell formation as well as *delta* gene

expression, (Butler et al., unpublished data). These data suggest that *atoh1* specifies a functional equivalence group and later regulates hair cell formation in vertebrates.

Pax2 orthologs in mouse, chick and zebrafish are another gene group expressed in hair cells (Lawoko-Kerali et al., 2002; Burton et al., 2004; Sanchez-Calderon et al., 2005). They are initially expressed in all placodal cells, but later, they are restricted to the ventromedial region of the otic vesicle and maintained in hair cells. As sensory patches are differentiated, their expression is upregulated and remains in hair cells (Riley et al., 1999). In spite of their similar expression pattern, respective depletion of *pax2a* or *pax2b* function affects different aspects of hair cell formation in zebrafish embryos. *pax2a* mutants fail to upregulate *delta* expression in hair cells, and this impaired lateral inhibition causes excess hair cell production in maculae. *pax2b* depleted embryos have fewer than normal hair cells in the macula and down regulation of both *pax2a* and *pax2b* function cause comparable hair cell defects (Whitfield et al., 2002). Therefore, it seems that *pax2b* regulates the initial hair cell specification and *pax2a* regulates the subsequent lateral inhibition by controlling *delta* expression in the hair cells. The relationship between *pax2* genes and proneural genes is not yet understood.

## DIFFERENTIATION AND MAINTENANCE OF THE HAIR CELL

Maintenance of hair cells has been studied mostly with respect to auditory function. A POU domain transcription factor, *Brn-3c,* is expressed in hair cells of all vestibular and auditory sensory patches. *Brn-3c* knockout mice produce hair cells but some of them do not express mature hair cell markers and are disorganized (Xiang et al., 1998). All hair cells, in this mutant eventually die around the day of birth. *Brn-3c* begins to be expressed in the postmitotic precursors of hair cells and early genes for hair cell fate specification are still expressed in the sensory epithelia in *Brn-3c* null mice. Therefore, Brn-3c appears to be required for the survival of hair cells immediately after their specification (Xiang et al., 1998). *Barhl1* is expressed later than *Brn-3c* in hair cells of the mouse ear. Absence of *Barh1* function causes defects in long term maintenance of hair cells in the cochlea. Outer hair cells and inner hair cells in the organ of Corti degenerate causing progressive hearing loss in the mouse (Li et al., 2002). *Gfi1* is another hair cell survival factor. This gene is expressed in hair cells of all sensory epithelia and is regulated by *Math1* and *Brn-3c* (Hertzano et al., 2004). However, knocking out *Gfi1* function causes apoptosis only in the organ of Corti. Saccular and utricular hair cells are disorganized but survive at least through five months after birth without this gene function whereas hair cells in cristae do not show any morphological defects (Wallis et al., 2003). These results indicate that all hair cells rely on common survival factors (Math1, Brn-3c and Barhl1) but also show regional differences (Gfi1) in

survival., probably reflecting functional specialization of hair cells: vestibular vs. auditory function.

## DEVELOPMENT OF STATOACOUSTIC GANGLION

The VIIIth cranial ganglion originates from the otic vesicle and is differentiated through several phases. In zebrafish, neuroblasts of the SAG are specified in the ventral region of the otic vesicle and begin to delaminate from the otic epithelium by 22 hpf. Delaminated neuroblasts migrate and accumulate beneath the anterior part of the otic vesicle (Fig. 4). They undergo further divisions and coalesce to form a ganglion (Haddon and Lewis, 1996). Some components of Delta- Notch signaling such as *Delta1*, *Jagged1* and *L-fng* are expressed in the neurogenic domain of the otic vesicle, suggesting its involvement in the specification of neuroblasts in the otic vesicle (Adam et al., 1998; Lewis et al., 1998; Morsli et al., 1998). Zebrafish *mind bomb* mutants produce excess neuroblasts (Haddon et al., 1998a; Haddon et al., 1999). *Ngn1* a basic helix loop helix transcription factor, was identified as a regulator in early development of neuroblasts in mouse and zebrafish. This gene begins to be expressed in neuroblasts in the otic vesicle even before neuroblasts delaminate from the otic epithelium. After delamination, expression of *ngn1* downregulates soon. Depletion of *ngn1* gene function results in complete loss of neuroblasts (Ma et al., 2000, Andermann et al., 2002). A

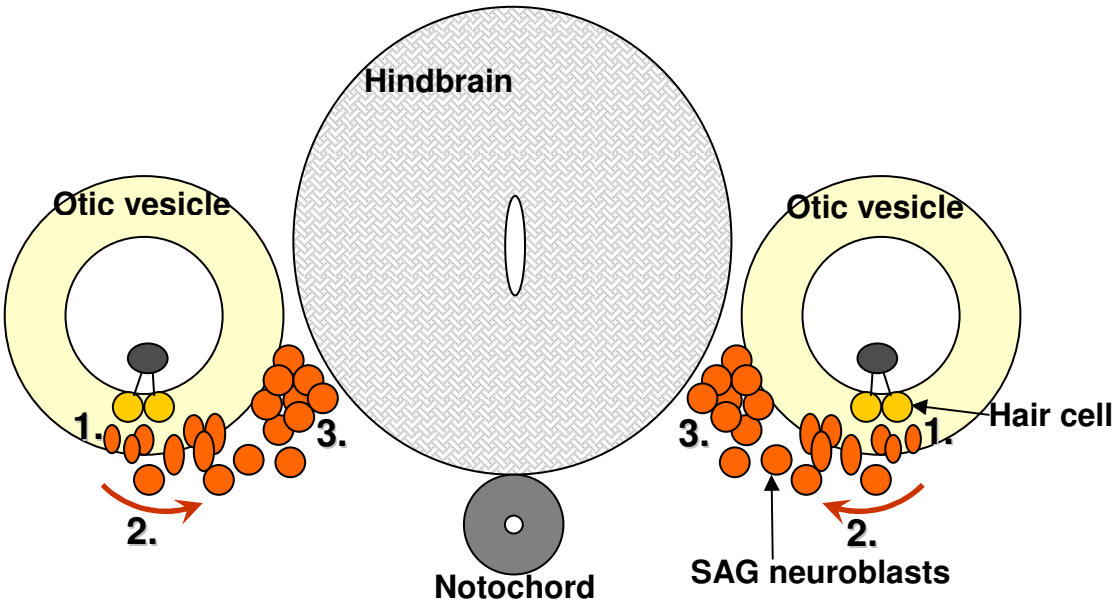


**Fig. 4.** Development of statoacoustic ganglia (SAG). A diagram to overview development of statoacoustic ganglia (SAG) in the transverse section at the level of the anterior otolith. SAG neuroblasts are specified in the ventral otic vesicle wall and delaminate from the otic vesicle. Delaminated neuroblasts migrate medially, accumulate and aggregate in the position between the hindbrain and the anterior part of the otic vesicle.

similar gene product, *neuroD* is also expressed in nascent neuroblasts, but its expression is maintained in differentiating neuroblasts suggesting a later role. The function of *neuroD* has been studied only in mouse. In the absence of *NeuroD,* SAG neurons are produced but they can not survive due to failure to express neurotrophin receptors, *TrkB* and *TrkC* (Kim et al., 2001).

Shh is implicated as an upstream regulator of *Ngn1* and *NeuroD* (Riccomangno et al., 2002). Shh knockout mice produce small cochleovestibular ganglia and reduced expression of *Ngn1* and *NeuroD.* In contrast, *ShhP1*, a transgenic mouse which ectopically expresses *Shh* in the otic vesicle has upregulated *Ngn1* and *NeuroD* and enlarged cochleovestibular ganglia. Development of the statoacoustic ganglion in zebrafish *shh* mutant is not well described, but the initial specification and the movement of SAG neuroblasts appear to be normal suggesting that other signals may be involved in zebrafish SAG development (Hammond et al., 2003).

The function of neurotrophins is important for the survival and target innervations of SAG neurons. BDNF, NT-3 and their receptors, TrkB and TrkC are expressed in the otic sensory epithelium and SAG neurons, respectively (Farinas et al., 1994; Enfors et al., 1995; Schimmang et al., 1997, reviewed in Fritzsch et al., 1999). *BDNF* is expressed in hair cells of all ear sensory epithelia. The expression of *NT-3* is excluded from all cristae, but in other sensory epithelia, utricle, saccule and cochlea, all hair cells and support cells express *NT-3* mRNA. High affinity receptors of both neurotrophins are expressed in SAG neurons. Although they show overlapping expression patterns, respective disruption of each gene or their receptors affects only a

specific subgroup of SAG neurons. The cochlea is poorly innervated without NT-3 or TrkC function, and BDNF and TrkB are required for vestibular neurons innervating utricle, saccule, and semicircular canals (reviewed in Fritzsch et al., 1999; Fritzsch et al., 2002).

## *Pax* GENE FAMILY

*Pax* genes play crucial roles in otic development. Pax genes are transcription factors which share a conserved 128 amino acid DNA binding domain, the Paired domain. Paired domain proteins are found across the animal kingdom and originally identified in *Drosophila* (Czerny et al., 1997; Dahl et al., 1997; Walther et al., 1991). In mammals, nine *Pax* genes exist and these genes are sub-grouped by their composition of functional domains, such as paired domain, homeo domain, octa peptide domain, transactivation domain and inhibitory domain (Table 1) (reviewed in Robson, et al., 2006; Chi and Epstein, 2002; Dahl et al., 1997; Mansouri et al., 1996). Genes within an individual group show a very high degree of sequence similarity within the paired domain and a similar expression pattern during embryogenesis. The paired domain is a DNA binding domain that consists of independent amino- and carboxy-terminal subdomains which are connected by a flexible linker. Each subdomain is composed of three α-helices and structurally resembles a helix-turn-helix motif. In addition to its role in DNA binding,

the paired domain also functions as a protein-protein interaction domain (Underhill and Gros, 1997; Plaza, et al., 2001). Except subgroup I, all other *Pax* genes have a homeodomain as an additional DNA binding domain. This domain can recognize TATA sequence in DNA (Wilson et al., 1993). However, a partial homeodomain in the *Pax2/5/8* gene family functions as an interaction surface for the retinoblastoma and TATA binding proteins (TBP) (Cvekl et al., 1999; Eberhard and Busslinger, 1999). The octapeptide domain is composed of eight amino acids, (H/Y)S(I/V)(N/S)G(I/L)LG. This domain is known to be a protein-protein interaction domain, for the octapeptide domain of Pax5 interacts with Groucho protein to repress transcription of target genes (Eberhard et al., 2000). In the C-terminal region, Pax proteins have a transactivation domain (PTS rich domain) and an inhibitory domain, suggesting their function as an activator or a repressor of the target gene expression. The relative activities of these two domains and alternative splicing seem to finely modulate transcriptional activity of Pax proteins in various contexts.

## *Pax* GENE FUNCTION IN THE DEVELOPMENT OF VARIOUS ORGANS

*Pax* genes are involved in the development of various organs including placode derived sensory organs (reviewed in Robson, et al., 2006; Chi and Epstein, 2002; Dahl et al., 1997). Mutations in *Pax* genes result in a faulty development of specific organs where

**Table 1.** The structure of *Pax* genes and their expression domains. Nine vertebrate *Pax* genes and their expression domains are listed. Based on their protein structures, these genes are classified into four groups. Diagrams show schematic locations of functional domains in each *Pax* gene group. Pale blue boxes indicate paired box domains, blue ovals indicate octapeptide domains and dark blue boxes indicate homeo-box. The smaller dark blue box in group 2 indicates the partial homeo-box. N: amino-terminus, C: carboxyl-terminus.

| | Gene | Structure | Expression domain |
|---|---|---|---|
| | | **Paired box OP Homeo box** | |
| Group 1 | Pax1 | 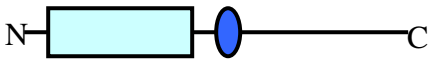  | Skeleton, Thymus |
| | Pax9 | | Skeleton. Cranio-facial., Tooth |
| Group 2 | Pax2 | | CNS. Kidney, Ear |
| | Pax5 | 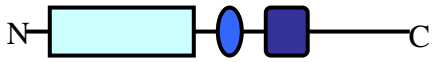  | CNS, B cell, Ear |
| | Pax8 | | CNS. Kidney, Thyroid, Ear |
| Group 3 | Pax4 | 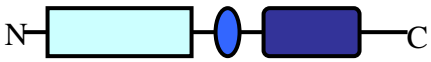  | Pancreas |
| | Pax6 | | CNS, Eye, Pancreas |
| Group 4 | Pax3 | 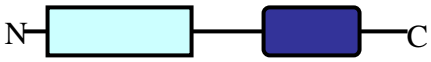  | CNS, Neural crest, Skeletal muscle |
| | Pax7 | | CNS, Neural crest, Skeletal muscle |

the genes are expressed (Table 1). Most of organogenesis occurs through tissue-tissue interactions mediated by various signaling molecules. Many *Pax* genes are implicated in such interactions. Detailed examples will be discussed in the following section

Many cancer studies have demonstrated tumor-associated *Pax* gene expression and have identified altered *Pax* gene activities. In alveolar rhabdomyosarcoma, Chromosomal translocations produce chimera proteins composed of the *Pax* DNA binding domains of *Pax3* or *Pax7* and the potent transcriptional activation domain of FKHR (a forkhead transcription factor) (Frascella et al., 1998; Sorensen et al., 2002). Homologous translocations resulting in chimera proteins with Pax5 and Pax8 protein domains were discovered in a lymphoma and a thyroid cancer (Ohno et al., 2000; Lui et al., 2005). Involvement of *Pax* gene activity in cancer has been verified by downregulating *Pax* genes in tumor cells. Inhibition of *Pax2* activity with antisense oligonucleotides in renal cell carcinoma cell lines suppressed cell growth (Gnarra and Dressler, 1995). The precise function of *Pax* genes in cancer is not known yet, but *in vitro* analyses showing *Pax2/5/8* genes activity in inhibiting *p53* expression (Stuart et al., 1995) and an interaction of Pax8 with *Bcl-2*, apoptosis suppressor gene (Hewitt, et al., 1997) suggest that aberrant regulations of these interactions could be a reason for various cancers.

## *Pax2/5/8* GENES IN ORGANOGENESIS

*Pax2/5/8* genes constitute one subgroup of the *Pax* gene family. They are expressed in developing CNS, eye, ear, kidney, thyroid and B cells. *Pax2* and *Pax8* are expressed in the nephric region from early stages of nephric development. In spite of early expression, *Pax2*$^{-/-}$ mice show only defects well after *Pax2* expression is initiated and *Pax8*$^{-/-}$ mice have no clear kidney defects (Torres et al., 1995; Favor et al., 1996; Mansouri, et al., 1998). These mild phenotypes are attributed to functional redundancy of *Pax2* and *Pax8* because double knockout mice show total loss of kidney from early stages (Bouchard, et al., 2002). In the process of kidney development, transition of metanephric mesenchymal cells to an epidermal structure (kidney tubules) is a well known process. Bmp7 is the inducing signal for this mesenchymal-epithelial transition (Luo, et al., 1995; Dudley, et al., 1995). *Pax2* is induced by Bmp7 in mesenchymal cells and mediates Bmp7 signaling in this process (Rothenpieler and Dressler, 1993; Dudley, et al., 1995).

Among the *Pax2/5/8* gene, *Pax8* is the only one expressed in the thyroid. The thyroid is composed of two structures originating from the floor of the pharynx and neural crest cells, respectively. *Pax8* expression begins in the floor of the pharynx and is continuously expressed in the derivatives of the pharynx floor (Plachov et al., 1990). Together with another homeodomain protein, TTF1, Pax8 regulates thyroid specific gene expression (Mansouri et al., 1998). Thus, *Pax8* deficient mice show impaired

development of the thyroid gland and *Pax8* mutation in humans causes hypothyroidism (Mansouri et al., 1998, Maccia et al., 1998).

The function of *Pax5* is well described in hematopoiesis. Hematopoietic stem cells give rise to myeloid and lymphoid cells, and they gradually restrict their competence into various hematopoietic cell types depending on environment. *Pax5* is expressed in the lymphoid cells and specifies the B cell fate. Pax5 represses non-B-cell genes and activates B-cell specific genes including the components of the B-cell receptor complex, membrane proteins, and immunoglobulins (Fitzsimmons et al., 1996). These two regulatory activities are controlled by its interactions with other coregulators such as Groucho family and TATA-binding proteins (Eberhard and Busslinger, 1999; Eberhard et al., 2000; Milili et al., 2002; Linderson et al., 2004). Ablation of Pax5 function arrests B-cell development at the pro-B-cell stage (Urbanek et al., 1994). Since arrested pro-B-cells are pluripotent and can give rise to other various hematopoietic cell types, the function of *Pax5* is highlighted in its clinical importance (Rolink et al., 1999; Schaniel et al., 2002). The function of *pax2/5/8* genes in ear development, and their interaction with other otic genes will be discussed in the following three chapters.

## *Pax2/5/8* GENES IN INNER EAR DEVELOPMENT

*Pax2/5/8* genes are expressed in key stages of otic development suggesting their involvement in vertebrate otic development (Fig. 5) (Pfeffer et al., 1998). In zebrafish, there are four members of *pax2/5/8* gene family: *pax2a*, *pax2b*, *pax5* and *pax8*. *pax8* is one of the earliest known otic markers, and its expression is detected in pre-otic cells of zebrafish embryos from the later half of gastrulation (9.5 hpf). *pax2a* and *pax2b* are two homologs, which are duplicated from an ancestral *pax2* gene. *pax2a* appears in preplacodal tissue by 11 hpf (1-2 somites), followed by *pax2b* at around 13.5 hpf (9 somites) just before formation of the placode. *pax2a* and *pax2b* continue to be expressed and is restricted to the medial half of the otic vesicle at 18.5 hpf. From 24 hpf, the expression is dramatically upregulated in hair cells but begins to be downregulated in other vesicle cells at 30 hpf. *pax5* expression begins in the anterior otic vesicle at 17 hpf as the otic vesicle forms and later remains in the anterior (utricular) macula (Fig. 5). Although *pax5* in the embryonic ear is only reported in amphibians and fish, the pattern of *pax8* and *pax2* expression shows significant similarity among vertebrates.

Functional studies of *pax2/5/8* genes in otic development have been performed in the mouse. *pax2* null mutant mice show abnormal differentiation of the auditory portion of the inner ear. They are not able to produce a normal cochlea or the cochlear ganglion where *pax2* gene is expressed (Torres et al., 1996). In contrast, *pax8* null mice do not show ear defects although *pax8* is expressed in very early stages of otic induction. *no isthmus* (*noi*) mutants, which produce non-functional truncated Pax2a proteins, are the

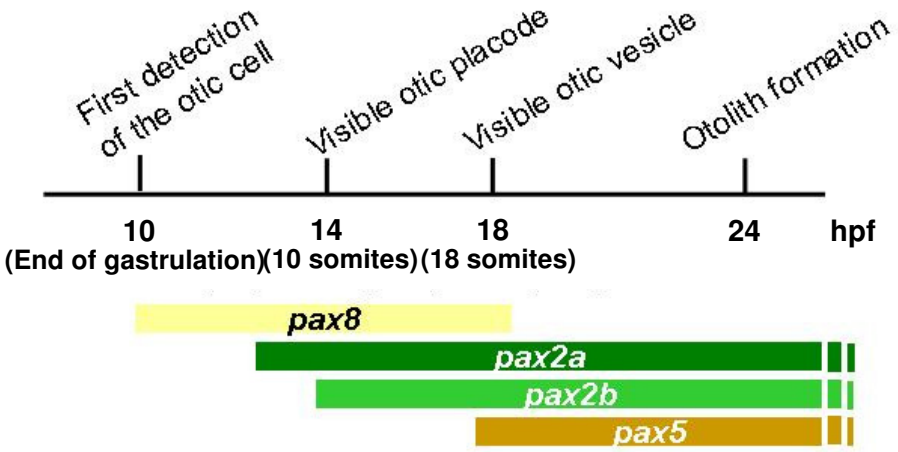


**Fig. 5.** The temporal expression of *pax2/5/8* genes in the zebrafish otic region. Based on the results of the whole-mount in situ hybridization analyses, the temporal expression patterns of *pax2/5/8* genes are demonstrated schematically. Each bar indicates each *pax* gene expression. *pax2a*, *pax2b* and *pax5* are continuously expressed in the otic region at least by 72 hpf, the latest observation time point in this study.

only identified zebrafish mutant of *pax2/5/8* gene family, and it also shows mildly affected ears. These mild otic phenotypes of single gene mutants could be explained by the redundancy among *Pax* genes as described in nephric development (Bouchard et al., 2002). Therefore, the specific function of each gene and their redundancy in otic development require more investigation.

Zebrafish is a good model system to study *Pax2/5/8* gene functions in inner ear development. Besides benefits of zebrafish in embryology and genetics, a gene specific knockdown technique using antisense oligonucleotides, morpholinos, is the most efficient way to downregulate multiple gene functions simultaneously. Furthermore, *pax2* is expressed in most otic developmental stages with very dynamic pattern in all vertebrates. Because of this dynamic expression pattern, manipulation of *pax2* function causes early defects which hinder investigation of *pax2* function in later stages. In zebrafish, *pax2a, pax2b* and *pax5* are expressed where *pax2* is expressed in other vertebrates. Since these three genes are structurally very homologous and functionally redundant (Bouchard et al., 2000), *Pax2* function in other vertebrates might be sub-specialized into zebrafish *pax2a, pax2b,* and *pax5* functions. Therefore, study of each gene function will uncover unidentified *Pax2* functions in other vertebrates.

## DISSERTATION OBJECTIVES

The objective of this dissertation is to address *pax2/5/8* gene functions in inner ear development, and their interaction with Fgf signaling, the key otic regulatory signaling using zebrafish as a model system.

Although Pax8 is one of the earliest transcription factors expressed in the preotic region of most vertebrates, its function in otic induction is not identified in any vertebrate. To investigate the role of Pax8, I cloned the full sequence of zebrafish *pax8* gene in the collaboration with Dr. A. Fritz's lab (Department of Biology, Emory University, Atlanta, GA), and performed a loss of function study using antisense oligonucleotide. Chapter II shows that *pax8* is required for normal otic induction, and it redundantly functions with *pax2a* and *pax2b* to maintain the otic fate mediating the major otic inducer, Fgf signaling.

After otic cells are induced and form the otic placode, expression of Fgf3 still persists in the hindbrain suggesting a later role. Zebrafish *valentino* mutants have perturbed expression of Fgf3 in the hindbrain but show relatively normal otic induction. By analyzing this mutant combined with the gene specific knockdown technique, I investigated the role of Fgf3 in otic vesicle differentiation in chapter III.

Under the control of Fgf3 signaling, *pax5* is expressed in one of the vestibular sensory epithelia, the utricular macula. The otic expression of *pax5* and its function in otic development have not been well described in any vertebrate. In chapter IV, I demonstrated that *pax5* is required for the utricular hair cell survival and the vestibular

function. In addition, the function of *pax5* with respect to the region specific mechanism for hair cell maintenance is discussed.

# CHAPTER II

# ZEBRAFISH Pax8 IS REQUIRED FOR OTIC PLACODE INDUCTION AND PLAYS A REDUNDANT ROLE WITH *pax2* GENES IN THE MAINTENANCE OF THE OTIC PLACODE*

## INTRODUCTION

Pax proteins are key regulators of developmental processes including specification, differentiation, growth, survival, migration and morphogenesis (Chi and Epstein, 2002; Dahl et al., 1997; Mansouri et al., 1996; Stuart et al., 1994). *Pax* genes are present in organisms ranging from worms to mammals (Czerny et al., 1997; Dahl et al., 1997; Walther et al., 1991). Pax proteins are named for and defined by the presence of a highly conserved, N-terminal, 128-amino acid DNA-binding domain, the paired domain (PD), which was first identified in the *Drosophila* pair-rule segmentation gene *paired* (Treisman et al., 1991).

---

* Reprinted from "Zebrafish Pax8 is required for otic placode induction and plays a redundant role with *pax2* genes in the maintenance of the otic placode"; by **Mackereth, M.D.†, Kwak, S.J.†, Fritz, A. and Riley, B.B.**, 2005, *Development* **132**, 371-382. †These authors contributed equally to this work.

The PD consists of two subdomains that each binds DNA in adjacent major grooves of the helix (Xu et al., 1995). Several Pax proteins can also interact with DNA via a complete or partial homeodomain (Dahl et al., 1997; Stuart et al., 1994; Underhill and Gros, 1997). Transcriptional activity of Pax proteins is controlled by a C-terminal regulatory region containing both activating and inhibitory domains (Dorfler and Busslinger, 1996).

Extensive alternative splicing has been reported for many vertebrate *Pax* genes, including mammalian *Pax2, Pax3, Pax5, Pax6, Pax7* and *Pax8*, and zebrafish *pax2a, pax3, pax7*, and *pax9* (Barber et al., 1999; Barr et al., 1999; Epstein et al., 1994; Kozmik et al., 1997; Kozmik et al., 1993; Nornes et al., 1996; Puschel et al., 1992; Seo et al., 1998; Tavassoli et al., 1997; Vogan et al., 1996; Zwollo et al., 1997). Similarly, *Pax2/5/8* transcripts of the invertebrate chordate amphioxus (*Branchiostoma floridae*) are alternatively spliced (Krelova et al., 2002). In most cases, alternative splicing has been shown to produce protein isoforms with drastically different DNA binding specificities and transactivation potentials (Barber et al., 1999; Barr et al., 1999; Epstein et al., 1994; Kozmik et al., 1997; Kozmik et al., 1993; Nornes et al., 1996; Puschel et al., 1992; Seo et al., 1998; Tavassoli et al., 1997; Vogan et al., 1996; Zwollo et al., 1997). Thus, alternative splicing is a highly conserved means of increasing the functional repertoire of *Pax* genes.

The nine vertebrate *Pax* genes are grouped into four categories, with *Pax2/5/8* constituting one of these classes (Pfeffer et al., 1998). This is an ancient group, with orthologs present in echinoderms, nematodes, and flies (Czerny et al., 1997). The

sequences of the functional regions are nearly invariant among the vertebrate *Pax2/5/8* genes (Pfeffer et al., 1998). *Pax2/5/8* genes are expressed in a spatially and temporally overlapping manner at the midbrain-hindbrain junction and in the CNS; this expression pattern has been conserved from zebrafish to mouse (Pfeffer et al., 1998). *Pax2* and *Pax8* homologs are also expressed in the otic placode and pronephros in these species (Pfeffer et al., 1998; Plachov et al., 1990). Recent evidence has shown that *Pax2* and *Pax8* perform redundant functions during mammalian kidney development and are required for the earliest steps of this process (Bouchard et al., 2002; Mansouri et al., 1998). However, otic development in *Pax2/Pax8*-deficient mouse embryos has not yet been described. In both zebrafish and mouse, *Pax8* is strongly expressed in the primordium of the otic placode during late gastrulation, making it the earliest known marker of otic induction (Pfeffer et al., 1998). *Pax8* expression is maintained throughout placode development and is lost soon after formation of the otic vesicle (Pfeffer et al., 1998). *Pax2* homologs are expressed in the otic anlagen during early somitogenesis stages and are maintained in portions of the otic vesicle (Pfeffer et al., 1998). The *Pax8* knockout mouse does not show an otic phenotype (Bouchard et al., 2002; Mansouri et al., 1998), and the *Pax2* knockout mouse shows variable defects in derivatives of the medial otic vesicle where *Pax2* is expressed after the vesicle forms (Bouchard et al., 2000; Burton et al., 2004; Favor et al., 1996; Torres et al., 1996). The absence of an earlier or more severe phenotype may reflect redundancy between these genes. There are two *Pax2* homologs in zebrafish, *pax2a* and *pax2b*, and functional disruption of both genes reduces hair cell production but does not impair formation of the placode or vesicle

(Whitfield et al., 2002). The extent to which *pax8* compensates for loss of *pax2a* and *pax2b* is not known.

Several upstream regulators of otic induction have been identified. The forkhead class transcription factor gene *foxi1* is expressed in the ventral ectoderm beginning at 50% epiboly. By mid-gastrulation *foxi1* expression is upregulated in the future otic placode prior to induction of *pax8*. Loss of *foxi1* prevents expression of *pax8* in the otic domain and severely compromises otic induction. Furthermore, misexpression of *foxi1* is sufficient to induce ectopic *pax8* (Nissen et al., 2003; Solomon et al., 2003). At least two other genes, *fgf3* and *fgf8*, are also necessary for *pax8* expression. These genes encode Fgf ligands that are expressed in the developing hindbrain between the prospective otic placodes. Loss of both *fgf* genes blocks otic induction, whereas misexpression of either gene is sufficient to induce ectopic otic tissue (Leger and Brand, 2002; Maroon et al., 2002; Phillips et al., 2001; Phillips et al., 2004). Thus, Fgf signaling and *foxi1* function converge to induce *pax8*, suggesting that *pax8* could be an important mediator of otic induction. In addition, zebrafish *dlx3b* and *dlx4b*, transcription factors with homeo-domains similar to *Drosophila distal-less* (Ekker et al., 1992a; Ellies et al., 1997), are required for otic placode formation. Combined loss of function of *dlx3b/4b* leads to a reduction or absence of otic placodes and *pax2a* expression in otic cells, but *pax8* expression initiates normally (Liu et al., 2003; Solomon and Fritz, 2002).

In this chapter, I describe a role for *pax8* during otic development. I have cloned full-length transcripts of zebrafish *pax8* and show that there are three main splice

variants that encode proteins with different N-terminal sequences. Depletion of Pax8 function leads to compromised otic vesicle and inner ear morphology, and my data suggest that different isoforms have both overlapping and unique functions. I show a strong genetic interaction between *pax8* and *pax2a*, and to a lesser extent *pax2b*, implicating these genes in the maintenance of otic cell fate. Depletion of *pax8* enhances otic placode and vesicle defects in embryos with reduced Fgf signaling or in embryos that have been depleted for *dlx3b* function. In contrast, depletion of *pax8* does not enhance defects in embryos depleted for *foxi1*. These and other data support the hypothesis that *pax8* helps mediate otic induction downstream of *foxi1* and *fgf3* and *8* but in parallel with *dlx3b*. At later stages, *pax8* acts redundantly with *pax2* genes to maintain otic fate.

## MATERIALS AND METHODS

### Fish strains

Embryos were developed at 28.5°C and staged according to standard criteria (Kimmel et al., 1995). Wild-type fish were derived from the AB line. $noi^{tu29a}$ and $ace^{ti282a}$ were derived from the Tu line (Brand et al., 1996) and used to assess functions of *pax2a* and *fgf8*, respectively. $noi^{tu29a}$ is thought to be a null allele (Lun and Brand, 1998) whereas $ace^{ti282a}$ is a strong hypomorph (Draper et al., 2001). Because *pax2a* and *fgf8* are closely

linked, producing *ace-noi* double homozygotes required that I first produce a recombinant line in which both mutant loci reside on the same chromosome. The rate of recombination between *fgf8* and *pax2a* is roughly 1.5%, so nearly 25% of intercross progeny produced in this line are double homozygotes.

### *pax8* 5' and 3' RACE cloning and sequencing

RNA was isolated from 3-5 somite and 24-hour embryos using TRIPURE reagent (Roche). For the 5' RACE reaction, 3-5 somite stage RNA was processed using the First Choice RLM-RACE kit from Ambion. cDNA was synthesized using a *pax8*-specific primer (CAGCGCCGCGGAGGGAAAGT) and C. therm polymerase (Roche) at 68°C for reverse transcription. Subsequently, PCR was performed using a second, nested *pax8*-specific primer (GCGGCGGTCGATTGGCAAAACTGTA) and the 5' RACE adaptor outer primer (Ambion). A fraction of this reaction was used as template in a second PCR amplification with a third, nested *pax8*-specific primer (AACGGGCGCAG ATGACGGAGACGAA) and the 5' RACE adaptor inner primer. All PCRs were performed using the Clontech Advantage-GC2 protocol with a final concentration of 1 M GC-melt. The resulting amplification products were cloned into pCRII Topo vector (Invitrogen) and sequenced. The 24-hour RNA was reverse transcribed using the CDS primer from the SMART II kit (Clontech) and C. Therm polymerase. 3' RACE was performed using a *pax8*-specific primer (CATCAATGGGCTGCTGGGAATCA) and the CDS primer (Clontech) in an initial PCR. A fraction of this reaction was used for a second PCR amplification with a nested *pax8*-specific primer (TCCGAGGGCTGAGGT

ATTTGTC) and the PCR primer supplied in the Clontech SMART II kit. A third round of PCR was performed using a fraction of the second PCR reaction as template and the *pax8*-specific primer (GCCAGTTCAGCAGCCCGTCCCTCAT) and the PCR primer (Clontech). The resulting products were cloned into the pCRII Topo vector and sequenced. For the splice variant analysis, *pax8*-specific primers located in the 5' UTR [exon 1a (Fig. 6A); GACAGACAACGGCGAACACCAACAC] and the 3'UTR [exon 13 (Fig. 6A); ACCCGGCCTCAGCTCAACATCAATAG] were used to amplify *pax8* transcripts from 24-hour cDNA (described above), using the Advantage-GC2 PCR protocol with a 1 M concentration of GC-melt. The resulting products were cloned into the pCRII Topo vector and sequenced.

**Morpholino injections**

Morpholino oligomers obtained from Gene Tools Inc. were diluted and injected as previously described (Nasevicius and Ekker, 2000; Phillips et al., 2001). A total of 1-5 ng MO was injected per embryo. At least 25 specimens were examined for each experiment. To knock down *pax8,* translation-blocking morpholinos and splice-blocking morpholinos were generated as follows: translation blocker for splice variant 1 (variant 1 MO): 5' GTTCACAAACATGCCTCCTAGTTGA 3'; translation blocker for splice variants 2 and 3 (variant 2/3 MO): 5' GACCTCGCCCAGTGCTGTTGGACAT 3'; splice blocker exon6/7 (splice donor site): 5' CTGCACTCACTGTCATCGTGTCCTC 3'; splice blocker exon6/7 (splice acceptor site): 5' CAGCTCTCCTGGTCACCTGCACAA C 3'; splice blocker exon3 (paired domain): 5' GTAGCGGTGACACACCCCCTCGGCC

3'; splice blocker exon7/8 (homeo domain): 5' TGCGGTGTTCTGCACCTGCTCTGCT 3'. Unless stated otherwise, *pax8* morphants were injected with 2.5 ng each of variant 1 MO and variant 2/3 MO to maximally disrupt *pax8* function. To knock down *fgf3*, two translation-blocking sequences were co-injected: *fgf3*-MO #1, 5' CATTGTGGCATCGC GGGATGTCGGC 3'; *fgf3*-MO #2, 5' GGTCCCATCAAAGAA GTATCATTTG 3'. Other morpholino sequences used were as follows: *dlx3b*-MO translation blocker, 5' ATATGTCGGTCCACTCATCCTTTAAT 3'; *foxi1*-MO translation blocker, 5' TAATC CGCTCTCCCTCCAGAAA 3'; *pax2b*-MO translation blocker: 5' GGTCTGCCTTACA GTGAATATCCAT 3'.

**Immunofluorescent staining**

Embryos were raised in 0.3% PTU solution to inhibit the formation of melanocytes. Embryos were fixed and stained as previously described (Riley et al., 1999) using polyclonal anti-mouse Pax2 antibody (Berkeley Antibody company, 1:100 dilution) and monoclonal anti-acetylated tubulin antibody (Sigma T-6793, 1:100). Alexa 546 goat anti-rabbit IgG (Molecular Probes A-11010, 1:50) and Alexa 488 goat anti-mouse IgG (Molecular Probes A-11001, 1:50) were used as secondary antibodies.

**In situ hybridization**

In situ hybridization was carried out as described in Phillips et al. (Phillips et al., 2001), and two-color staining was performed as described by Jowett (Jowett, 1996) with minor modifications. Antisense riboprobes were transcribed from plasmids containing the

following: *dlx3b* (Ekker et al., 1992a); *krox20* (Oxtoby and Jowett, 1993); *msxC* (Ekker et al., 1992b); *pax2a* (Krauss et al., 1991); *pax5* and *pax8* (Pfeffer et al., 1998).

## RESULTS

### *pax8* transcript structure

The previously published sequence for zebrafish *pax8* was incomplete, lacking 3' UTR sequences and 5' sequences, including the putative start codon (Pfeffer et al., 1998). In order to facilitate design of translation-blocking morpholinos, complete *pax8* cDNAs were generated using RACE by RT-PCR on adaptor ligated mRNA from 3-5 somite stage and 24-hour embryos. Sequence analysis of the 5' RACE clones indicated that *pax8* is alternatively spliced, resulting in two different predicted start codons (Fig. 6A). Because members of the *Pax* gene family are subject to alternative splicing (Barber et al., 1999; Barr et al., 1999; Epstein et al., 1994; Kozmik et al., 1997; Kozmik et al., 1993; Nornes et al., 1996; Puschel et al., 1992; Seo et al., 1998; Tavassoli et al., 1997; Vogan et al., 1996; Zwollo et al., 1997), primers in the predicted 5' UTR and 3' UTR were designed and RT-PCR was performed to obtain a collection of clones containing *pax8* transcripts with a complete coding sequence. A total of 54 clones were randomly selected and sequenced, and the results of this analysis are summarized in Fig. 6B. To verify these results, the cDNA sequences were used to search the genome assembly

database (assembly Zv2; http://www.sanger.ac.uk/Projects/D_rerio/). Based on this comparison and the previously available data, the zebrafish *pax8* gene consists of at least 13 exons, and I have renumbered them accordingly (Fig. 6A). The predominant class of transcripts (32/54, 59.5%; Fig. 6B) is variant 1.1, which contains exon 1a, then exon 2 and all subsequent exons. The predicted ORF for variant 1 starts ten amino acids within the canonical paired domain and is contiguous with the previously published sequence. Interestingly, Fugu *pax8* also encodes a methionine at position 10 of the paired domain (Pfeffer et al., 1998), and thus may encode a similar set of Pax8 proteins as zebrafish. The second most frequent class of transcripts (6/54, 11%; Fig. 6B) is variant 2.1, which contains exon 1a, exon 1c, and then exon 2 and all following exons. Exon 1c provides an alternate potential start codon, leading to a predicted protein that starts eight amino acids N-terminal to the canonical paired domain (Fig. 6A). Variant 3 transcripts appear to be rare (2/54, 4% of my clones) and encode the same predicted protein sequence as variant 2 transcripts.

Variants 1.2 (3.7%) and 2.2 (3.7%) lack exon 11, which encodes a portion of the transactivation domain. Similarly, variants 1.3 (5.5%) and 2.3 (3.7%) lack exons 9 and 10, which also encode part of the transactivation domain. Variants 1.4 (3.7%) and 1.5 (1.8%) use an alternate splice donor site, leading to an insert between exons 9 and 10; this insert is in frame and would add 11 amino acids to the transactivation domain (not shown in Fig. 6A sequence). In addition to the insert, variant 1.5 also lacks exon 11. Variant 2.6 lacks part of the transactivation domain due to the absence of exon 9.

The sequence analysis shows that *pax8* transcripts are subject to extensive alternative splicing. To address the potential functional significance of different Pax8 isoforms, artificial mRNA for variants 1.1 or 2.1 (full length) and 1.3 or 2.3 (nonfunctional transactivation domain) were injected into one-cell embryos. Ectopic overexpression of either full length variant leads to severe gastrulation defects, precluding a meaningful interpretation of *pax8* function in otic placode formation. Conversely, injection of the isoforms lacking the transactivation domain did not lead to any detectable phenotypes in otic placode or vesicle morphology (data not shown).

**Functional analysis of *pax8***

I designed morpholino oligonucleotides (MO) to knock down *pax8* function. Four MOs were designed to block pre-mRNA splicing at distinct splice junction sites (Draper et al., 2001), and two additional MOs were designed to target the sequence around each of the predicted start codons (Nasevicius and Ekker, 2000). Together, these two MOs are predicted to block translation of all isoforms (Fig. 6A). Co-injection of the translation-blocking MOs resulted in the most consistent and reproducible phenotypes, and this approach was used in all subsequent studies. Co-injection of the two translation blockers plus two of the four splice-blocking MOs did not produce any additional phenotypic

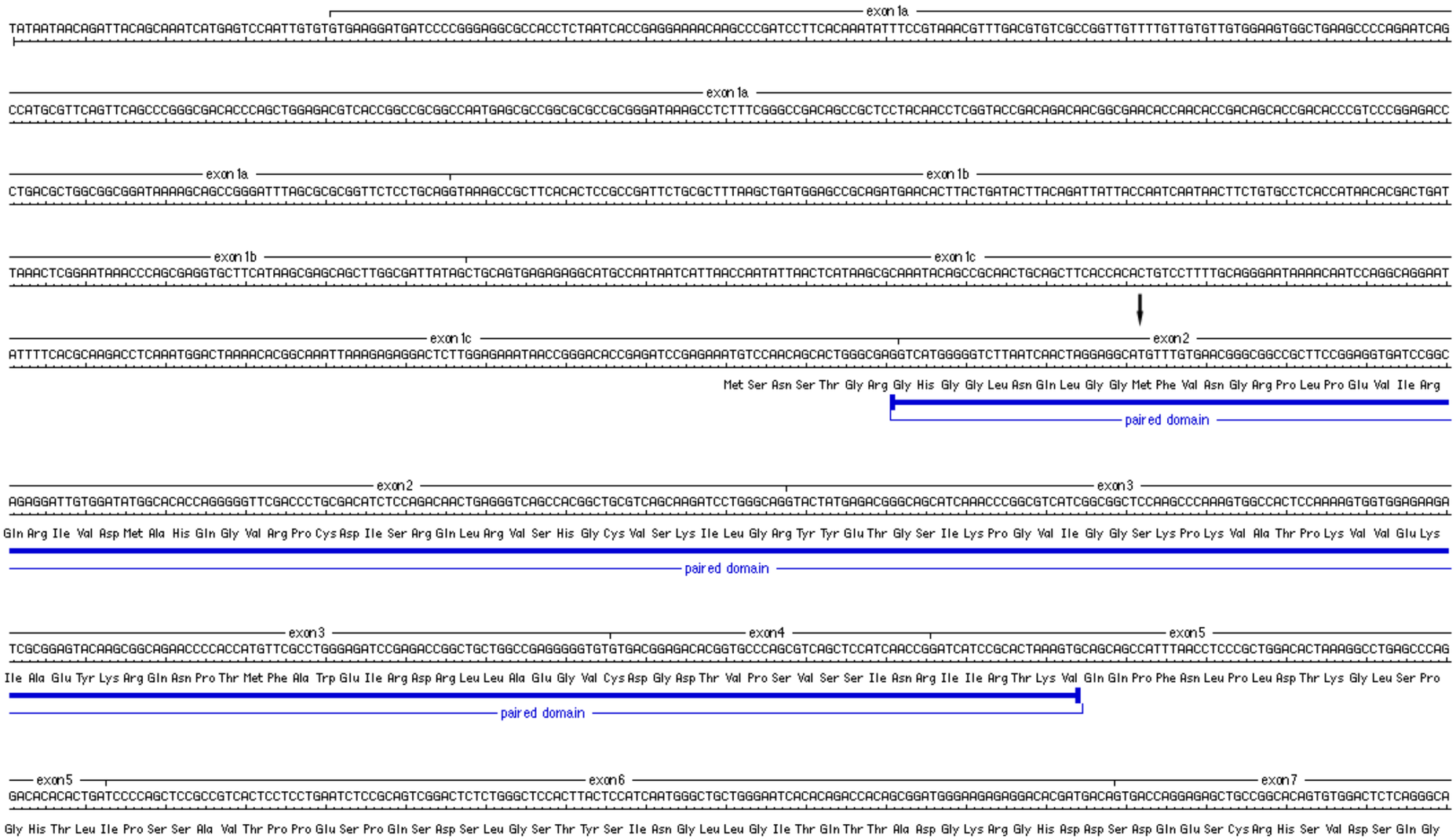


**Fig. 6**. Sequence and splice variants of *pax8*. Figure 6A shows the complete sequence of the *pax8* variant 3 transcript. Exons predicted by comparison to genomic sequence are indicated above the sequence. The transcription start site, preceded by a TATAA box, begins with exon 1a. Exon 1 is contiguous with genomic DNA sequence, but has been subdivided into exons 1a, 1b, and 1c to indicate that the splice variants shown in Figure 6B contain different parts of exon 1. The arrow indicates the putative start codon used in variant 1 transcripts. The star indicates that some transcripts use an alternate splice donor site that extends exon 9 by 33bp (sequence not shown). The canonical Paired domain and predicted transactivation and inhibitory domains are indicated below the sequence. Polyadenylation (polyA) sites are underlined in purple; the majority of transcripts (52/54) use the first polyA site.


**Fig. 6. (Continued)**

# B

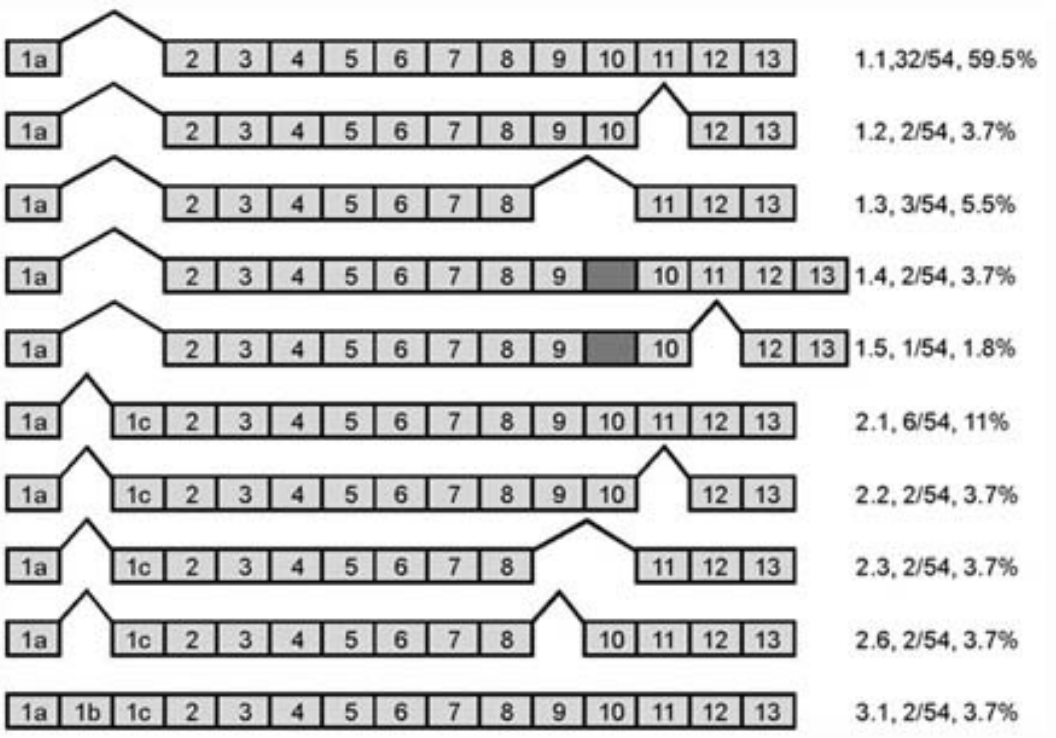


**Fig. 6. (Continued)** Figure 6B shows a schematic representation (not to scale) of the splice variants observed in *pax8* transcripts. The variant name (e.g. 1.1, 1.2), total number of representative transcripts out of 54 total sequenced, and % abundance are indicated after each schematic transcript. The unlabeled box between exon 9 and exon 10 in variants 1.4 and 1.5 indicates an additional 11 amino acid insert (see also Fig. 6A) resulting from the use of an alternate splice donor site. The predicted coding sequence for variants 2 and 3 begins with the start codon in exon 1c; all variant 1 transcripts use the start codon in exon 2 indicated by the arrow in Figure 6A.

defects, although nonspecific necrosis was seen at higher MO concentrations (not shown), further suggesting that the translation-blocking MOs effectively block *pax8* function.

At 24 hpf, reduction of *pax8* translation in embryos injected with both translation-blocking *pax8* MOs (*pax8* morphants) causes a slightly shortened trunk/tail axis and a reduced midbrain-hindbrain border with mild necrosis in adjacent brain tissue (Fig. 7A, D). Furthermore, the otic vesicle is reduced in its linear dimensions by roughly half (Fig. 7B, E). These phenotypic changes are observed in over 90% of *pax8* morphants. Embryos injected with only variant 1 MO (Fig. 7C) or variant 2/3 MO (Fig. 7F) display an otic vesicle phenotype of intermediate severity, with the variant 2/3 morphant embryos showing a slightly more affected otic vesicle. Because *pax8* is one of the earliest known markers of preotic development (Pfeffer et al., 1998), I analyzed the initial stages of otic induction in *pax8* morphants. Knockdown of *pax8* does not eliminate *pax8* mRNA expression in otic precursor cells, but reduces the size of the preotic domain of *pax8* expression at all stages examined (Fig. 7G, J). The level of *pax8* expression in these cells is also reduced, suggesting a certain degree of autoregulation. Two other preotic markers, *pax2a* and *dlx3b*, also display reduced preotic domains, but levels of expression are relatively normal (Fig. 7H, K, I, L). Hindbrain (HB) patterning is normal in *pax8* morphants as judged by expression patterns of *krox20, fgf3, fgf8, wnt8* and *wnt8b* (Fig. 7H, K; see also Fig. 10), suggesting that impairment of preotic development is not due to loss of HB signals. I infer that a reduced level of *pax8* impairs the response of preplacodal cells to otic-inducing signals (see Discussion). Alternatively,

otic induction may proceed normally in *pax8* morphants, but placodal cells proliferate less in the absence of Pax8. However, previously published work on the role of Fgf3 and Fgf10 during otic development in the mouse suggests that this latter explanation is not the case (Alvarez et al., 2003; Wright and Mansour, 2003). I also examined later aspects of otic patterning in *pax8* morphants. General features of anterior-posterior, dorso-ventral and medio-lateral patterning appear unaffected, as shown by normal expression of *pax5* in the anterior (Fig. 8B, F), *dlx3b* in the dorsal (Fig. 8C, G), and *pax2a* in the ventromedial portions of the otic vesicle (Fig. 8A, E). However, hair cell production is reduced by an average of 42±11% (*n*=59; compare Fig. 8A and E), and severely affected specimens produce only a single macula per ear (not shown). Cristae typically form by 72 hpf and express *msxC*, although the level of expression is usually reduced in the lateral crista (Fig. 8D, H). In severely affected specimens with very small otic vesicles, one or more cristae are fused or missing (not shown). Later stages of otic development become increasingly aberrant as embryos begin to degenerate and die (not shown). Since *pax8* is not expressed in the ear past 19 hpf, reduction in the vesicle and sensory epithelia presumably arise from earlier deficits in the placode or preplacode resulting from reduced levels of *pax8*.

**Interactions between *pax8* and *fgf* genes**

Fgf signaling appears to be the principal inducer of otic development in all vertebrates (Noramly and Grainger, 2002; Riley and Phillips, 2003). In zebrafish, *fgf3* and *fgf8* are expressed in periotic tissues during gastrulation and are essential for otic

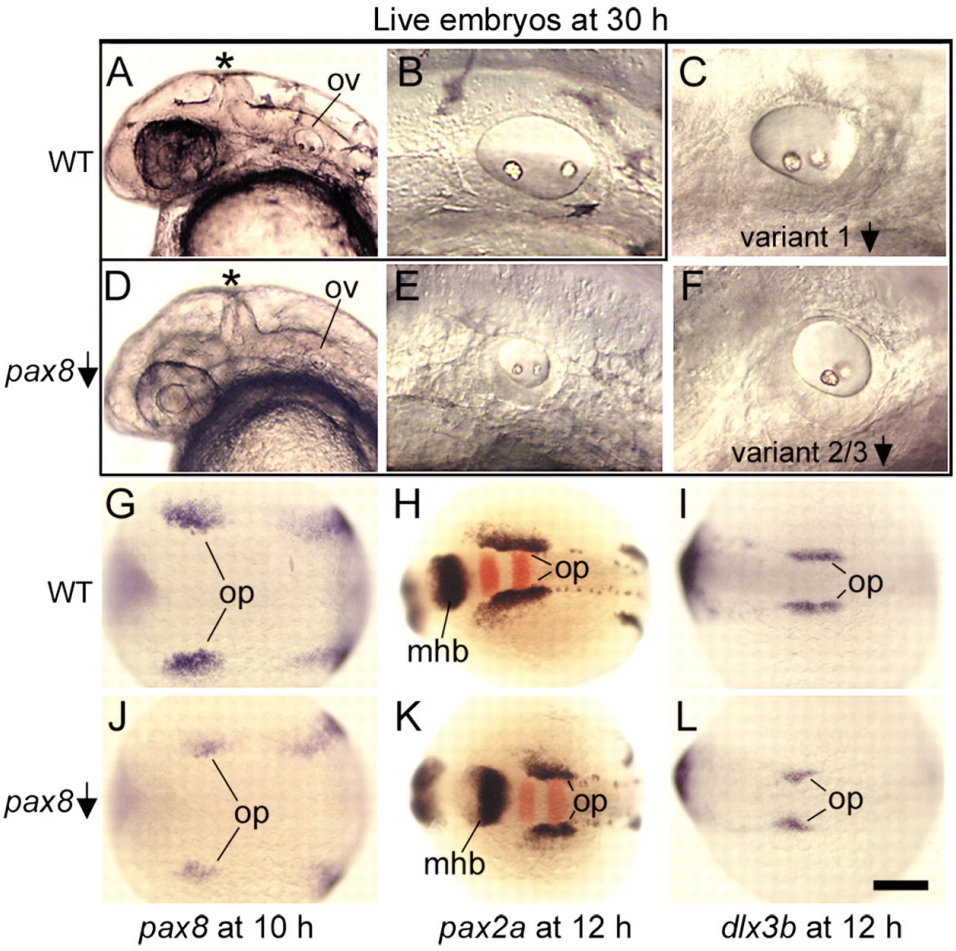


**Fig. 7.** Assessment of Pax8 function in otic induction. (A, D) Head region of live wild-type (A) and *pax8*-MO injected (D) embryos at 30 hpf. The *pax8*-MO injected embryo has a narrow midbrain-hindbrain border (asterisk), and small otic vesicles (ov). (B, E) Otic vesicles at 30 hpf in live wild-type (B) and *pax8*-MO injected (E) embryos. (C, F) Otic vesicles at 30 hpf in embryos injected with v1-MO to knock down variant 1-isoforms of *pax8* (C) or v2/3-MO to knock down variant 2 and 3-isoforms of *pax8* (F). (G, J) *pax8* expression at 10 hpf in wild type (G) and *pax8*-MO injected (J) embryos. H, K, Expression of *pax2a* (blue) and *krox20* (red) at 12 hpf in wild type (H) and *pax8*-MO injected (K) embryos. (I, L) *dlx3b* expression at 12 hpf in wild type (I) and *pax8*-MO injected (L) embryos. Images show lateral views with anterior to the left and dorsal to the top (A-F); or dorsal views with anterior to the left (G-L). Abbreviations: mhb, midbrain-hindbrain border; op, otic placode; ov, otic vesicle. Scale bar, 200 µm (H, K), 170 µm (G, J, I, L), 150 µm (A, D), and 40 µm (B, C, E, F).

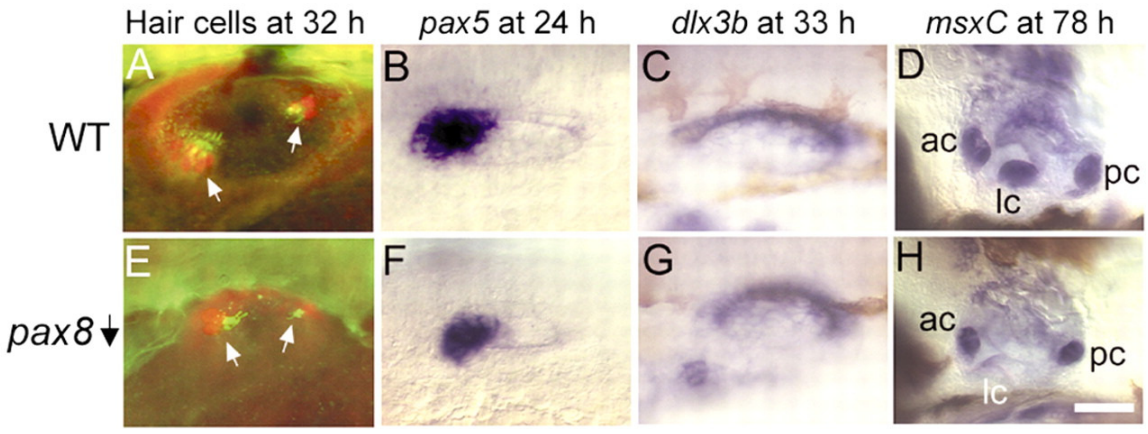


**Fig. 8.** Assessment of Pax8 function in otic vesicle patterning. (A, E) Otic vesicles at 32 hpf stained with anti-Pax2 (red) and anti-acetylated tubulin (green) antibodies to label hair cells (Riley et al., 1999) in wild-type (A) and *pax8*-MO injected (E) embryos. Hair cell patches are indicated (white arrows). Injected embryos produce fewer hair cells than normal. In the experiment shown here, an average of 5.2 ± 1.1 hair cells were seen in *pax8* morphants (n = 59 ears), compared to 9.2 ± 1.4 hair cells in wild-type embryos (n = 10 ears). 5-10% of *pax8* morphants produce only one macula per ear (not shown). (B, F) *pax5* expression at 24 hpf in wild-type (B) and *pax8*-MO injected (F) embryos. (C, G) *dlx3b* expression at 33 hpf in wild-type (C) and *pax8*-MO injected (G) embryos. (D, H) *msxC* expression marks developing cristae in the otic vesicle at 78 hpf in wild-type (D) and *pax8*-MO injected (H) embryos. The lateral crista is present in the injected embryo but shows strongly reduced expression of *msxC*. Defects in development of cristae and semicircular canals are highly variable in *pax8* morphants. Images show lateral views with anterior to the left and dorsal to the top. Abbreviations: ac, anterior crista; lc, lateral crista; pc, posterior crista. Scale bar, 90 µm (D, H), 40 µm (C, G), and 30 µm (A, B, E, F).

induction (Leger and Brand, 2002; Maroon et al., 2002; Phillips et al., 2001). Furthermore, in the experimental context of the whole embryo, misexpression of *fgf3* or *fgf8* can lead to the formation of ectopic otic placodes (Phillips et al., 2004). Induction of *pax8* expression is the earliest response to Fgf signaling and does not occur in the absence of Fgf signaling. I hypothesized that *pax8* helps mediate otic induction or early differentiation in response to Fgf signaling. In support of this hypothesis, the phenotype observed in *pax8* morphants (Fig. 7, 8) resembles that observed in embryos disrupted for either *fgf3* or *fgf8* (Fig. 9E, M). I tested this relationship further by examining the effects of disrupting *pax8* and either *fgf3* or *fgf8*. Because *fgf3* and *fgf8* are partially redundant, blocking either function alone causes only moderate reduction in the expression domains of preotic markers *pax8, pax2a*, and *dlx3b* (Fig. 9F-H, N-P), with corresponding reduction in the size of the otic vesicle (Fig. 9E, M). These tissues are further reduced in embryos depleted for both *pax8* and *fgf3* (Fig. 9I-L). Depleting *pax8* in *ace* (*fgf8*) mutants causes even more severe deficiencies in otic development: at early stages, expression domains of *pax8* and *pax2a* are strongly reduced, upregulation of *dlx3b* does not occur, and at later stages the otic vesicle is rudimentary and produces no hair cells or otoliths (Fig. 9Q-T). It is unclear whether the stronger interaction of *pax8* with *fgf8* compared to *fgf3* reflects functional differences between these ligands or differing degrees of functional disruption. A recent report suggests that *fgf8* plays a more dominant role than *fgf3* in early hindbrain patterning (Wiellette and Sive, 2004), and may thus also have a more pronounced role in otic induction. In either case, the above data are consistent with the hypothesis that *pax8* helps mediate the effects of both Fgfs. The

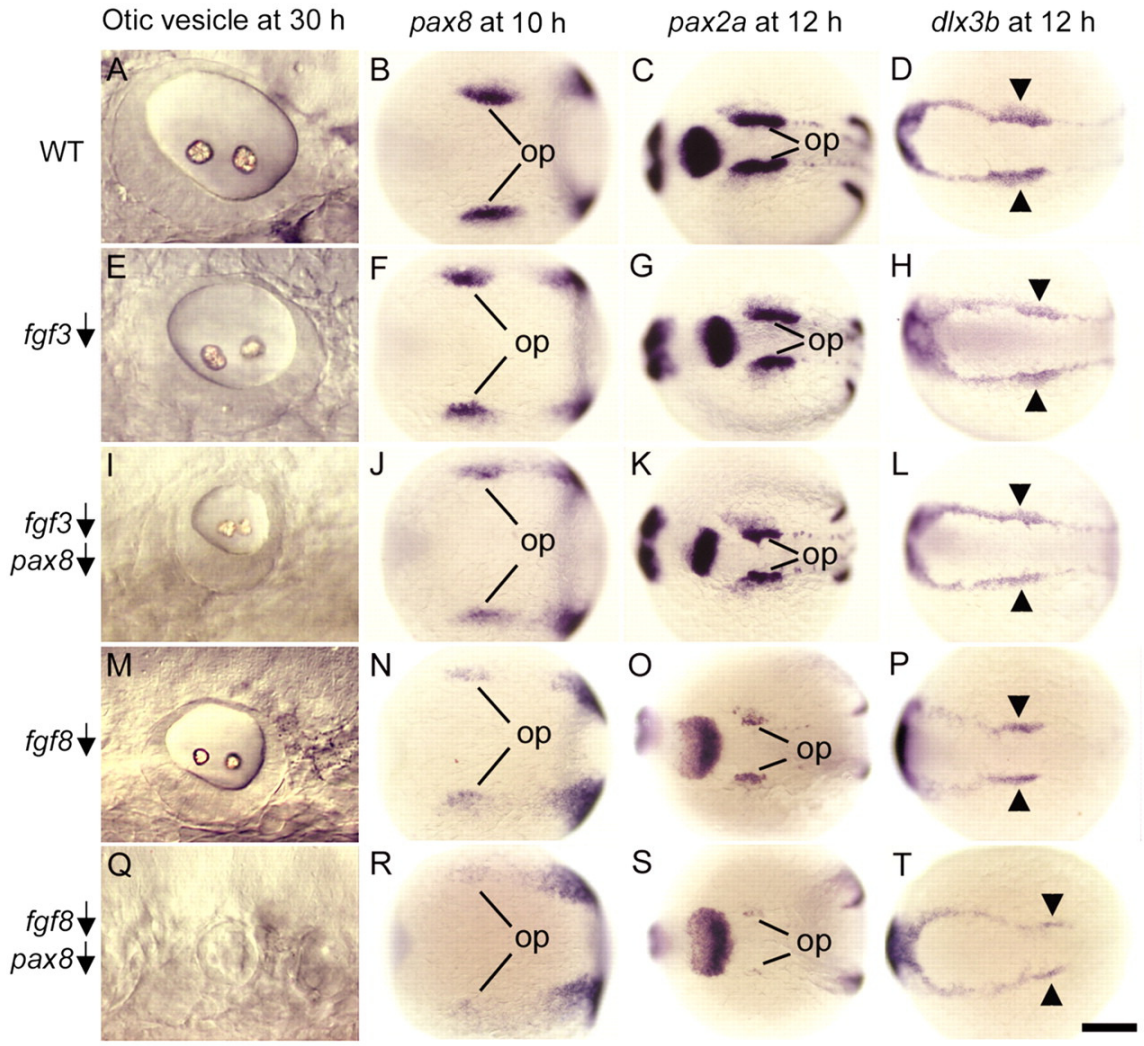


**Fig. 9**. Interaction of *pax8* with *fgf3* and *fgf8*. Wild-type embryos (A-D), wild-type embryos injected with *fgf3*-MO (E-H), wild-type embryos coinjected with *fgf3*-MO and *pax8*-MO (I-L), *ace* (*fgf8*) mutants (M-P), and *ace* mutants injected with *pax8*-MO (Q-T). Images show lateral views of the otic vesicle at 30 hpf (A, E, I, M, Q), and dorsal views of *pax8* expression at 10 hpf (B, F, J, N, R), *pax2a* expression at 12 hpf (C, G, K, O, S) and *dlx3b* expression at 12 hpf (D, H, L, P, T). op, otic placode. Arrowheads mark the otic region where *dlx3b* expression normally shows marked upregulation. Anterior is to the left in all specimens. Scale bar, 30 µm (A, E, I, M) and 200 µm (B-D, F-H, J-L, N-P, R-T).

fact that otic development is not totally ablated is consistent with the notion that *pax8* is not the only gene involved in the early response to Fgf signaling.

**Interactions between *pax8* and *pax2* genes**

Two other *pax* genes are coexpressed with *pax8* in preotic cells, albeit at slightly later stages: *pax2a* is expressed in the otic anlagen by 11 hpf (3 somites) and *pax2b* is expressed by 13.5 hpf (9 somites) (Pfeffer et al., 1998). As closely allied members of the *pax2/5/8* family, these three genes could provide multiple levels of redundancy during otic development. Notably, embryos deficient in both *pax2a* and *pax2b* produce relative normal otic vesicles, with defects being limited to reduced hair cell production (Whitfield et al., 2002). This surprisingly mild phenotype possibly reflects compensation by *pax8*. Similarly, later expression of *pax2a* and *pax2b* could ameliorate the effects of disrupting *pax8* function. To address these possibilities, I injected *pax8*-MO and *pax2b*-MO into *noi* (*pax2a*) mutants (Fig. 10A'-D'). Early placode development in *pax2a-pax2b-pax8*-deficient embryos is similar to that in *pax8* morphants. However, by 18 hpf, the otic domain of *pax2a* is severely reduced in *pax2a-pax2b-pax8*-deficient embryos (Fig. 10B'). By 24 hpf, the otic domain of *pax2a* is lost entirely in about half of *pax2a-pax2b-pax8*-deficient embryos (47%, *n*=36; Fig. 10C'), and there are no morphological signs of otic development (Fig. 10D'). Staining with acridine orange indicates that there is no noticeable increase in cell death in the periotic region (not shown), suggesting that otic cells dedifferentiate in the absence of *pax2/8* function. In agreement, about half of *pax2a-pax2b-pax8*-deficient embryos show diffuse expression of *dlx3b* in the otic region

or no otic expression at all (11/30 and 3/30, respectively, Fig. 10E', F'). In addition, a scattering of *dlx3b*-expressing cells appears between the otic territory and pharyngeal arches, a region normally devoid of *dlx3b* expression. It is possible that these ectopic *dlx3b*-expressing cells are the dispersed remnants of the otic vesicle. Expression of other otic markers shows similar results. For example, *sox9a* expression is initially induced but is barely detectable in *pax2a-pax2b-pax8*-deficient embryos by 13.5 hpf (Fig. 10I, I'). *claudinA* is expressed in a reduced otic domain at 13.5 hpf. By 24 hpf, about half of *pax2a-pax2b-pax8*-deficient embryos show either no *claudinA* expression (9/25, Fig. 10K') or a diffuse scattering of expressing cells, again suggesting dispersal of otic remnants (5/25, Fig. 10L'). In summary, otic induction appears no worse in *pax2a-pax2b-pax8*-deficient embryos than in *pax8* morphants, but the otic placode is not maintained properly at later stages. Various hindbrain markers including *krox20, fgf3, fgf8, wnt8*, and *wnt8b* (Fig. 10B', G', H', and data not shown) are induced and maintained normally, suggesting that the failure to maintain otic fate is not due to loss of hindbrain signaling.

A similar phenotype to the *pax2a-pax2b-pax8*-deficient phenotype is seen in *noi (pax2a)-pax8*-deficient embryos (not shown). Because *pax2b* is still expressed, I infer that *pax2b* alone is not sufficient to maintain otic development. Nevertheless, the frequency of total ear loss in *noi* (*pax2a*)*-pax8*-deficient embryos (22%, *n*=23) is lower than in *pax2a-pax2b-pax8*-deficient embryos (47%, *n*=36), suggesting that *pax2b* can contribute to otic maintenance. To test this further, I injected wild-type embryos with *pax2b*-MO and *pax8*-MO. Otic development is similar to that seen in *pax8*-deficient

**Fig. 10.** Relative functions of *pax8*, *pax2a* and *pax2b*. (A-C) *pax2a* expression in wild-type embryos at 14 hpf (A), 18 hpf (B) and 24 hpf (C). D, Head region of an uninjected *noi* (*pax2a*) mutant at 30 hpf. The otic vesicle has essentially normal morphology. (A'-D') *noi* (*pax2a*) mutants coinjected with *pax8*-MO and *pax2b*-MO showing *pax2a* expression at 14 hpf (A'), 18 hpf (B') and 24 hpf (C'), and a live specimen with no otic vesicles at 30 hpf (D'). *krox20* expression in the hindbrain is shown in red (B, B'). E, E', F, F', *dlx3b* expression at 24 hpf in a wild-type embryo (E), a wild-type embryo injected with *pax8*-MO (F), and *noi* (*pax2a*) mutants coinjected with *pax8*-MO and *pax2b*-MO (E', F'). The specimen in E' lacks morphological otic vesicles but does show a scattering of *dlx3b*-expressing cells in the otic region (asterisk). The specimen in F' lacks morphological signs of otic development and also shows no *dlx3b* expression in the otic region (asterisk). (G, G', H, H') *fgf3* expression in wild-type embryos at 14 hpf (G) and 19 hpf (H) and in *pax2ba-pax2b-pax8*-deficient embryos at 14 hpf (G') and 19 hpf (H'). Expression in the hindbrain (r4) is normal in all specimens, whereas expression in the otic vesicle (ov) is strongly reduced at 19 hpf in *pax2a-pax2b-pax8*-deficient embryos (compare H, H'). (I, I') sox9a expression at 13.5 hpf in wild-type (I) and *pax2a-pax2b-pax8*-deficient (I') embryos. (J-L, J'-L') claudinA expression in wild-type embryos at 13.5 hpf (J) and 24 hpf (K, L), and in *pax2a-pax2b-pax8*-deficient embryos at 13.5 hpf (J') and 24 hpf (K', L'). (M-P) wild-type embryos coinjected with *pax8*-MO and *pax2b*-MO showing expression of *pax2a* at 14 hpf (M) and 18 hpf (N), the head region of a live specimen with a small otic vesicle at 30 hpf (O), and an enlargement of the otic vesicle of the same specimen (P). Images show dorsal views with anterior to the left (A, A', G-J, G'-J', M), dorsal views with anterior to the top (B, B', C, C', K, K', N), or lateral views with anterior to the left (D-F, D'-F', L, L', O, P). Abbreviations and symbols: a, pharyngeal arches; asterisk, region where otic vesicle normally forms; mhb, midbrain-hindbrain border; op, otic placode; ov, otic vesicle; r4, rhombomere 4 of the hindbrain. Scale bar, 170 µm (A, A', G, G', I, J, I', J', M), 75 µm (B-F, B'-F', H, H', K, L, K', L', N, O) and 19 µm (P).

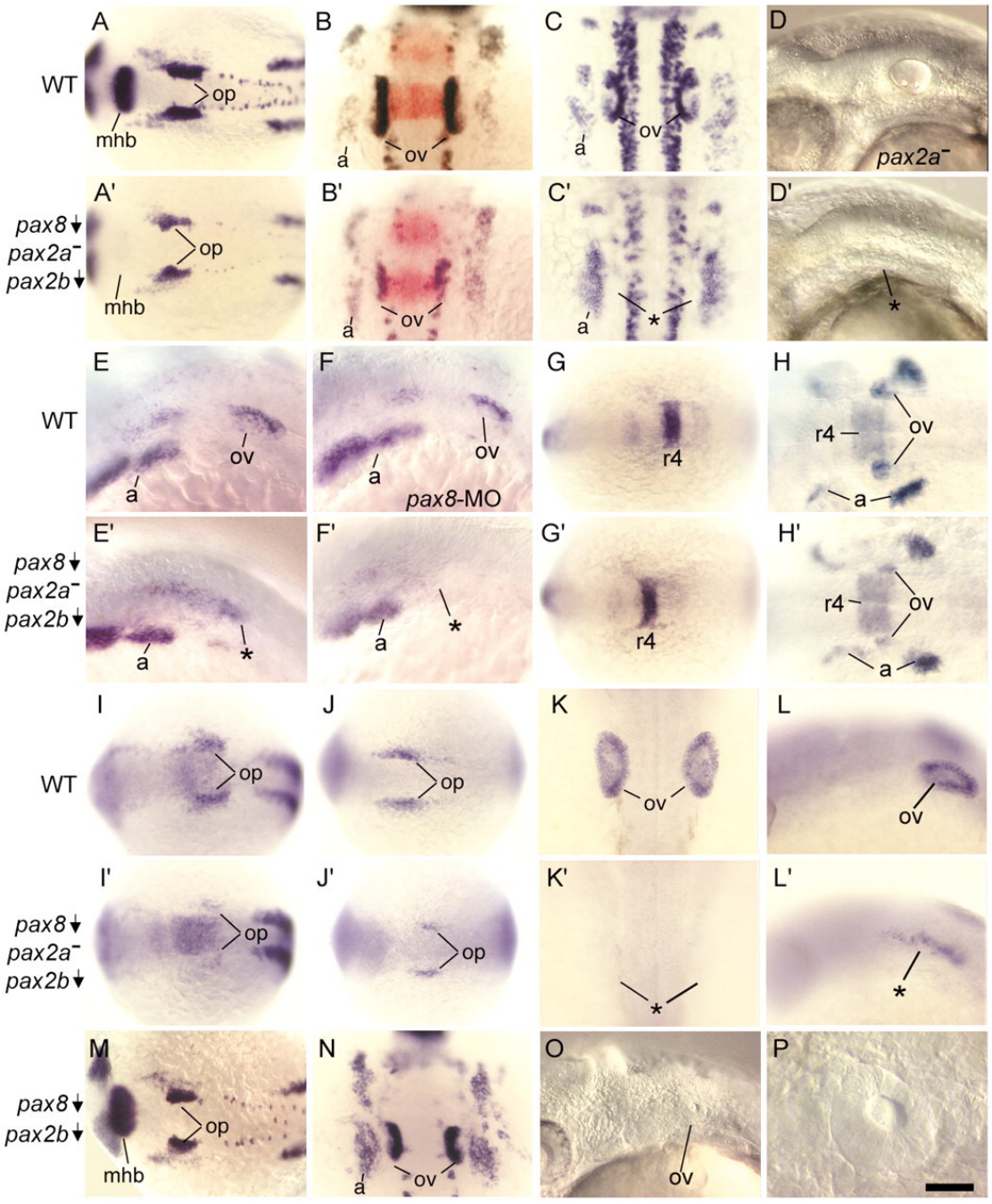
A
B
C
D
WT
op
mhb
a
ov
pax2a⁻
A'
B'
C'
D'
pax8↓
pax2a⁻
pax2b↓
*
E
F
G
H
WT
ov
a
pax8-MO
r4
E'
F'
G'
H'
pax8↓
pax2a⁻
pax2b↓
I
J
K
L
WT
op
I'
J'
K'
L'
pax8↓
pax2a⁻
pax2b↓
M
N
O
P
pax8↓
pax2b↓

embryos through 18 hpf (Fig. 10M, N, and data not shown). However, *pax2b-pax8*-deficient embryos produce a much smaller otic vesicle than *pax8*-deficient embryos and usually lacks otoliths (Fig. 10O, P), suggesting significant loss of otic tissue after the vesicle begins to form. Thus, both *pax2a* and *pax2b* play a role in otic maintenance, but the requirement for *pax2a* appears more critical.

Because of the strong interaction between *pax8* and *pax2a*, I used the *noi* (*pax2a*) mutation to provide a sensitized background in which to test the relative roles of different *pax8* splice variants. *pax8* variant 1 MO blocks translation of variant 1 isoforms, which lack the N-terminal paired domain, whereas *pax8* variant 2/3 MO blocks translation of isoforms predicted to include the entire paired domain. Injection of *pax8* variant 1 MO into *noi* (*pax2a*) mutants usually results in production of a moderately reduced otic vesicle containing hair cells but no otoliths (83%, *n*=84, Fig. 11A, B). In contrast, injection of *pax8* variant 2/3 MO into *noi* (*pax2a*) mutants ablates the ear entirely (21/76) or results in production of a relatively small otic vesicle (55/76). In the latter case, however, otoliths are usually produced (Fig. 11C, D). The two translation blockers also differentially affect brain development in the region of the midbrain-hindbrain border (MHB). The MHB does not form in *noi* (*pax2a*) mutants. Mutants injected with *pax8* variant 2/3 MO invariably show a persistent and intense band of cell death localized to the ventral midline of the MHB region (Fig. 11C, H). This pattern of cell death is never observed in uninjected *noi* (*pax2a*) mutants nor in mutants injected with *pax8* variant 1 MO (Fig. 11A, F). Instead, 20-30% of *noi* (*pax2a*) mutants injected with *pax8* variant 1 MO show a moderate increase in cell death in the dorsolateral MHB

region (Fig. 11G). The significance of these differences is unclear at present, but the data strongly suggest that Pax8 isoforms containing a complete vs. partial paired domain have at least some distinct developmental functions.

**Interactions between *pax2a* and *fgf* genes**

A role for *pax2* genes in placode maintenance has not been previously reported, so this function was further investigated by analyzing the interaction between *fgf* genes and *pax2a*. In *ace-noi* (*fgf8-pax2a*) double mutants, expression of preotic markers is initially comparable to that seen in *ace* single mutants. However, the otic domain of *pax2a* shrinks dramatically in *ace-noi* double mutants such that, by 14 hpf, it is much smaller than in either *ace* or *noi* single mutants (Fig. 12D, E, G, H). *ace-noi* double mutants produce only very small otic vesicles containing few hair cells and no otoliths (Fig. 12I; and data not shown). In severely affected specimens, otic vesicles are so small that they can only be detected at high magnification using DIC optics. Similar results are obtained when *fgf3* is knocked down in *noi* (*pax2a*) mutants (not shown). Presumably, Fgf depletion impairs early preotic development such that *pax2a* function becomes critical for this process. When *pax2a* is disrupted in addition to *fgf3* or *fgf8*, the majority of placodal cells are unable to maintain otic fate.

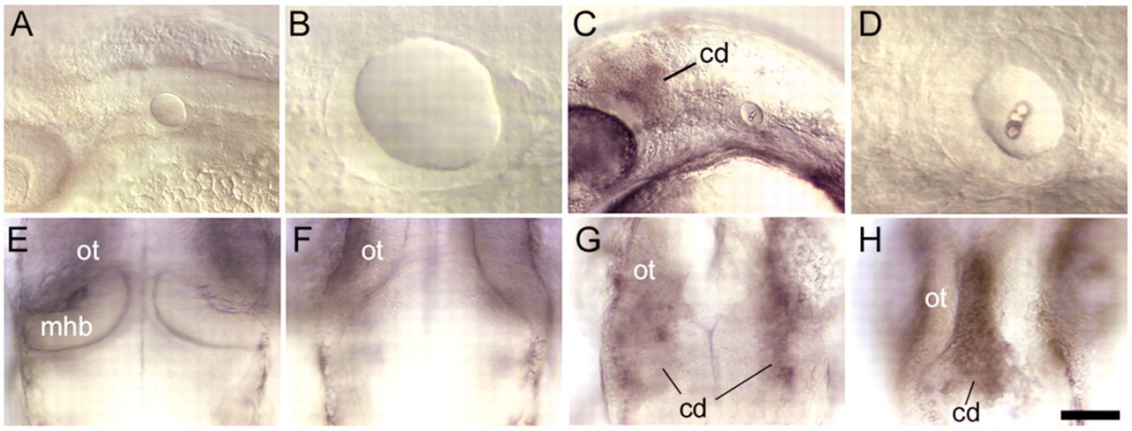


**Fig. 11.** Distinct functions of *pax8* splice isoforms**.** (A-D) Lateral views of the head and otic structures at 30 hpf in *noi* (*pax2a*) mutants injected either with *pax8* variant 1 MO (A, B) or *noi* mutants injected with *pax8* variant 2/3 MO (C, D). Most *noi* mutants knocked down for variant 1 isoforms produce a moderate-sized otic vesicle containing hair cells but lacking otoliths (B). In contrast, *noi* mutants knocked down for variant 2 and 3 isoforms typically produce a small otic vesicle containing both hair cells and otoliths (D) or no otic vesicle at all (data not shown). In addition, all *noi* mutants knocked down for variant 2 and 3 isoforms show persistent cell death (cd) in the midbrain-hindbrain region. (E-H) Dorsal views of the midbrain-hindbrain border region at 30 hpf in an uninjected wild-type embryo (E), an uninjected *noi* mutant (F), a *noi* mutant injected with *pax8* variant 1 MO (G) and a *noi* mutant injected with *pax8* variant 2/3 MO (H). Increased cell death is not evident in the majority of *noi* mutants knocked down for variant 1 isoforms (A) and, if present (G), cell death is diffuse and limited to dorsolateral tissue. In *noi* mutants knocked down for variant 2&3 isoforms, cell death is invariably present, intense, and localized to the midline of the midbrain-hindbrain border region (H). Anterior is to the left (A-D) or to the top (E-F). Abbreviations: cd, cell death; mhb, midbrain-hindbrain border; ot, optic tectum. Scale bar, 75 µm (A, C), 50µm (E-H), 19 µm (B, D).

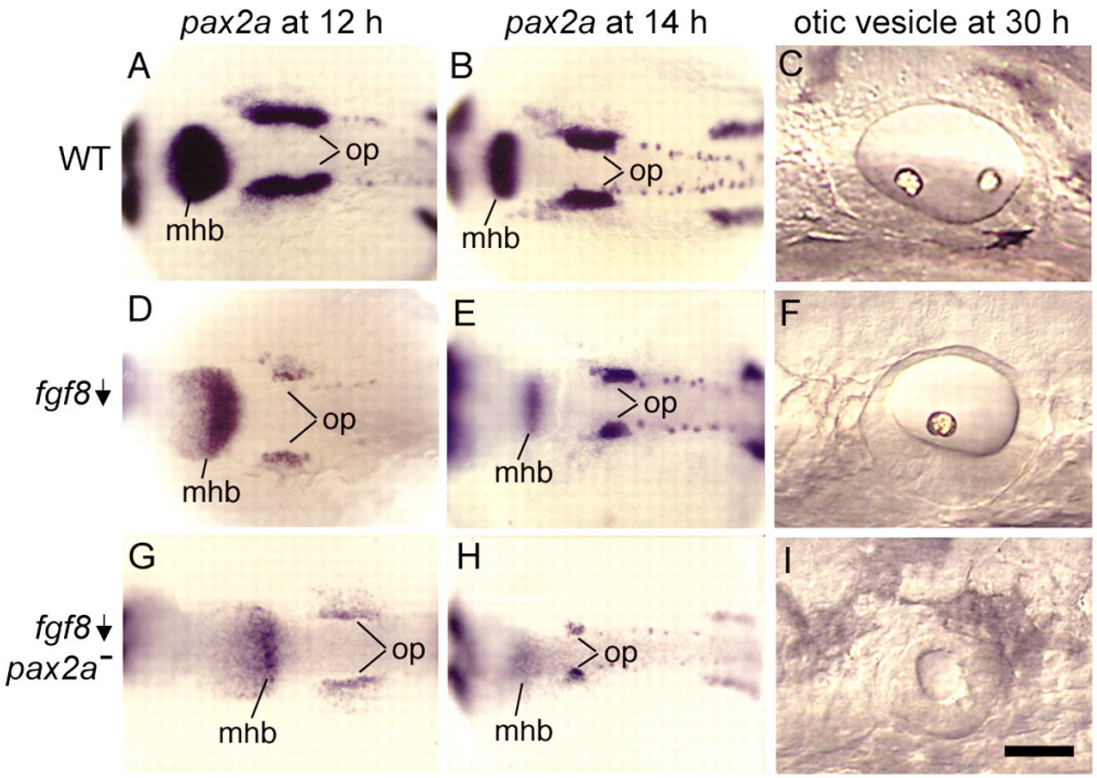


**Fig. 12.** *pax2a* interacts with *fgf8***.** Wild-type embryos (A-C), *ace* (*fgf8*) single mutants (D-F) and *ace-noi* (*fgf8-pax2a*) double mutants (G-I). Images show dorsal views of *pax2a* expression at 12 hpf (A, D, G) and 14 hpf (B, E, H), and lateral views of otic vesicles at 30 hpf (C, F, I). The specimen in B is the same as in Fig. 9A, and the specimen in C is the same as in Fig. 10B. Anterior is to the left in all specimens.
Abbreviations: mhb, midbrain-hindbrain border; op, otic placode. Scale bar, 170 µm (A, B, D, E, G, H) and 35 µm (C, F, I).

**Pax8 interaction with other transcription factors, *foxi1* and *dlx3b***

*foxi1* is one of the earliest regulators of preotic development identified (Nissen et al., 2003; Solomon et al., 2003). Loss of *foxi1* causes a severe phenotype characterized by production of very small otic vesicles or, in severe cases, complete loss of otic tissue. Expression of *pax8* in the otic domain is not detectable in *foxi1* mutants, presumably contributing to the mutant phenotype. Conversely, misexpression of *foxi1* is sufficient to induce ectopic expression of *pax8*, suggesting that Foxi1 serves as an upstream activator of *pax8* expression. To test this predicted epistatic relationship, I co-injected *foxi1*-MO and *pax8*-MO into wild-type embryos. Knockdown of *foxi1* and *pax8* causes defects in otic development that are indistinguishable from the effects of injecting *foxi1*-MO alone (Fig. 13A-F), supporting the notion that *foxi1* and *pax8* function in a simple linear pathway.

*dlx3b* is another early regulator of preotic development, and mutants homozygous for a deletion that removes *dlx3b* (as well as *dlx4b* and *sox9a*) show severe deficiency of otic tissue. However, they show nearly normal expression of *pax8* (Solomon and Fritz, 2002). Furthermore, early expression of *dlx3b* along the edges of the neural plate is independent of Fgf signaling and *pax8* function (Fig. 13). These and other data strongly suggest that *pax8* and *dlx3b* are at least initially in independent pathways. To investigate the epistatic relationship between these genes, embryos were co-injected with *dlx3b*-MO and *pax8*–MO. In *dlx3b-pax8* double morphant embryos, preotic domains of *dlx3b* and *pax2a* are reduced relative to those seen in embryos depleted for *dlx3b* or *pax8* alone (Fig. 13H, I, K, L). Otic vesicles are dramatically reduced in size and typically produce

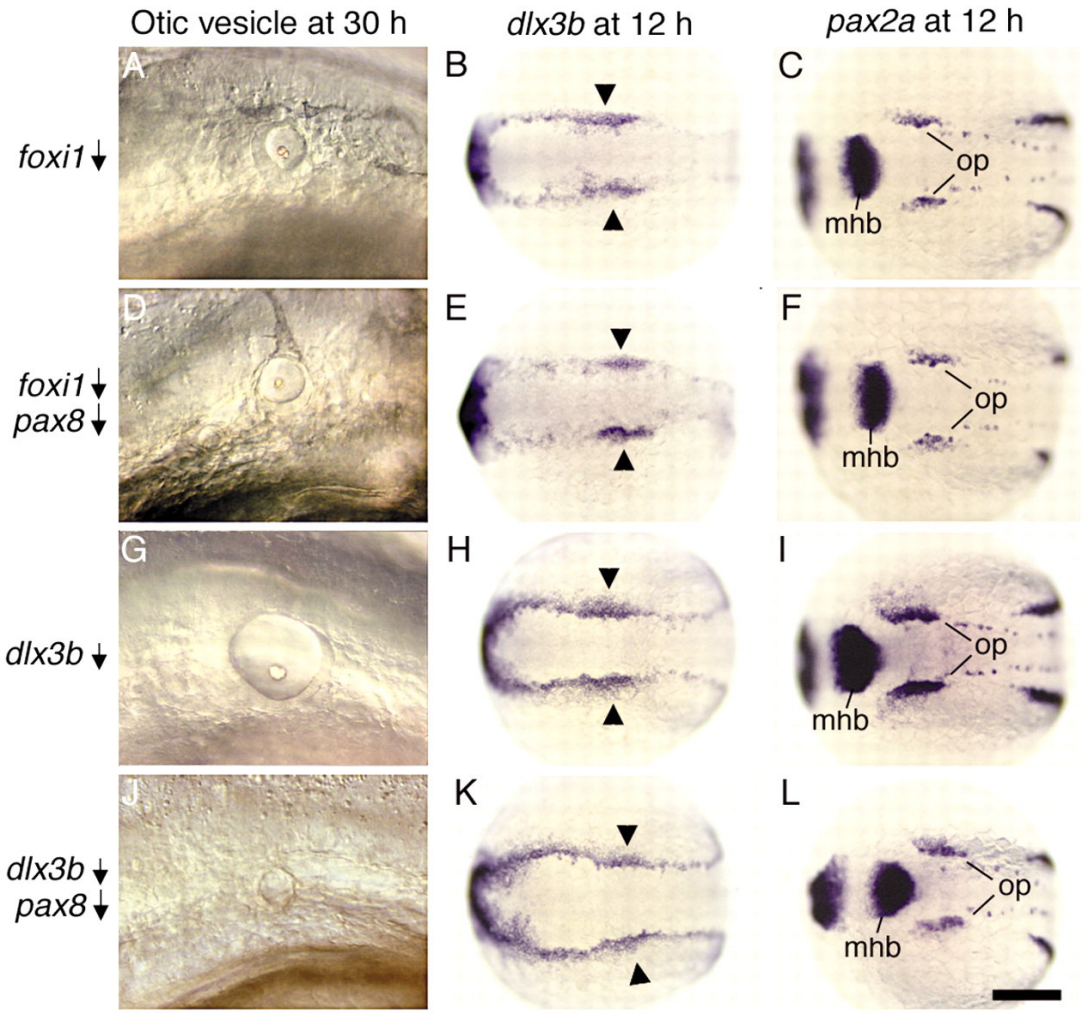


**Fig. 13**. *pax8* acts downstream of *foxi1* and in parallel with *dlx3b*. Wild-type embryos injected with *foxi1*-MO (A-C), *foxi1*-MO plus *pax8*-MO (D-F), *dlx3b*-MO (G-I), or *dlx3b*-MO plus *pax8*-MO (J-L). Images show lateral views of the otic vesicle at 30 hpf (A, D, G, J), or dorsal views of *dlx3b* expression at 12 hpf (B, E, H, K) and *pax2a* expression at 12 hpf (C, F, I, L). Anterior is to the left in all specimens. Abbreviations: mhb, midbrain-hindbrain border; op, otic placode. Arrowheads mark the otic region of *dlx3b* expression. Scale bar, 50 µm (A, D, G, J) and 200 µm (B, C, E, F, H, I, K, L).

no hair cells or otoliths (Fig. 13G, J; and data not shown), indicating severe deficiencies in otic differentiation. These findings show that *pax8* and *dlx3b* do not operate in a simple linear pathway.

## DISCUSSION

### Exonic structure of *pax8*

I have completed the *pax8* cDNA sequence and identified three main variants of transcripts with several subvariants present. While most features of the exon-intron structure are conserved with mammalian *Pax8*, the zebrafish sequence shows several unique features. Most significantly, I identified three main categories of splice variants that vary in their N-terminal sequences, leading to the use of two alternative start codons. The predicted ORF for variant 1 begins ten amino acids within the canonical paired domain and would presumably disrupt the DNA-binding ability of the N-terminal portion of this domain (Xu et al., 1995). Variants 2 and 3 encode proteins that contain the entire canonical paired domain. The paired domain comprises N-terminal and C-terminal subdomains, which mediate binding to distinct parts of a conserved DNA consensus sequence. Although no isoforms using alternate start codons have been identified in the mouse or human, one mammalian isoform, Pax8(S), contains an additional serine residue in the N-terminal subdomain. This insertion functionally

inactivates the N-terminal subdomain, causing Pax8(S) to bind a different DNA consensus sequence through its C-terminal subdomain, perhaps analogous to the zebrafish variant 1 vs. variant 2-3 isoforms. Pax8(S) accounts for roughly one-third of Pax8 produced in all tissues, extending the range of target genes potentially regulated by the *Pax8* locus (Kozmik et al., 1997). It is possible that the zebrafish isoform with an incomplete N-terminal subdomain has altered binding properties similar to mammalian Pax8(S). Interestingly, Fugu *pax8* also encodes a methionine at position 10 of the paired domain (Pfeffer et al., 1998), and thus may encode a set of Pax8 proteins similar to zebrafish. Although the exact functional differences between these isoforms remain to be elucidated, my data suggest that variant 1 and variant 2/3 isoforms appear to have both overlapping and unique functions as revealed by knockdown in the *noi* (*pax2*) mutant background.

At least six splice variants found in the mouse and human show changes in C-terminal sequences (Kozmik et al., 1993), and even more C-terminal variants are found in zebrafish. Other Pax8 functional domains, including the transactivation domain and the inhibitory domain, are disrupted in these isoforms. The functional significance of C-terminal variation is presently unknown; however, altering the structure of the functional domains may create proteins with altered DNA sequence specificity or varying transactivation potentials, as has been previously reported for other members of the zebrafish and mammalian *Pax* gene families (Barber et al., 1999; Barr et al., 1999; Epstein et al., 1994; Kozmik et al., 1997; Kozmik et al., 1993; Nornes et al., 1996; Puschel et al., 1992; Seo et al., 1998; Tavassoli et al., 1997; Vogan et al., 1996; Zwollo et

al., 1997). It should be noted that these alternatively spliced isoforms appear to be rare in zebrafish.

**Redundancy among *pax2* and *pax8* genes**

Knockdown of *pax8* causes significant reduction in the amount of otic tissue produced during induction, and the deficit persists through subsequent stages of otic development. The small vesicle that is eventually produced expresses regional markers normally but shows deficiencies in sensory epithelia. In severe cases, various maculae or cristae are missing or fused, possibly as a nonspecific consequence of the presence of too little otic tissue. The closely related genes *pax2a* and *pax2b* are expressed at slightly later stages of preotic development and appear to partially overlap in function with *pax8*. Disruption of both *pax2a* and *pax2b* function causes only subtle defects in otic development, suggesting that *pax8* can substantially compensate for their loss. When the function of all three *pax* genes is disrupted, otic tissue shows progressive diminution during placodal development and is lost entirely by 24 hpf. Staining with acridine orange does not reveal an obvious increase in otic cell death, suggesting that otic these cells eventually dedifferentiate in the absence of otic maintenance mediated by *pax2a, pax2b*, and *pax8*. This notion is further supported by the observation that the otic domain of *dlx3b* expression appears to be progressively lost beginning around 24 hpf. These data strongly support the hypothesis that *pax8* and *pax2* functions are partially redundant. A similar relationship among murine *Pax2/5/8* family members seems likely as well. *Pax8* and *Pax2* are expressed in the developing murine ear at the same relative stages as in

zebrafish (Pfeffer et al., 1998). No ear defects have been reported in *Pax8* knockout mice (Bouchard et al., 2002; Mansouri et al., 1998), and defects in *Pax2* knockout mice are limited to disturbances in medial otic vesicle development (Bouchard et al., 2000; Burton et al., 2004; Favor et al., 1996; Torres et al., 1996). Otic development has not yet been described in *Pax8-Pax2* double knockout mice, but it seems likely that much more severe otic defects will result in such embryos. Indeed, such has been observed with respect to kidney development (Bouchard et al., 2002). The developing kidney undergoes apoptotic cell death at an early stage in *Pax8-Pax2* double mutants, a phenotype not observed in either of the single mutants (Bouchard et al., 2002).

### *pax8* as part of a genetic network

Induction of *pax8* expression requires at least two distinct pathways, one mediated by *foxi1* and the other by Fgf signaling (Leger and Brand, 2002; Maroon et al., 2002; Nissen et al., 2003; Phillips et al., 2001; Solomon et al., 2003; Solomon et al., 2004). These inductive pathways are partially independent, but some aspects of *foxi1* expression appear to be regulated by Fgf signaling. *foxi1* is initially expressed in ventral ectoderm but then shows upregulation in periotic ectoderm roughly 30-60 minutes before induction of *pax8*. The spatial pattern of *foxi1* expression is unaltered in embryos depleted for Fgf3 and Fgf8 (Solomon et al., 2004), but misexpression of *fgf3* or *fgf8* is sufficient to induce *foxi1* expression in ectopic locations (Phillips et al., 2004). It is possible that *foxi1* is sensitive to residual Fgf signaling in *fgf* morphants or, alternatively, Fgf3 and Fgf8 may act in concert with other factors to regulate *foxi1*. In any case,

expression of *pax8* occurs in the region where *foxi1* and Fgf signaling overlap, and serves as an important nexus linking these pathways.

My data also indicate that *pax8* positively regulates its own expression since the level of *pax8* expression is reduced in *pax8* morphants. I speculate that *pax8* helps mediate otic induction and that this feedback loop magnifies the efficacy of Fgf signaling, extending the range of Fgf action to cells farther from the source. Thus, loss of *pax8* would be expected to limit otic induction to cells in close proximity to the signaling source, a prediction borne out by my studies. Subsequent expression of *pax2a* and *pax2b*, which require Fgf signaling but not *pax8*, presumably stabilizes otic fate within the diminished population of preotic cells. Such a model could explain why eliminating *Pax8* in the mouse has such mild consequences; in the mouse, *Fgf3* is expressed directly within preotic cells, making the need for signal amplification less critical during initial stages of otic induction. Later expression of *Pax2* might then be sufficient to stabilize otic development initiated by prior Fgf signaling.

A number of other transcription factors have been implicated in early otic development, the best characterized of which are *dlx3b* and *dlx4b*. *dlx3b/4b* are initially expressed in ventral ectoderm but become restricted by 9 hpf to a contiguous line of cells surrounding the neural plate (Akimenko et al., 1994). By 11 hpf, *dlx3b/4b* show strong upregulation in preotic cells. The early phases of *dlx3b/4b* expression are independent of Fgf signaling, but later upregulation in the otic anlagen fails to occur in embryos depleted for Fgf3 and Fgf8 (Liu et al., 2003; Solomon, 2004); (this report). As such, *dlx3b* and *dlx4b* could serve as another mediator of Fgf signaling (Solomon, 2004).

Knockdown of either *dlx* gene causes mild to moderate deficiencies in otic development, with much more severe deficiencies seen in embryos knocked down for both (Liu et al., 2003; Solomon and Fritz, 2002). Embryos homozygous for a deletion that removes *dlx3b, dlx4b* and *sox9a* (a third preotic marker under control of Fgf signaling) fail to produce an ear, although roughly one-third of mutant embryos produce a few disorganized otic cells that belatedly express *pax2a*. This severe disruption occurs despite the fact that *pax8* is initially expressed normally (Solomon and Fritz, 2002). Thus, *pax8* is clearly not sufficient to sustain early otic development. Other transcription factors also play crucial roles during otic induction.

In this study, I have shown that knockdown of both *pax2a* and *pax8* causes much more severe loss of ear tissue than knocking down either alone. I have previously shown that *foxi1*, which is required for *pax8* expression in the otic domain, and *dlx3b* act in parallel pathways in early otic placode formation and show a strong synergistic genetic interaction (Solomon, 2004). The *pax8-dlx3b* morphant analysis confirms these previous results and furthermore suggests that a significant aspect but not all of *foxi1* function is mediated by *pax8*. Thus, there appear to be multiple regulatory genes that respond to Fgf signaling and help mediate its effects. Each is likely to control both redundant and specific functions; hence there is neither a single `master regulator', analogous to the role played by *pax6/eyeless* during eye development, nor an `all-or-none' combinatorial code required for otic induction. This model partly accounts for the remarkable resilience and regulative capacity of the developing inner ear (Baker and Bronner-Fraser, 2001; Noramly and Grainger, 2002; Riley and Phillips, 2003; Torres and Giraldez, 1998). A

similar series of experiments involving *pax2-pax8, dlx3b, foxi1, fgf3-fgf8* and *sox9* genes has been performed by Hans and colleagues (Hans et al., 2004). They propose a model that fully agrees with the findings and conclusions presented here (Hans et al., 2004), as well as the model proposed by Solomon et al. (Solomon et al., 2004).

# CHAPTER III

# AN EXPANDED DOMAIN OF Fgf3 EXPRESSION IN THE HINDBRAIN OF ZEBRAFISH *valentino* MUTANTS RESULTS IN MISPATTERNING OF THE OTIC VESICLE *

## INTRODUCTION

Development of the inner ear requires interactions with adjacent hindbrain tissue. Many studies have shown that the hindbrain can induce otic placodes in adjacent ectoderm (Stone, 1931; Yntema, 1933; Harrison, 1935; Waddington, 1937; Jacobsen, 1963; Gallagher et al., 1996; Woo and Fraser, 1998; Groves and Bronner-Fraser, 2000). A number of the relevant hindbrain signals have recently been identified (reviewed by Whitfield et al., 2002). In zebrafish, two members of the Fgf family of signaling molecules, Fgf3 and Fgf8, are expressed in the anlagen of rhombomere-4 (r4) during late gastrulation when induction of the otic placode begins (Reifers et al., 1998; Phillips et al., 2001; Maroon et al., 2002). At this time, *pax8* is induced in the adjacent otic anlagen

---

* Reprinted from "An expanded domain of Fgf3 expression in the hindbrain of zebrafish *valentino* mutants results in mis-patterning of the otic vesicle."; by **Kwak, S.J., Phillips, B.T., Heck, R. and Riley, B.B**., 2002, *Development* **129**, 5279-5287.

. Disruption of both *fgf3* and *fgf8* prevents induction of the otic placode, and conditions that expand the expression domains of these genes lead to production of supernumerary or ectopic otic vesicles (Phillips et al., 2001; Raible and Brand, 2001; Vendrell et al., 2001; Maroon et al., 2002). In addition, disruption or depletion of *Fgf3* perturbs inner ear development in chick and mouse (Represa et al., 1991; Mansour et al., 1993) and misexpression of *Fgf3* in chick is sufficient to induce ectopic otic vesicles (Vendrell et al., 2000). It has also been shown that chick Fgf19, which is expressed in a pattern similar to that of Fgf3 (Mahmood et al., 1995), cooperates with the hindbrain factor Wnt8c to induce a range of otic placode markers in tissue culture (Ladher et al., 2000). Thus, multiple hindbrain factors are involved in otic placode induction, and Fgf signaling plays an especially prominent role.

Much less is known about the role played by hindbrain signals in later stages of inner ear development. Experiments in chick embryos show that rotation of the early otic vesicle about the anteroposterior axis reorients gene expression patterns in a manner suggesting that proximity to the hindbrain influences differentiation of cells within the otic vesicle (Wu et al., 1998; Hutson et al., 1999). In zebrafish, *Xenopus*, chick, and mouse embryos, *Fgf3* continues to be expressed in the hindbrain after otic placode induction (Mahmood et al., 1995, 1996; McKay et al., 1996; Lombardo et al., 1998; Phillips et al., 2001). This raises the question of whether this factor also helps regulate subsequent development of the otic placode or otic vesicle.

Analysis of the *valentino* (*val*) mutant in zebrafish provides indirect evidence that hindbrain signals are necessary for normal development of the otic vesicle (Moens et al.,

1996, 1998). *val* encodes a bZip transcription factor that is normally expressed in r5 and r6. *val/val* mutants produce an abnormal hindbrain in which the r5/6 anlagen fails to differentiate properly and gives rise to a single abnormal segment, rX, which shows confused segmental identity. Although the *val* gene is not expressed in the inner ear, *val/val* mutants produce otic vesicles that are small and malformed. Since otic induction appears to occur normally in *val/val* mutants (Mendonsa and Riley, 1999), I infer that altered hindbrain patterning perturbs signals required for later aspects of otic development. Mice homozygous for a mutation in the ortholologous gene, *kreisler*, also show later defects in development of the otic vesicle (Deol, 1964; Cordes and Barsh, 1994). The inner ear defects in *kreisler* mutants are thought to result from insufficient expression of *Fgf3* in the hindbrain (McKay et al., 1996). In contrast to zebrafish, mouse *Fgf3* is initially expressed at moderate levels in the hindbrain from r1 through r6. As development proceeds, expression downregulates in the anterior hindbrain but upregulates in r4 (Mahmood et al., 1996). After formation of the otic placodes, *Fgf3* expression also upregulates in r5 and r6. This upregulation fails to occur in *kreisler* mutants, possibly accounting for subsequent patterning defects in the inner ear (McKay et al., 1996).

To examine the relationship between hindbrain and otic vesicle development in zebrafish, I have examined patterning of these tissues in wild-type and *val/val* mutant embryos. I find that *val/val* mutants produce excess and ectopic hair cells at virtually any position in the epithelium juxtaposed to the hindbrain. Expression of the anterior otic markers *nkx5.1* and *pax5* is also seen ectopically throughout this region of the otic

vesicle. Conversely, expression of the posterior marker *zp23* is ablated in *val/val* embryos. Analysis of hindbrain patterning shows that *fgf3* is misexpressed in the rX region of *val/val* mutants. Disruption of *fgf3* function by injection of an antisense morpholino oligomer blocks formation of ectopic hair cells and suppresses A-P patterning defects in the otic vesicle of *val/val* mutants. In contrast, *fgf8* is expressed normally in *val/val* embryos, and loss of *fgf8* does not suppress the inner ear defects caused by the *val* mutation. These data indicate that the expanded domain of *fgf3* plays a crucial role in the etiology of inner ear defects in *val/val* mutants and suggest that Fgf3 secreted by r4 normally specifies anterior fates, suppresses posterior fates, and stimulates hair cell formation in the anterior of the otic vesicle.

## MATERIALS AND METHODS

### Strains

Wild-type embryos were derived from the AB line (Eugene, OR). Mutations used in this study were *valentino* (*val*$^{b337}$) and *acerebellar* (*ace*$^{ti282a}$). Both of mutations were induced with ENU and are thought to be functional null alleles (Moens et al., 1996, 1998; Brand et al., 1998). Embryos were developed at 28.5ºC in water containing 0.008% Instant Ocean salts. Embryonic ages are expressed as hours post-fertilization (h).

**Identification of mutant embryos**

Live *val/val* homozygotes were reliably identified after 19 h by the small size and round shape of the otic vesicle. In addition, fixed *val/val* embryos stained for *pax2a*, *pax5*, or *zp23* showed characteristic changes in posterior hindbrain patterning. At earlier stages, *val/val* mutants were identified by loss of *krox20* staining in rhombomere 5 (Moens et al., 1996). Live *ace/ace* mutants were readily identified after 24 h by the absence of a midbrain-hindbrain border and enlarged optic tectum (Brand et al., 1996). In addition, *ace/ace* specimens that were fixed and stained for *pax2a* or *pax5* showed no staining in the midbrain-hindbrain border. At earlier stages (14 h), *ace/ace* mutants were identified by loss of *fgf3* expression in the midbrain-hindbrain border.

**Whole-mount immunofluorescent staining**

Embryos were fixed in MEMFA (0.1 M MOPS at 7.4, 2 mM EGTA, 1 mM $MgSO_4$, 3.7% formaldehyde) and stained as previously described (Riley et al., 1999). Primary antibodies used in this study were: Polyclonal antibody directed against mouse Pax2 (Berkeley Antibody Company, 1:100 dilution), which also recognizes zebrafish Pax2a (Riley et al., 1999); Monoclonal antibody directed against acetylated tubulin (Sigma T-6793, 1:100), which binds hair cell kinocilia (Haddon and Lewis, 1996). Secondary antibodies were Alexa 546 goat anti-rabbit IgG (Molecular Probes A-11010, 1:50) or Alexa 488 goat anti-mouse IgG (Molecular Probes A-11001, 1:50).

**Whole-mount in situ hybridization**

Whole-mount in situ hybridization was performed as described (Stachel *et al*., 1993) using riboprobes for *fgf*3 (Kiefer et al., 1996b), *fgf8* (Reifers et al., 1998), *dlA* (Appel and Eisen, 1998; Haddon et al., 1998b), *pax5* (Pfeffer et al., 1998), *dlx3* and *msxC* (Ekker et al., 1992a, b), *nkx5.1* (Adamska et al., 2000), *otx1* (Li et al., 1994), and *zp23* (Hauptmann and Gerster, 2000). Two color in situ hybridization was performed essentially as described by Jowett (1996) with minor modifications (Phillips et al., 2001).

**Morpholino Oligomer Injection**

*fgf3*-specific morpholino oligomer obtained from Gene Tools Inc. was diluted in Danieaux solution (58 mM NaCl, 0.7 mM KCl, 0.4 mM $MgSO_4$, 0.6 mM $Ca(NO_3)_2$, 5.0 mM HEPES, pH 7.6) to a concentration of 5 µg/µl as previously described (Nasevicius and Ekker, 2000; Phillips et al., 2001). Approximately 1 nl (5 ng *fgf3*-MO) was injected into the yolk cell at the 1- to 2-cell stage.

**Misexpression of *val***

Wild-type *val* was ligated into pCS2 expression vector by Andrew Waskiewicz (Cecilia Moens' lab) and was kindly provided as a gift. RNA was synthesized in vitro and approximately 1 ng of RNA was injected into the yolk of cleaving embryos at the 1- to 4-cell stage.

# RESULTS

## Altered patterns of hair cells in *val/val* mutants

*val/val* mutants produce small otic vesicles with shortened antero-posterior axes but relatively normal dorso-ventral axes. This gives the mutant ear a characteristic circular shape that is quite distinct from the ovoid shape of the wild-type ear. This is thought to arise secondarily from abnormal development of the hindbrain (Moens et al., 1998), signals from which are required for normal ear development. To test this idea directly, I characterized early patterning of the otic vesicle and hindbrain in *val/val* mutants. In *val/val* mutants, the size, number, and distribution of otoliths in the inner ear vary considerably (Fig. 14A, B). In wild-type embryos, otoliths form only at the anterior and posterior ends of the otic vesicle where they attach to the kinocilia of tether cells (Fig. 14C; Riley et al., 1997). Tether cells are the first hair cells to form and occur in pairs at both ends of the nascent otic vesicle where they facilitate localized accretion of otolith material. The supernumerary and ectopic otoliths observed in *val/val* embryos were each associated with pairs of tether cells, as seen in live embryos under DIC optics (not shown). Visualizing tether cells by their expression of *deltaA* (Haddon et al., 1998a; Riley et al., 1999) confirms that *val/val* mutants produce excess and ectopic tether cells (Fig. 14D). In both wild-type and *val/val* embryos, tether cells acquire the morphology of mature hair cells by 22 h (Riley et al., 1997, and data not shown) and can be visualized by nuclear staining with anti-Pax2 antibody. This antibody was originally directed against mouse Pax2 but also binds zebrafish Pax2a, which is preferentially

expressed in maturing hair cells (Riley et al., 1999). Because of the unusual positions of some hair cells in *val/val* mutants, their cell type identity was confirmed in some specimens by staining with anti-acetylated tubulin, which labels hair cell kinocilia (Haddon and Lewis, 1996). This confirmed the presence of excess and ectopic hair cells at 24 h in *val/val* mutants (Figs. 14F). *val/val* mutants continue to show greater numbers of hair cells than wild-type embryos through at least 33 h (Fig. 15, Table 2 on page 88). In addition, ectopic patches of hair cells continue to develop between the anterior and posterior maculae in most *val/val* mutants (Fig. 14G). However, the spatial distribution of hair cells varies widely from one specimen to the next (Figs. 14G, I-K). In general, hair cells can emerge at any position along the ventro-medial surface of the otic vesicle in *val/val* mutants, unlike wild-type embryos in which hair cells are restricted to the anterior (utricular) and posterior (saccular) maculae. These data suggest that the signal(s) that normally regulate the location and number of hair cells are misregulated in *val/val* mutants, an interpretation further supported by analysis of Fgf expression in the hindbrain (see below).

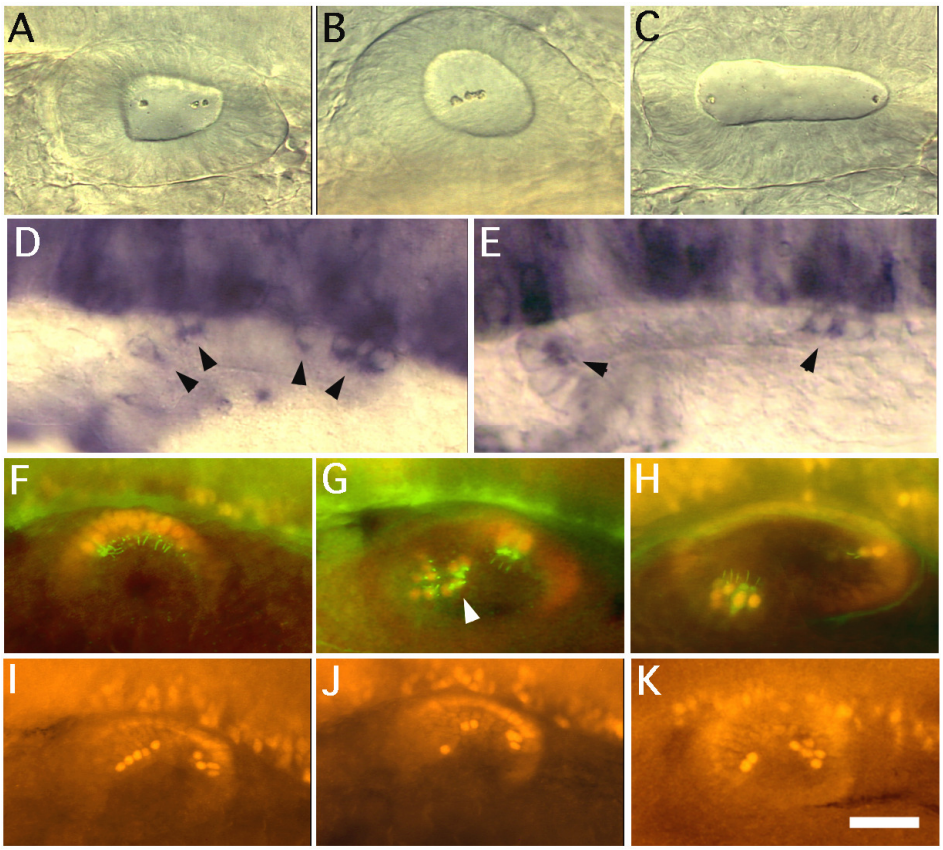


**Fig. 14.** Patterns of hair cells in the otic vesicle**.** Lateral view of otic vesicles of live *val/val* (A, B) and wild-type (C) embryos viewed under DIC optics at 21h. *val/val* mutants have small, round otic vesicles, and otoliths vary in number and position. (D, E) Dorsolateral view of *deltaA* expression in the otic vesicle at 19 h in *val/val* (D) and wild-type (E) embryos. Arrowheads indicate nascent tether cells. (F-H) Dorsolateral view of otic vesicles showing hair cells stained with anti-Pax2 (red) and anti-acetylated tubulin (green) antibodies. (F) *val/val* mutant at 24 h. Seven hair cells are distributed along the length of the anteroposterior axis of the otic vesicle. (G) *val/val* mutant at 30 h. An ectopic patch of hair cells (arrowhead) is evident between the anterior and posterior maculae. (H) wild-type embryo at 30 h. (I-K) Dorsolateral view of *val/val* mutants at 27 h stained with anti-Pax2 to visualize hair cell nuclei. The number and distribution of hair cells are variable. Anterior is to the left in all specimens. Scale bar, 20 µm (A-C), 15 µm (D, E), 30 µm (F-H), or 40 µm (I-K).

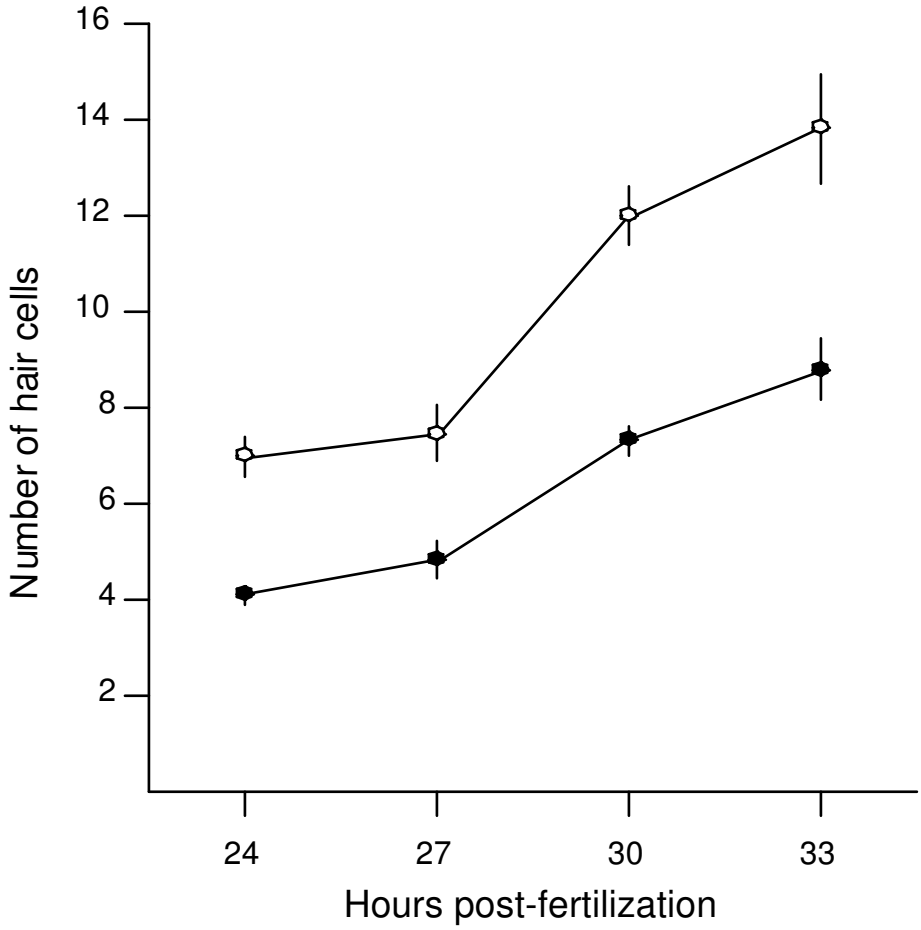


**Fig. 15.** Time course of hair cell formation in the otic vesicle. Embryos were fixed at the indicated times and hair cells were visualized by Pax2 staining. Each datum is the mean number of hair cells per ear (± standard deviation) of 10 or more specimens. *val/val* mutants produce excess hair cells throughout the time course. Symbols: (●) wild-type and (○) *val/val* embryos.

**Altered antero-posterior patterning in *val/val* mutants**

I next examined expression of various otic markers to further characterize altered patterning in *val/val* embryos. Expression of *pax5* is first detectable in the inner ear at 17.5-18 h (Pfeffer et al., 1998). This expression domain is normally restricted to the anterior part of the otic vesicle adjacent to r4 and is maintained through at least 30 h (Fig. 16A, C). In *val/val* embryos, *pax5* expression extends along the entire length of the medial wall of the otic vesicle (Fig. 16B, D). Another anterior marker, *nkx5.1*, is also expressed throughout the medial wall of the otic vesicle in *val/val* mutants (Fig. 16F). In contrast, *zp23* is normally expressed in posterior medial cells adjacent to r5 and r6 in the wild-type but is not detectably expressed in *val/val* embryos (Fig. 16G, H). Otic patterning is not globally perturbed, however. Mutant embryos show a normal pattern of *dlx3* expression in the dorso-medial epithelium (Fig. 17F). Similarly, *otx1* is expressed normally in ventral and lateral cells of *val/val* mutants (Fig. 17A-D). Based on studies in mouse, the dorsal and lateral domains of *dlx3* and *otx1* probably help regulate development of the semicircular canals and sensory cristae (Depew at al., 1999; Krauss and Lufkin, 1999; Morsli et al., 1999; Mazan et al., 2001). It was previously reported that formation of semicircular canals is totally disrupted in *val/val* mutants (Moens et al., 1998). However, I find that this is a highly variable phenotype, ranging from grossly abnormal morphogenesis to nearly normal patterning at day 3 (Fig. 17G-I). Morphology typically becomes increasingly aberrant with time, possibly resulting from improper regulation of endolymph, as seen in *kreisler* mutant mice (Deol, 1964; Brigande et al., 2000; see Discussion). Regardless of whether semicircular canals develop properly,

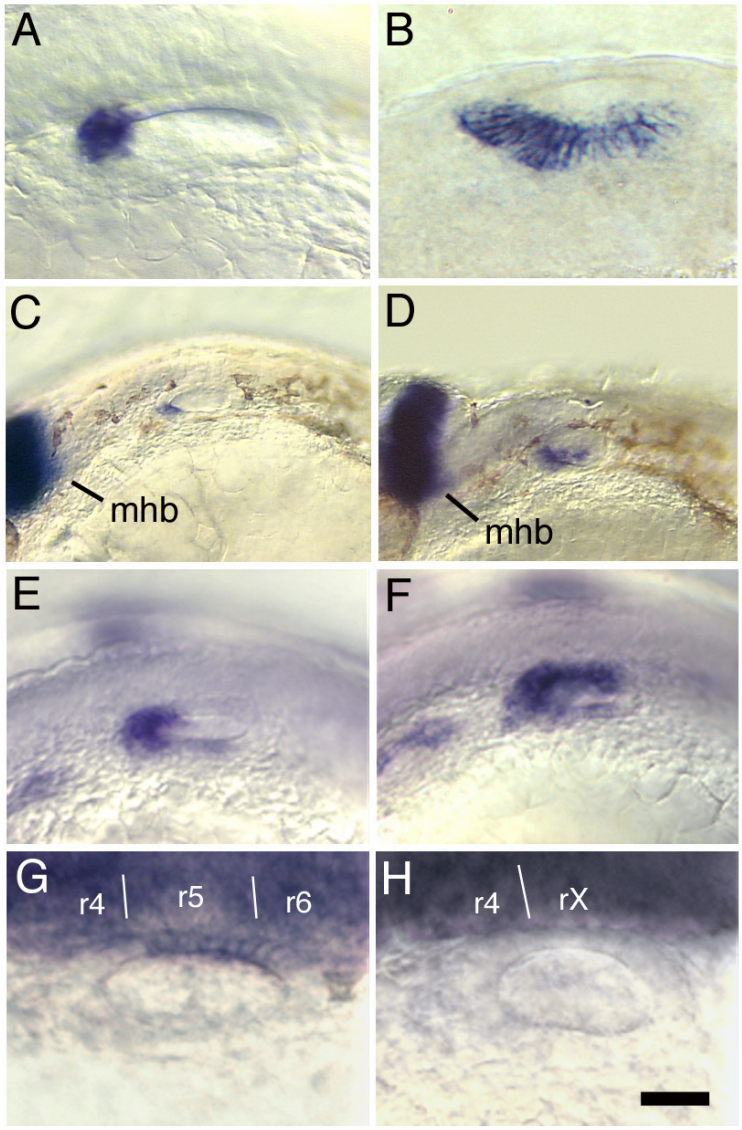


**Fig. 16.** Expression of A-P markers in the inner ear. Lateral or dorsolateral views of the otic vesicle (anterior to the left). (A-D) *pax5* expression at 24 h (A, B) and 30 h (C, D). Staining is limited to the anterior end of the otic vesicle in wild-type embryos (A, C) but is greatly expanded in *val/val* mutants (B and D). The midbrain-hindbrain border (mhb) is indicated. (E, F) Expression of *nkx5.1* at 24 h in wild-type (E) and *val/val* (F) embryos. Expression is expanded posteriorly in *val/val* mutants. (G, H) Expression of *zp23* at 24 h in wild-type (G) and *val/val* (H) embryos. No expression is detectable in the ear in *val/val* mutants. Relative positions of rhombomeres are indicated. Scale bar, 25 µm (A, B, G, H), 75 µm (C, D), or 50 µm (E, F).

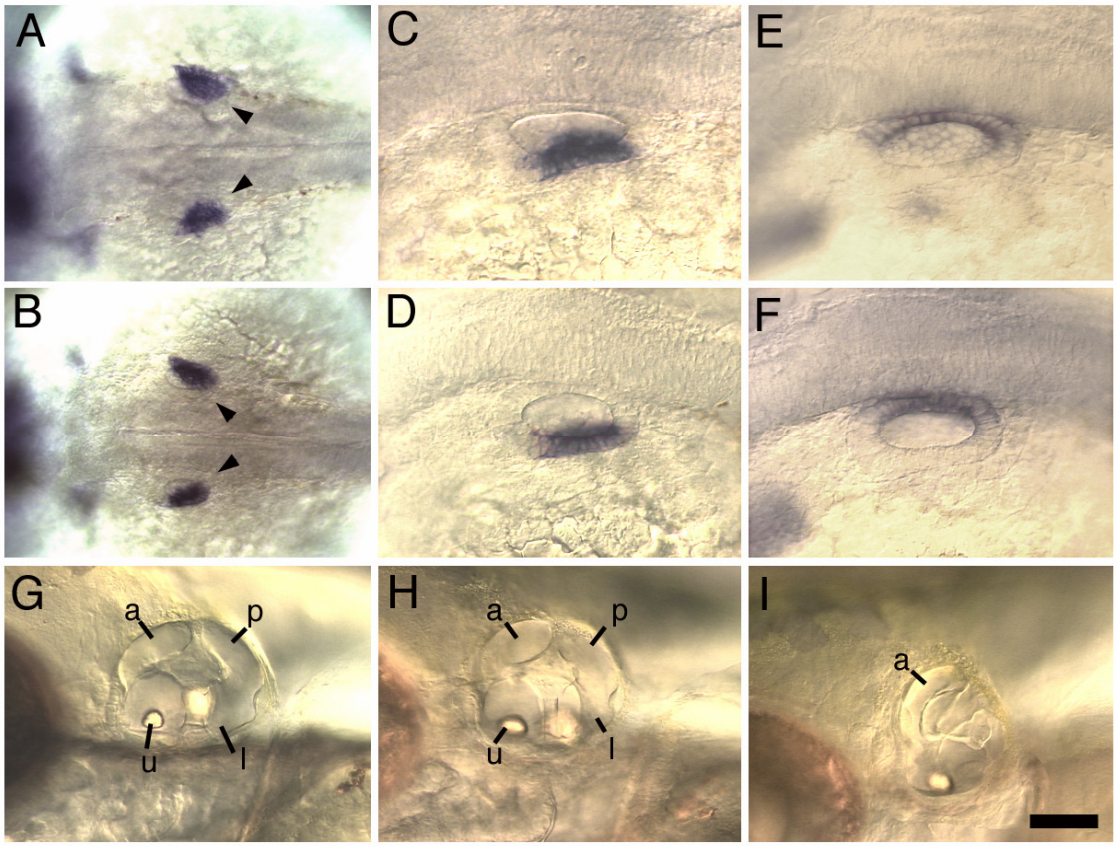


**Fig. 17.** D-V and M-L patterning in the inner ear. (A-D) Expression of *otx1* at 24 h in wild-type (A, C) and *val/val* (B, D) embryos. Dorsal views (A, B) show expression in the lateral epithelium of the otic vesicle (arrow heads), and lateral views (C, D) show expression in the ventral epithelium. (E, F) Dorsolateral views showing expression of *dlx3* at 24 h in wild-type (E) and *val/val* (F) embryos. Gene expression patterns are normal. (G-I) Lateral views of the inner ear at 72 h in wild-type (G) and *val/val* (H, I) embryos. Morphology ranges from nearly normal to highly aberrant. Anterior is to the left in all specimens. Abbreviations: a, anterior semicircular canal; l, lateral semicircular canal; p, posterior semicircular canal; u, utricle. Scale bar, 100 µm (A, B, G-I) or 50 µm (C-F).

all three sensory cristae are produced and express *msxC* (data not shown). Thus, some aspects of axial patterning are relatively normal in *val/val* embryos at early stages, and the only consistent defect is that medial cells abutting the hindbrain all show anterior character. This is consistent with the hypothesis that factors locally expressed in the hindbrain regulate anterior-posterior fates in the medial wall of the otic vesicle, and that such factors are misregulated in the rX region of *val/val* mutants. Such misexpression could also explain the abnormal pattern of hair cells produced in *val/val* mutants.

**Expression of *fgf3* and *fgf8* in the *val/val* hindbrain**

Fgf3 and Fgf8 are both expressed in the r4 anlagen during late gastrulation and cooperate to induce the otic placode (Phillips et al., 2001). I hypothesized that persistent expression of one or both of these factors in r4 plays a later role in patterning the otic placode and vesicle. In both wild-type and *val/val* embryos, *fgf8* is expressed at high levels in r4 at 12 h (Fig. 18A, B) but is downregulated by 14 h (not shown). This argues against a role for Fgf8 in the etiology of the inner ear phenotype in *val/val* embryos. In contrast, *fgf3* expression shows a consistent difference between *val/val* and wild-type embryos. In the wild-type, hindbrain expression of *fgf3* is restricted to r4 and is maintained through at least 18 h when the otic vesicle forms (Fig. 18C, E, and data not shown). In *val/val* mutants, *fgf3* shows similar developmental timing but is expressed in an expanded domain extending from r4 through rX (Fig. 18D, F). Within rX, the level of expression falls off gradually towards the posterior such that there is no clear posterior limit of expression. Ectopic expression of *fgf3* in *val/val* embryos is first

detectable at 10 h, corresponding to the time when *val* normally begins to function in the r5/6 anlagen (data not shown). Initially, ectopic expression of *fgf3* in rX is much weaker than in r4. Expression in rX subsequently increases to a level similar to that seen in r4 by 12 h (Fig 18D). These data suggest that expansion of the domain of *fgf3* in the hindbrain could play a role in misexpression of A-P markers and production of ectopic hair cells in the inner ear.

The above data also suggest that *val* normally functions, directly or indirectly, to exclude *fgf3* expression from r5/6. To explore this more fully, I examined the effects of *val* misexpression by injecting *val* RNA into wild-type embryos. In more than half (55/98) of *val*-injected embryos, hindbrain expression of *fgf3* was dramatically reduced or ablated (Fig. 19A, B). Similar effects were seen at 10, 12, and 14 h (data not shown). At 24 h, otic vesicles were usually small (15/64) or totally ablated (36/64) (Fig. 19C, D). Disrupting *fgf3* by itself impairs, but does not ablate, otic tissue (Phillips et al., 2001; Vendrell et al., 2001; Maroon et al., 2002). This indicates that *val* misexpression affects other processes in addition to *fgf3* expression. Indeed, ubiquitous misexpression of *val* frequently caused truncation of the trunk and tail (46/64, Fig. 19C) and could therefore impair mesendodermal signals on which otic development relies (reviewed by Whitfield et al., 2002). However, even amongst embryos with normal axial development, about half showed partial loss of *fgf3* expression (5/10) and impaired otic development (18/34). In many of these cases, these defects were limited to one side of

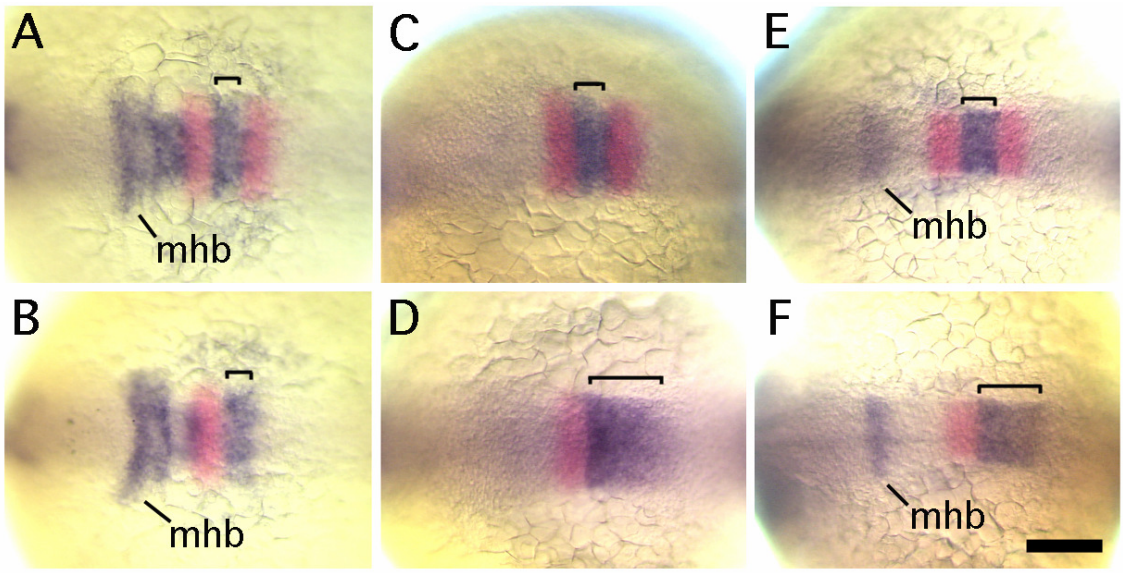


**Fig. 18.** Expression of *fgf8* and *fgf3* in the hindbrain. Dorsal view (anterior to the left) of specimens double stained for *fgf* gene expression (blue) and *krox-20* (red). Loss of *krox20* staining in r5 identifies *val/val* mutants. (A, B) *fgf8* expression at 12 h in wild-type (A) and *val/val* (B) embryos. Brackets indicate the r4 domain of *fgf8*. No change is detected in the mutant. (C, D) *fgf3* expression at 12 h in wild-type (C) and *val/val* (D) embryos. (E, F) *fgf3* expression at 14 h in wild-type (E) and *val/val* (F) embryo. Brackets indicate the domain of *fgf3* corresponding to either r4 (C, E) or r4 though rX (D, F). *fgf3* is ectopically expressed in the rX region in *val/val* embryos. Scale bar, 80 µm.

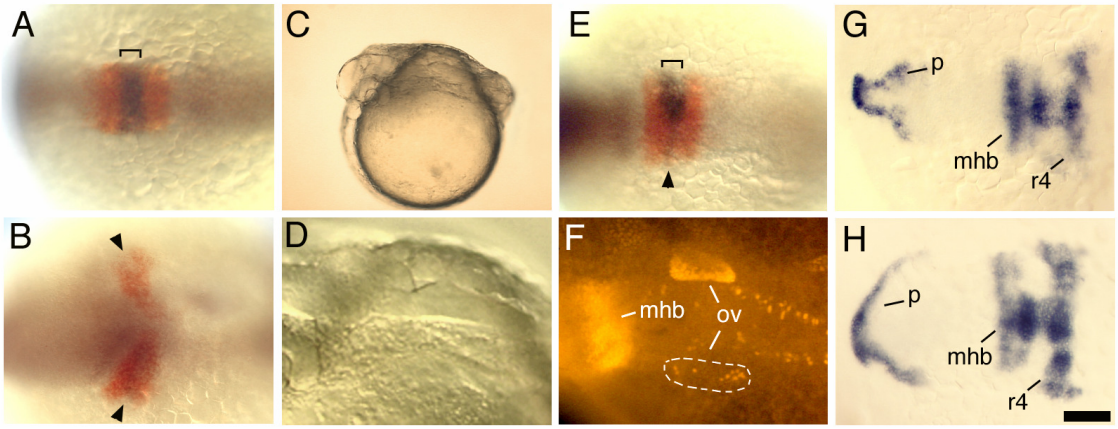


**Fig. 19.** Effects of misexpressing *val*. (A, B) Dorsal views showing expression of *fgf3* (blue) and *krox20* (red) at 14 h in a normal embryo (A) and an embryo injected with *val* RNA (B). The val-injected embryo shows little or no *fgf3* expression in the r4 domain (arrowheads) and has undergone less convergence than normal. (C, D) Lateral view of a *val*-injected embryo at 24 h. Trunk and tail tissues are ablated (C) and no otic vesicle is visible (D). (E, F) Dorsal views of *val*-injected embryos with relatively normal axial development. (E) Expression of *fgf3* (blue) and *krox20* (red) at 14 h. The left side of r4 shows little *fgf3* expression (arrowhead) whereas the right side is nearly normal (bracket). (F) Expression of *pax2a* at 24 h in the midbrain-hindbrain border (mhb) and otic vesicles (ov). The left otic vesicle (dashed circle) is severely disrupted. (G, H) Expression of *fgf8* at 12 h in a normal wild-type embryo (G) and a *val*-injected embryo (H). The *val*-injected embryo has a truncated axis (not shown) and has undergone less convergence than normal. Nevertheless, *fgf8* is expressed relatively normally in the prechordal plate (p), midbrain-hindbrain border (mhb), and rhombomere 4 (r4). Anterior is to the left in all panels. Scale bar, 100 µm (A, B, D-H) or 250 µm (C).

the embryo (Fig. 19E, F), possibly resulting from variation in the amount of RNA inherited by early cleavage stage blastomeres. In contrast to *fgf3*, expression of *fgf8* was relatively normal in most (82/85) *val*-injected embryos, even those with axial truncations (Fig. 19H). These data support the hypothesis that *val* specifically represses *fgf3* expression in the hindbrain. This is in sharp contrast to the function of the mouse homolog *kreisler*, which is required to activate high level expression of *Fgf3* in r5 and r6 (McKay et al., 1996). Such species differences may have been important for evolutionary changes in inner ear structure and function (see Discussion).

**Dependence of inner ear patterning on Fgf3**

To test the role of Fgf3 in otic vesicle patterning, embryos were injected with *fgf3*-MO, an antisense oligomer that specifically inhibits translation of *fgf3* mRNA (Nasevicius and Ekker, 2000; Phillips et al., 2001; Maroon et al., 2002). Injection of *fgf3*-MO into wild-type embryos results in a range of defects with varying degrees of severity (Phillips et al., 2001). The size of otic vesicle is usually reduced and about half (42/86) of Fgf3-depleted wild-type embryos show little or no *pax5* expression in the inner ear (Fig. 20A). Expression of *nkx5.1* is also reduced or ablated in the otic vesicle and vestibulo-acoustic ganglion in about half (30/62) of injected wild-type embryos (data not shown). In contrast, expression of *zp23* often expands anteriorly in the otic vesicle to include medial cells adjacent to r4 (21/32 embryos, Fig. 20D). Hair cell production is reduced by up to 70% in severely affected embryos (Fig. 20G; Table 2 on page 88, note range of data). Injection of *fgf3*-MO into *val/val* mutants leads to further reduction in the size of otic

vesicle. Expression of *pax5* is strongly reduced in most cases: In one experiment, 37% (26/71) showed *pax5* expression limited to the anterior of the otic vesicle (Fig. 20B), and 38% (27/71) showed no detectable expression (Fig. 20C). Similarly, *nkx5.1* is strongly reduced or ablated in about half (16/30) of injected *val/val* embryos (Fig. 20F). Most (12/15) *val/val* embryos injected with *fgf3*-MO express *zp23* in the otic vesicle, including tissue adjacent to r4 (Fig. 19E). Hair cell production is reduced to a level comparable to that seen in Fgf3-depleted wild-type embryos (Table 2 on page 88). In addition, depletion of Fgf3 prevents formation of ectopic hair cells in the majority (19/25) of *val/val* embryos (Fig. 20H, I). Thus, Fgf3-depletion prevents formation of excess and ectopic hair cells as well as misexpression of A-P markers in *val/val* mutants. Since the hindbrain is the only periotic tissue known to express *fgf3* at this time, I infer that the expanded domain of *fgf3* in *val/val* mutants is critical for generation of the above inner ear defects.

**Dependence of inner ear patterning on Fgf8**

Although expression of *fgf8* did not appear to correlate with changes in inner ear patterning in *val/val* mutants, I sought to characterize patterning defects in *ace/ace* mutants and examine genetic interactions between *ace* and *val*. Defects in *ace/ace* embryos are less variable than in embryos injected with *fgf3*-MO (Phillips et al., 2001). The otic vesicle in *ace/ace* mutants is reduced in size but usually retains an ovoid shape at 24h. Hair cell production is reduced by more than half in the majority of *ace/ace* mutants (Table 2), and more than a third (7/19) of specimens produce no posterior hair

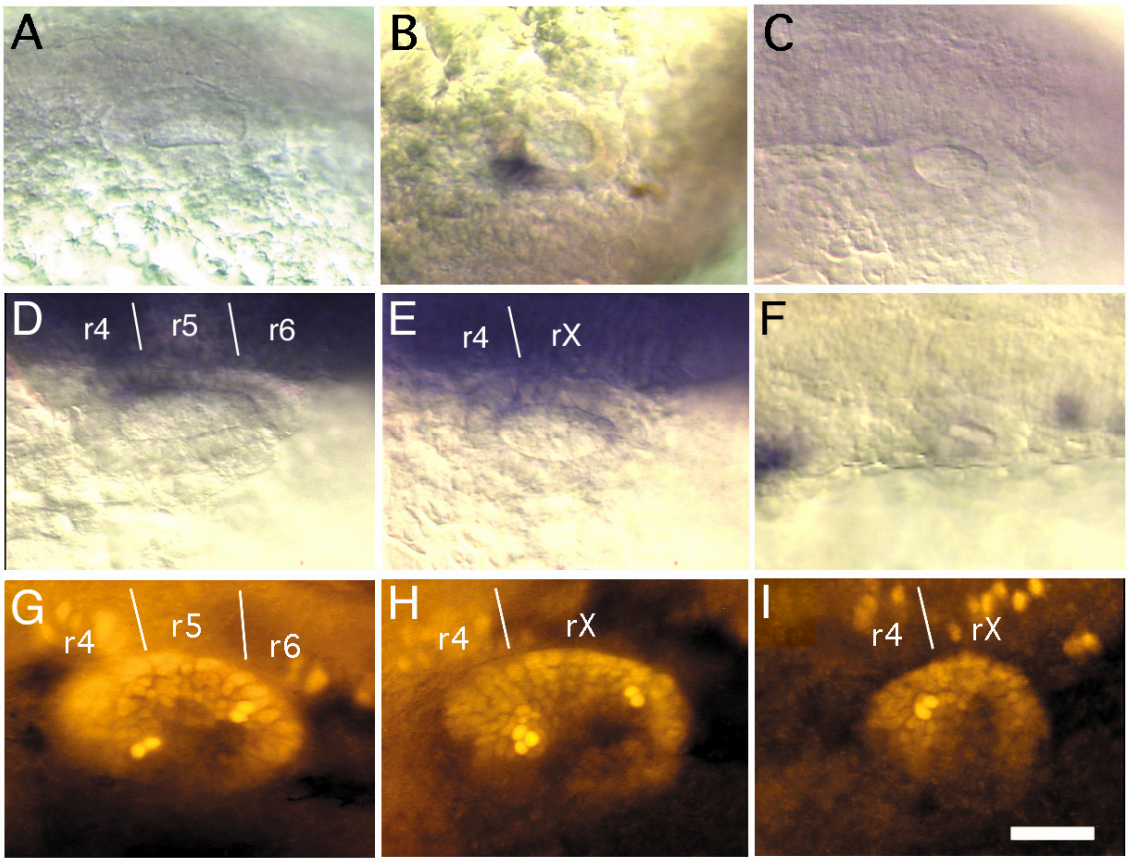


**Fig. 20.** Effects of *fgf3* knockdown on inner ear development. Dorsolateral view (anterior to the left) of otic vesicles in embryos injected with *fgf3*-MO. (A-C) in situ hybridization of *pax5* at 24 h in injected wild-type (A) and injected *val/val* (B, C) embryos. Expression levels are greatly reduced in 1/2 to 2/3 of embryos (see text for details). (D, E) Expression of *zp23* at 24 h in injected wild-type (D) and injected *val/val* (E) embryos. Expression is detected throughout the medial wall of the otic vesicle, including cells adjacent to r4. (F) in situ hybridization of *nkx5.1* at 24 h in an injected *val/val* embryo. No expression is detected in the otic vesicle. (G-I) Anti-Pax2 staining at 30 h in injected wild-type (G) and injected *val/val* (H, I) embryos. The number of hair cells is reduced relative to uninjected controls, and the majority (19/25) of *val/val* embryos do not produce ectopic hair cells. Fgf3-depleted *val/val* embryos with extremely small otic vesicles (I) produced anterior hair cells only. Relative positions of rhombomeres are indicated. Scale bar, 70 µm (A-C, F), 50 µm (D, E), or 30 µm (G-I).

cells at all (Fig. 21E). In *ace/ace*; *val/val* double mutants, the size of otic vesicle is further reduced and the number of hair cells is comparable to that in *ace/ace* single mutants (Fig. 21F; Table 2). Hair cells often form adjacent to r4 and/or rX in *ace/ace; val/val* double mutants and are usually located in a more medial position than are hair cells in *ace/ace* mutants (Fig. 21F). In addition, *pax5* is expressed along the full length of the anteroposterior axis of the ear (Fig. 21D). Expression of *nkx5.1* is also expanded in *ace/ace;val/val* double mutants, while *zp23* is not expressed (data not shown). Thus, the *ace* mutation strongly perturbs inner ear patterning, but loss of *fgf8* function does not suppress the patterning defects associated with the *val* mutation. This is probably because expression of *fgf3* is expanded in the hindbrain of *ace/ace;val/val* double mutants as in *val/val* mutants (Fig. 21B). Together, these data indicate that *val* and *ace* affect different developmental pathways, and that the early patterning defects seen in the *val/val* mutant ear are not caused by misregulation of *fgf8* expression.

**Table 2.** Number of hair cells at 30 hpf.

| | number hair cells/ear at 30h | | |
|---|---|---|---|
| Genotype | mean ± s.d. | range | number |
| +/+ | 6.9 ± 1.1 | 6-9 | 28 |
| val/val | 12 ± 1.3 | 10-14 | 32 |
| fgf3 kd | 5.3 ± 1.7 | 2-8 | 21 |
| fgf3 kd in val/val | 5.7 ± 2.4 | 2-11 | 33 |
| ace/ace | 2.9 ± 1.0 | 2-5 | 19 |
| ace/ace;val/val | 2.5 ± 0.7 | 1-4 | 28 |

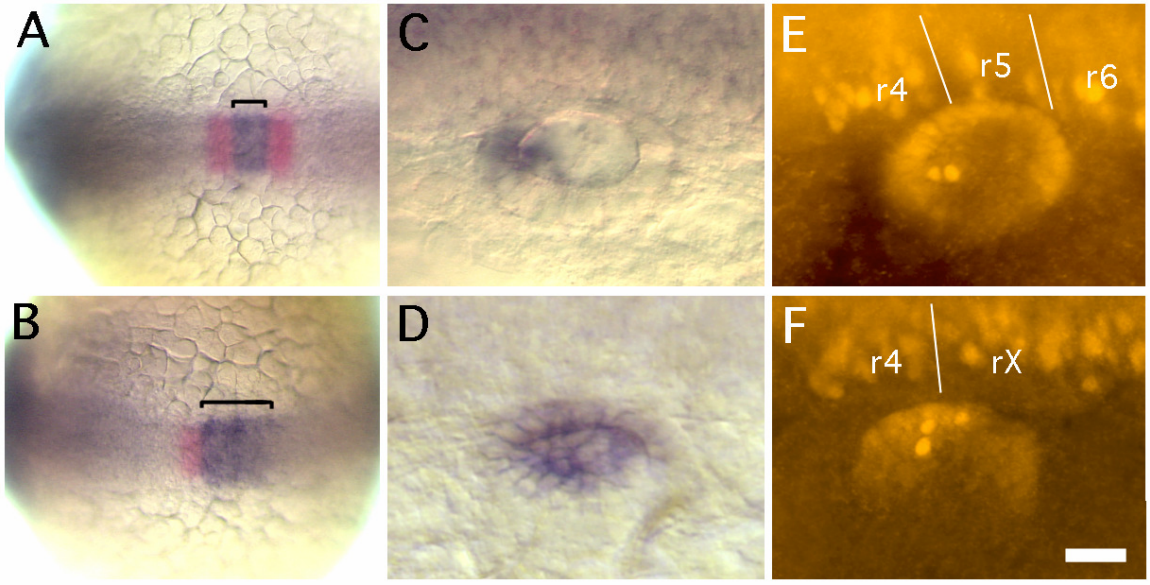


**Fig. 21.** Effects of *fgf8* dysfunction on inner ear development. (A, B) Dorsal view of the hindbrain at 14h showing expression of *fgf3* (blue, with brackets) and *krox20* (red) in *ace/ace* (A) and *ace/ace; val/val* (B) embryos. (C, D) Dorsolateral view showing *pax5* expression in the otic vesicle at 24 h in *ace/ace* (C) and *ace/ace; val/val* (D) embryos. (E, F) Dorsolateral view showing anti-Pax2 staining in the otic vesicle at 30 h in *ace/ace* (E) and *ace/ace; val/val* (F) embryos. Relative positions of rhombomeres are indicated. Double mutants show ectopic expression of *fgf3* in rX (B), ectopic expression of *pax5* (D) and ectopic hair cells in the otic vesicle (F). Anterior is to the left in all specimens. Scale bar, 80 µm (A, B), or 30 µm (C-F).

# DISCUSSION

## Fgf3, Fgf8, and hindbrain signaling

Development of the first hair cells is normally restricted to regions of the otic placode directly adjacent to r4 and r6 (Fig. 14), suggesting that signals emitted by those rhombomeres specify the equivalence groups from which hair cells emerge. Data presented here suggest that Fgf3 is an important r4-derived factor that regulates formation of anterior hair cells, as well as expression of various A-P markers in the ear. In *val/val* embryos, *fgf3* is expressed ectopically in rX (Fig. 18), and ectopic hair cells form within the adjacent otic vesicle (Fig. 14). Expression of *nkx5.1* and *pax5*, which are normally restricted to the anterior portion of the placode next to r4, expand posteriorly in *val/val* mutants to include all cells abutting the hindbrain (Fig. 16). The posterior marker *zp23* is not expressed in the otic vesicle in *val/val* mutants. Depletion of Fgf3 suppresses all of the above patterning defects in the *val/val* mutant ear. Moreover, in many Fgf3-depleted embryos, anterior otic markers are totally ablated and *zp23* expression expands anteriorly to include cells adjacent to r4.

The fact that any hair cells are produced at all in Fgf3-depleted embryos indicates that additional hair cell-inducing factors must be present. *fgf8* is clearly required for normal hair cell formation and could partially compensate for loss of *fgf3* (Reifers et al., 1998; Phillips et al., 2001). However, several observations indicate that the role of *fgf8* is distinct from that of *fgf3*. First, periotic expression of *fgf8* declines sharply just before the placode forms at 14 h, thereby limiting its ability to influence later otic patterning.

Second, expression patterns of *nkx5.1*, *pax5*, and *zp23* are not altered in *ace/ace* embryos (Fig. 21C, and data not shown), indicating that A-P patterning is relatively normal. Third, loss of *fgf8* inhibits hair cell formation but does not prevent formation of ectopic hair cells in *val/val* mutants. The latter are dependent on *fgf3* instead. Thus, in contrast to *fgf3*, there is little evidence to suggest that the r4 domain of *fgf8* regulates regional patterning in the otic placode. Instead, *fgf8* may play a more general role in stimulating hair cell competence during the process of placode induction.

Paradoxically, anterior hair cells are not as severely impaired in *ace/ace* mutants as are posterior hair cells. Posterior hair cells are totally ablated in about 1/3 of *ace/ace* mutants. This is difficult to explain based solely on the expression domain of *fgf8*, but may reflect changes in the dimensions of the otic placode. In *ace/ace* mutants, the otic placode is often reduced to a domain juxtaposed to r4 and r5 only. Thus, secretion of Fgf3 from r4 may be sufficient to induce some anterior hair cells in the absence of Fgf8, whereas cells in the posterior otic placode may lie too far from r6 to benefit from inductive factors possibly secreted from there. No clear candidates for r6-specifc inducers are known, but the Fgf-inducible genes *erm*, *pea3*, and *sprouty4* are expressed in r6 (Fürthauer et al., 2001; Raible and Brand, 2001; Roehl and Nüsslein-Volhard, 2001; and my unpublished observations), suggesting that at least one as yet unidentified Fgf homolog is expressed there.

The reason for expanded expression of *fgf3* in *val/val* mutants is not clear, but there are several possibilities. First, this could result from misspecification of segment identity in the rX territory. Several other genes normally expressed in adjacent

segments, including *hoxb1* in r4 and *hoxb4* in r7, eventually come to be expressed in rX (Prince et al., 1998). However, these changes do not occur until 20 somites (19 h). In contrast, expression of *fgf3* in rX is first detected at 10 h in *val/val* mutants, corresponding to the time when *val* normally begins to function (Moens et al., 1998). This raises the alternative possibility that Val protein normally acts to transcriptionally repress *fgf3*. In support of this, misexpression of *val* inhibits r4-expression of *fgf3*, but not *fgf8* (Fig. 19). Direct support for transcriptional regulation by Val will require analysis of the promoter/enhancer regions of *fgf3*.

**Comparison of *val* and *kr***

In sharp contrast to *val* function in zebrafish, mouse Kreisler is required, directly or indirectly, for upregulation of Fgf3 in r5 and r6 (McKay et al., 1996). This difference is notable because so many other aspects of early hindbrain and ear development are conserved between these species. The high degree of sequence-identity leaves little doubt that the zebrafish genes are orthologous to *kr* and *Fgf3*, respectively (Kiefer et al., 1996a; Moens et al., 1998). There are, however, differences in the N- and C-terminal regions of Fgf3 in zebrafish vs. mouse. These regions are thought to be important for mediating the characteristic receptor binding preferences and signaling properties of Fgf3. Nevertheless, these functional properties are actually quite similar between the fish and mouse proteins (Kiefer et al., 1996a). This, combined with the broad similarities in their expression patterns and involvement in early otic development, strengthen the notion that the fish and mouse *Fgf3* genes are indeed orthologs. Because

zebrafish often has multiple homologs of specific tetrapod genes, it is possible that a second *fgf3* gene might be present in the zebrafish genome that shows an expression pattern more like the mouse gene. If so, it will be important to address its function as well. However, I have shown that the known *fgf3* ortholog plays an essential role in the etiology of the ear phenotype in *val*/*val* embryos, since key aspects of the phenotype are suppressed by injecting *fgf3*-MO. Morpholino oligomers are highly gene-specific in their effects, and even though they do not totally eliminate gene function, they generate phenotypes that are indistinguishable from those caused by known null mutations (Nasevicius and Ekker, 2000; Phillips et al., 2001; Raible and Brand, 2001; Maroon et al., 2002). On balance, it appears that the general role of Fgf3 in otic development has been conserved in mouse and fish but that differential regulation in the hindbrain represents a real difference between these species.

Considering the above differences in hindbrain signaling, one might expect the ear phenotypes in *val/val* and *kr/kr* mutants to be quite different. Instead, the phenotypes appear strikingly similar. In *kr/kr* embryos, as in *val/val* embryos, development of the otic vesicle is highly variable and defects can be seen in virtually all regions of the labyrinth (Deol, 1964). In *kr/kr* mutants, formation of the wall of the otic capsule is often incomplete, with large gaps through with membranous epithelia protrude, and morphology of the labyrinth is usually grossly abnormal. Such global disruption may be related to buildup of excess fluid pressure due failure of the endolymphatic duct to form in many or most *kr/kr* mutants (Deol, 1964; Brigande et al., 2000). Whether a similar problem occurs in *val/val* mutants is not clear. The existence of an endolymphatic duct

in zebrafish was only recently documented (Bever and Fekete, 2002), but it does not begin to form until around day 8. Most *val/val* mutants die before this time, and they often begin to show defects in morphogenesis (e.g. of the semicircular canals) by 72 h (Fig. 17, and data not shown). While these early defects cannot be explained by the absence of an endolymphatic duct, mutant ears often appear swollen and distended by day 3, suggesting a buildup of endolymphatic pressure. It is possible that cellular functions normally required to maintain a proper fluid balance in the early vesicle are misregulated in *val/val* mutants. Thus, hydrops may be an important contributing factor to the defects in both *kr/kr* and *val/val* mutants.

Another similarity between *kr/kr* and *val/val* mutants is that they both form ectopic patches of hair cells. However, this phenotype has a completely different etiology in the two species. In tetrapod vertebrates, sensory epithelia do not begin to differentiate until after the various chambers of the labyrinth begin to form. Thus, formation of ectopic hair cells in *kr/kr* mutants probably reflects the general disorganization of, and chaotic protrusions from, the labyrinth (Deol, 1964). In contrast, sensory epithelia in zebrafish begin to differentiate much earlier. Macular equivalence groups are already specified at 14 h when the placode first forms (Haddon et al., 1998a; Whitfield et al., 2002), and the first hair cells (visualized by the presence of kinocilia) are evident as soon as the lumen of the vesicle forms at 18.5 h (Riley et al., 1997). Thus, formation of ectopic hair cells in *val/val* mutants reflects an early defect in cell fate specification rather than a later defect in morphogenesis. It is noteworthy that there have

been no detailed molecular studies of otic development in *kr/kr* mutants, so a direct comparison of early pattern formation is not yet possible.

**Evolutionary implications**

It is interesting to consider that the altered pattern of *fgf3* expression in the *val/val* mutant hindbrain closely resembles the normal pattern of *Fgf3* expression in chick and mouse embryos (Mahmood, 1995, 1996; McKay et al., 1996). Analysis of *val/val* mutants suggests that misexpression of *fgf3* in rX leads to development of excess and ectopic hair cells in the otic vesicle. It is possible that evolutionary changes that led to normal expression of *Fgf3* in r5/6 in amniotes were crucial for evolution of the cochlea, which has no known counterpart in anamniote vertebrates (Lewis et al., 1985). In the mouse, development of the cochlea requires Fgf signaling at early otic vesicle stages (Pirvola et al., 2000). The Fgf receptor isoform Fgfr-2(IIIb) is expressed in the otic epithelium juxtaposed to the hindbrain. Targeted disruption of this isoform leads to severe dysgenesis of the cochlea. Cochlear development is also impaired in *Fgf3*-null and *kr/kr* mutant mice (Deol, 1964; Mansour et al., 1993). In *Xenopus*, *Fgf3* expression shows a pattern intermediate between that of zebrafish and amniotes: The frog gene is initially expressed in r3 through r5 and only later becomes restricted to r4 (Lombardo et al., 1998). Although amphibians do not possess a cochlea, they do show modifications of the posterior otic vesicle that give rise to the basilar and amphibian papillae, auditory organs not found in fishes (reviewed by Lewis et al., 1985). Thus, expression of *fgf3* in

more posterior regions of the hindbrain correlates with elaborations of the inner ear that may have been essential for enhancing auditory function in terrestrial environments.

# CHAPTER IV

# THE REQUIREMENT OF *pax5* IN UTRICULAR HAIR CELL MAINTENANCE

## INTRODUCTION

The vertebrate inner ear is a conserved organ system comprising a series of interconnected chambers, each of which is dedicated to either vestibular or auditory function. Each chamber contains a sensory patch consisting of hair cells and support cells. The hair cells synapse with neurons of the statoacoustic ganglion (SAG), or the VIIIth cranial nerve, axons of which project to functional processing nuclei in the hindbrain.

All sensory patches originate from the prosensory region in the ventromedial wall of the otic vesicle, and each sensory patch subsequently differentiates with specific structural and functional attributes. For example, hair cells in the utricle detect linear motions and gravity through an attached otolith whereas semicircular canals have hair cells with long cilia to sense angular acceleration through the fluid motion in the canal. Saccular hair cells are also associated with an otolith but in fish, these hair cells transmit auditory signals. Differential gene expression in the otic vesicle presumably underlies functional specification as well as structural development. Supporting this idea,

impaired function of specific genes in the prosensory region can cause defective development in discrete chambers and associated sensory patches. A conditional knockout of *Fgfr1* function in the otic epithelium blocks the formation of hair cell only in the cochlear epithelium (Pirvola et al., 2002). *Otx1* is expressed in the presumptive lateral crista and *Otx1*$^{-/-}$ mice do not produce the lateral crista or a normal lateral semicircular canal (Morsli et al., 1999). After formation, hair cells in a given sensory region appear to be maintained in a specific manner too. A mouse zinc finger transcription factor, *Gfi1,* is expressed in hair cells of all sensory epithelia. Knocking out *Gfi1*, however, affects hair cells in each sensory epithelium differentially. Hair cells in the cochlea are disorganized and start to die from P0. Maculae in the utricle and the saccule show disorganized layers of hair cells and support cells but hair cells are survived at least by 5 month after birth. Moreover, hair cells in cristae are produced and maintained normally (Wallis et al., 2003). In spite of a widespread expression pattern, the differential effects of *Gfi1* on each sensory region suggest that unique combinations of localized factors establish different properties and requirements for each sensory patch. To date, many genes have been identified in a specific sensory patch. However, it is not easy to address their function in a sensory patch because their expression pattern are temporally and spatially very dynamic and null mutations often cause severe defects in the morphogenesis that preclude assessment of later functions.

*pax*2/5/8 genes are involved in the various organogenesis events, interacting with other regulatory genes including themselves (Dahl et al., 1997; Pfeffer et al. 1998; Chi and Epstein, 2002). Members of this gene family often show functional redundancy by

virtue of their structural homology (Bouchard et al., 2000; Bouchard et al., 2002; Hans et al., 2004; Mackereth et al., 2005). In zebrafish, there are four genes identified in *pax2/5/8* gene family, *pax8*, *pax5*, *pax2a* and *pax2b*. Interestingly, all of them are expressed in the developing inner ear (Pfeffer et al., 1998). *pax8*, *pax2a* and *pax2b* function early to induce and maintain the otic placode (Hans et al., 2004; Mackereth et al., 2005) and *pax2a* and *pax2b* play later roles in hair cell differentiation (Riley et al., 1999; Whitfield et al., 2002). However, there have been no functional studies of *pax5*. Expression of *pax5* begins in the anterior otic vesicle (Pfeffer et al., 1998) and later is localized to the utricular macula. This expression pattern suggests that *pax5* may be involved in development, maintenance or functional organization of the utricular macula. Two genes are known to regulate regional expression of *pax5*: *pax2a* and *fgf3*. A null mutant for *pax2a*, *no isthmus* (*noi*), completely lacks *pax5* expression in the otic vesicle (Pfeffer et al., 1998). *fgf3* knockdown embryos also show severely reduced *pax5* expression indicating *fgf3* as another regulator for *pax5* (Kwak et al., 2002). Although these genes have been well studied, it is still unknown how they regulate sensory development and what extent *pax5* mediates their functions.

To investigate *pax5* function in the otic vesicle, I cloned the full sequence of *pax5* cDNA and performed loss of function studies using antisense oliginucleotide technique. Knocking down *pax5* function caused vestibular defects in zebrafish larvae with a normal overt morphology of the ear. I provided evidences that vestibular deficits in *pax5* depleted embryos result from defects in maintaining utricular hair cells with secondary SAG neuronal defects in the utricular macula. I also examined *noi* and an

*fgf3* null mutant, *lim abscent* (*lia*), in comparison with *pax5* depleted embryos to understand their interaction.

## MATERIALS AND METHODS

### Fish strains and maintenance

Wild-type zebrafish strains were derived from the AB line (Eugene, OR). Null mutants for *pax2a, noi*$^{tu29a}$ (Brand et al., 1996; Lun and Brand, 1998) and *fgf3, lia*$^{t24152}$ (Herzog et al., 2004) were used in this study. ENU-derived *monolith (mnl)* mutants which exhibit vestibular dysfunction were also used (Riley and Grunwald, 1996; Riley and Moorman, 2000). Embryos were raised under standard laboratory conditions at 28.5˚ C and staged as described by Kimmel et al., 1995. In some case, 0.2 mM phenylthiourea (PTU) was added to prevent melanin formation. Embryos were fixed in 4% formaldehyde for 2 hours at room temperature or overnight at 4˚C.

### Cloning of *pax5*

Using zebrafish genomic sequence database (http://www.ensembl.org), I searched trace files which contain sequences matching putative exon1 and exon2 sequences. With the known partial sequence of exon2 as a bait, I found at least 3 trace files, zfishB-a1351c05.q1c.scf, zfish41364-125e05.p1c.scf and, zfish41361-170c09.p1c.scf. They

show exactly 639 overlapping nucleotides containing the full exon2 sequence. For exon1, I used the Fugu *pax5* exon1 sequence to search the most homologous trace files. The four searched trace files, zfish44907-611f07.p1k, zfish43943-534d01.p1c, z35725-a6211g06.p1c and, z35725-a6498f09.p1c contain identical 51 nucleotides with 80% identity to the Fugu *pax5* exon1 sequence. The full sequence of exon 11 in the carboxyl terminal end of *pax5* gene was found in the trace file, zfish44764-1131a01.p1k. The identified sequences are confirmed by RT-PCR followed by cloning and sequencing using primers for the putative full ORF; *pax5*(-6): 5'GGGAATTCAACACGATGGAAA TCCACTG3', *pax5*(1128):5'GGTCTAGATTATTTCGTGCCTCCCACTC 3'.

**Behavioral analysis**

Vestibular function was assayed by three tests between 3 and 7dpf. Balance was assessed by the ability of larvae to rest with their dorsal sides up one minute after initiating a startle response by tapping petridishes of larvae. This was determined three or more times for each population. Larvae were tested individually, three times, for motor coordination. The percentage of larvae capable of swimming rapidly in a straight course, in response to tapping the dish or dropping a drop of water near the embryo, were scored as normal. Swim bladder inflation was observed under a dissecting microscope (Riley and Moorman 2000).

**Morpholino injection**

Splice-, and translation-blocking morpholino oligomers were generated to knock-down *pax5*. Translation blocker for splice variant 1 (TB1); 5'CAGTGGATTTCCATCTGTTT TAAA3′; translation blocker for splice variant 2 (TB2): 5′CTCGGATCTCCCAGGCA-ACATGGT3′; splice blocker for exon-intron boundary on exon 2 (SB1): 5′TACTCAT-AACTTACCTGCCCAGTA3′; splice blocker for exon-intron boundary on exon 3 (SB2) : 5′ATGTGTTTTACACACCTGTTGATTG3′; splice blocker for exon-intron boundary on exon 5: 5′TTGACCCTTACCTAAATTATGCGCA3′. A cocktail of all five morpholinos was prepared in Danieaux solution to a concentration of 12 µg/µl (3µg/µl each TB1 and TB2; and 2 µg/µl each SB1, 2 and 3). Approximately 1 nl was injected into wild-type zebrafish embryos at one-cell stage to generate morphants.

**Injection of *pax5* RNAs**

Two splice variants, *pax5*-v1and *pax5*-v2 were cloned in pCS2p+ expression vector. RNAs for both variants were synthesized *in vitro* and ~200 pg of *pax5*-v1 and *pax5*-v2 RNA mixture (100 pg of each variant) was injected into the embryos at the one- to two-cell stage.

**Immunohistochemistry**

Embryos raised in PTU were fixed and processed as previously described (Riley et al., 1999). The following primary antibodies were used: mouse anti-Pax2a (Berkeley Antibody Company, 1:100 dilution)) which stains zebrafish Pax2a, anti-acetylated

tubulin (Sigma T-6793, 1:100) and Islet-1(DSHB 39.4D5, 1:100). Alexa 546 goat anti-rabbit IgG (Molecular Probes A-11010, 1:50) and Alexa 488 goat anti-mouse IgG (Molecular Probes A-11001, 1:50) were used as secondary antibodies.

**Rhodamine-Phalloidin staining**

Embryos raised in PTU were fixed and rinsed in 0.1% PBT for 15 minutes followed by incubation in PBT (2-3% Triton-X-100) at room temperature for 4 hours and then overnight at 4˚C. Permeabilized embryos were incubated in Rhodamine-Phalloidin (Molecular Probes R415, 1:30 dilution in 1% Bovine Serum Albumin in PBS) for 2 hours at room temperature, washed four times in PBT (0.5% Triton-X-100) for 30 minutes each and observed.

**DiI labeling**

3-7 day old larvae were fixed and then washed in PBS. The larvae were mounted in 0.6% low-melting-temperature agarose made in PBS. To examine the neuronal projections from the statoacoustic ganglion (SAG), DiI (1,1-dioctadecyl-3,3,3,3 -tetramethylindocarbocyanine perchlorate, Molecular probes D-282, 4 mg/ml in 100% ethanol) was injected into the utricular macula of larvae. Glass micropipettes were backfilled with the DiI solution and directed to the utricular macula using a micromanipulator. Injected embryos were incubated at 33˚C overnight and observed.

**Whole-mount in situ hybridization**

Whole-mount in-situ hybridizations were carried out as described previously (Phillips et al. 2001) using the following riboprobes: *nkx5.1* (Adamska et al., 2000), *otx1* (Li et al., 1994), *zp23* (Hauptmann and Gerster, 2000), *dlx3* (Ekker et al., 1992a), *krox20* (Oxtoby and Jowett, 1993), *msxC* (Ekker et al., 1992b), *pax5* (Pfeffer et al., 1998), *fgf8* (Reifers et al., 1998) and *fgf3* (Kiefer et al., 1996).

**Cell death analysis**

Embryos were dechorinated and incubated in the solution of acridine orange in PBS for 1 hour, at room temperature. This was followed by two 10 minute washes in PBS prior to observation. In situ TUNEL assay (TdT-mediated dUTP Nick-End Labeling) was performed as suggested by the manufacturer to detect apoptotic cell nuclei (Promega TUNEL assay kit).

**RESULTS**

**Cloning of zebrafish *pax5***

The known sequence for zebrafish *pax5* cDNA was incomplete, with sequences missing from both the 5' and 3' ends (Pfeffer et al., 1998). Using the zebrafish genomic sequence database (http://www.ensembl.org) and comparison with Fugu *pax5*, I found

tracer files with the putative missing zebrafish sequences. To confirm the identity of these sequences, I designed primers based on the new sequences and successfully amplified the complete *pax5* cDNA. Analysis of multiple cDNA clones revealed two distinct sequences representing different splice isoforms, *pax5*-variant 1 (*pax5*-v1) and *pax5*-variant 2 (*pax5*-v2) (Fig. 22-1). *pax5*-v1 is 1176 nucleotides long matching full-length of *pax5* cDNA. *pax5*- v2 has a partial paired domain caused by splicing out the second exon (nucleotides 47-212). This splice variant is predicted to use an alternative translation start codon in exon 3. In mouse, 6 splice variant forms are known. The two splice variants, *pax5*-v1and *pax5*-v2 are homologous to mouse splice variants *Pax-5a* and *Pax-5b* respectively suggesting that splicing events for *pax5* gene are conserved in vertebrates (Zwollo et al., 1997). The relative abundance of cloned cDNAs suggests that *pax5*-v1 (8 out of 10 clones) is more prevalent than *pax5*-v2 (2 out of 10 clones).

**Expression of *pax5* in the otic vesicle**

*pax5* is first detected in the anterior end of the otic placode at about 17 hpf, just before formation of the otic vesicle (Fig. 22-2A). By 24 hpf, the anterior quarter of the otic vesicle shows a uniformly high level of *pax5* expression (Fig. 22-2B). Expression is subsequently restricted to the anterior (utricular) macula and remains in the macula until at least 72 hpf (Fig. 22-2C and D). At these later stages, all cells in the utricular macula express *pax5*, but hair cells show higher expression than support cells (Fig. 22-1D). In addition to the predominant signal in the utricle, I observed expression in a small number

**Fig. 22.** cDNA structure and expression of *pax5*. (A) Structure and sequence of *pax5* gene. A schematic drawing of *pax5* splice variants on a relative scale. Square brackets indicate each exon. Conserved functional domains, paired (PD), octapeptide (OP), homeo (HD), transactivation (TAD) and inhibitory (ID) are marked. Putative start sites (M) for each splice variant are indicated. Bars show the binding sites for five *pax5* morpholinos, 2 translation blockers (TB1 and 2) and 3 splice blockers (SB1, 2 and 3). The missing N-terminus (i) and C-terminus regions (ii) sequences in comparison with Fugu *pax5* sequences in the corresponding regions. The amino acid sequence of zebrafish *pax5* and Fugu *pax5* is 100% identical with 80% DNA sequence identity in exon1 and exon11. (B-E) Otic expression of *pax5* in wild-type at 17 hpf (B) in the otic placode, 24 hpf (C) in the otic vesicle and 48 hpf (D) in the hair cells. (D) Enlarged view of area marked in C. Arrows indicate *pax5* expression in the saccule, arrowheads mark *pax5* expression in hair cells and bracket indicates support cell layer. (B) Dorsal, (C) dorsolateral and (D, E) lateral views, with anterior to the left. Scale bar, 30 µm (B), 40 µm (C, D), 12.5 µm (E).

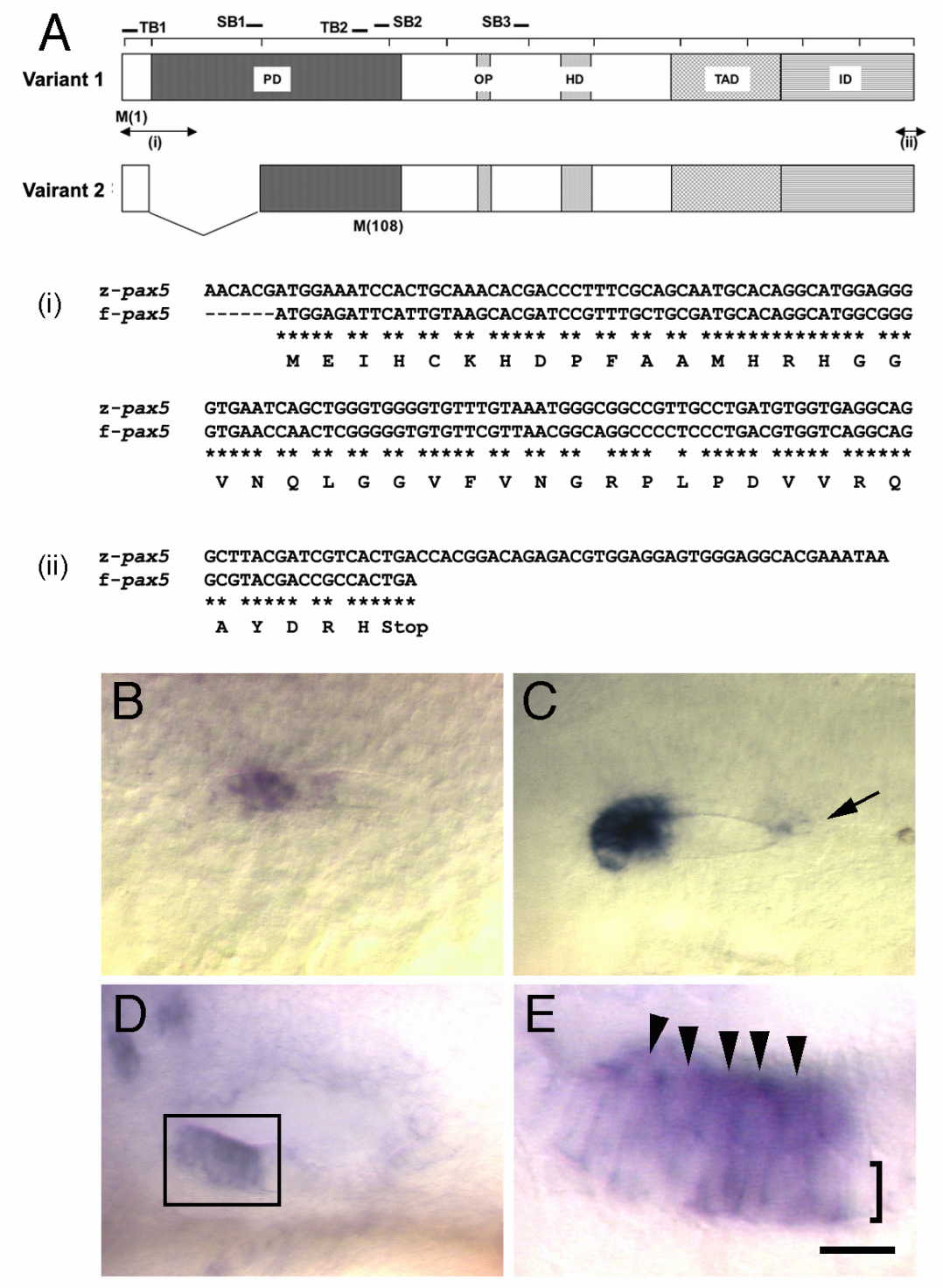
A
TB1
SB1
TB2
SB2
SB3
Variant 1
PD
OP
HD
TAD
ID
M(1)
(i)
(ii)
Vairant 2
M(108)
(i)
z-pax5 AACACGATGGAAATCCACTGCAAACACGACCCTTTCGCAGCAATGCACAGGCATGGAGGG
f-pax5 ------ATGGAGATTCATTGTAAGCACGATCCGTTTGCTGCGATGCACAGGCATGGCGGG
M E I H C K H D P F A A M H R H G G
z-pax5 GTGAATCAGCTGGGTGGGGTGTTTGTAAATGGGCGGCCGTTGCCTGATGTGGTGAGGCAG
f-pax5 GTGAACCAACTCGGGGGTGTGTTCGTTAACGGCAGGCCCCTCCCTGACGTGGTCAGGCAG
V N Q L G G V F V N G R P L P D V V R Q
(ii)
z-pax5 GCTTACGATCGTCACTGACCACGGACAGAGACGTGGAGGAGTGGGAGGCACGAAATAA
f-pax5 GCGTACGACCGCCACTGA
A Y D R H Stop
B
C
D
E

of saccular hair cells (Fig. 22-1B). This posterior expression is maintained through at least 48 hpf.

**Vestibular defects in *pax5* knockdown embryos**

To study *pax5* function in the inner ear development I generated morpholinos. Two morpholinos were designed to block translation from two putative translation start codons and three splice-blocking morpholinos were designed to induce aberrant splicing of sequences encoding the paired domain and the homeo domain (Fig. 22-1). Each of these morpholinos, used individually, disrupted vestibular function (discussed below) but varied in efficiency. However, a cocktail of all five morpholinos proved most efficient and was used for the remainder of this study. Embryos injected with *pax5* morpholino cocktail (*pax5* morphants) show no overt morphological defects. A normal sized otic vesicle is produced and otoliths are formed in right positions at the right time. Although *pax5* is also expressed in the midbrain hindbrain boundary (MHB), and is required for normal MHB development in mouse, knocking down *pax5* function does not impair the morphology of MHB in zebrafish embryos (not shown). Although there were no overt defects, the predominant expression in the utricle led me to test for vestibular deficits. I performed three tests to assay vestibular function (Riley and Moorman, 2000). In a test for balance, the ability to maintain a dorsal-up posture was examined. Coordinated movement following a startle response is another aspect of vestibular function. In response to touch, embryos with normal vestibular function rapidly swim away from the stimulus in a straight line. Embryos with vestibular deficits

respond aberrantly, typically swimming in circles, spirals or erratic zig-zag motions. Lastly, I examined swim bladder inflation of embryos. Normally, embryos must swim to the surface of water to obtain air for inflation of the swim bladder. Vestibular deficits impede this motion and thereby prevent swim bladder inflation. These tests were used previously to study *monolith* (*mnl*) mutants, which show a severe and permanent loss of vestibular function due to the lack of utricular otoliths (Riley and Grunwald, 1996; Riley et al., 1997). *mnl* mutants fail all three tests unless they are rescued by experimental manipulations that restore the formation of utricular otoliths (Riley and Moorman, 2000). I therefore used these assays to test *pax*5 morphants, which show delays in development of vestibular function (Fig. 23). Although most *pax5* morphants eventually display normal vestibular behaviors, about 20% never do so and continue to show severely impaired vestibular function (Fig. 23). These data support the hypothesis that *pax5* function is required for development and/or function of the vestibular system.

**Inner ear development of *pax5* morphants**

The vestibular defects in *pax5* morphants could be caused by molecular changes in the utricular sensory epithelium possibly related to defects in otic vesicle patterning and/or deficits in neurons of statoacoustic ganglion (SAG). Therefore, I examined expressions of molecular markers for otic vesicle and SAG development in *pax5* morphants. *nkx5.1*, which marks the anterior end of the otic vesicle as well as the SAG, is expressed normally in *pax5* morphants (Fig. 24A, B). *zp23,* a marker of the posterior medial wall adjacent to r5 and r6 of hindbrain, is also expressed normally in *pax5* morphants,

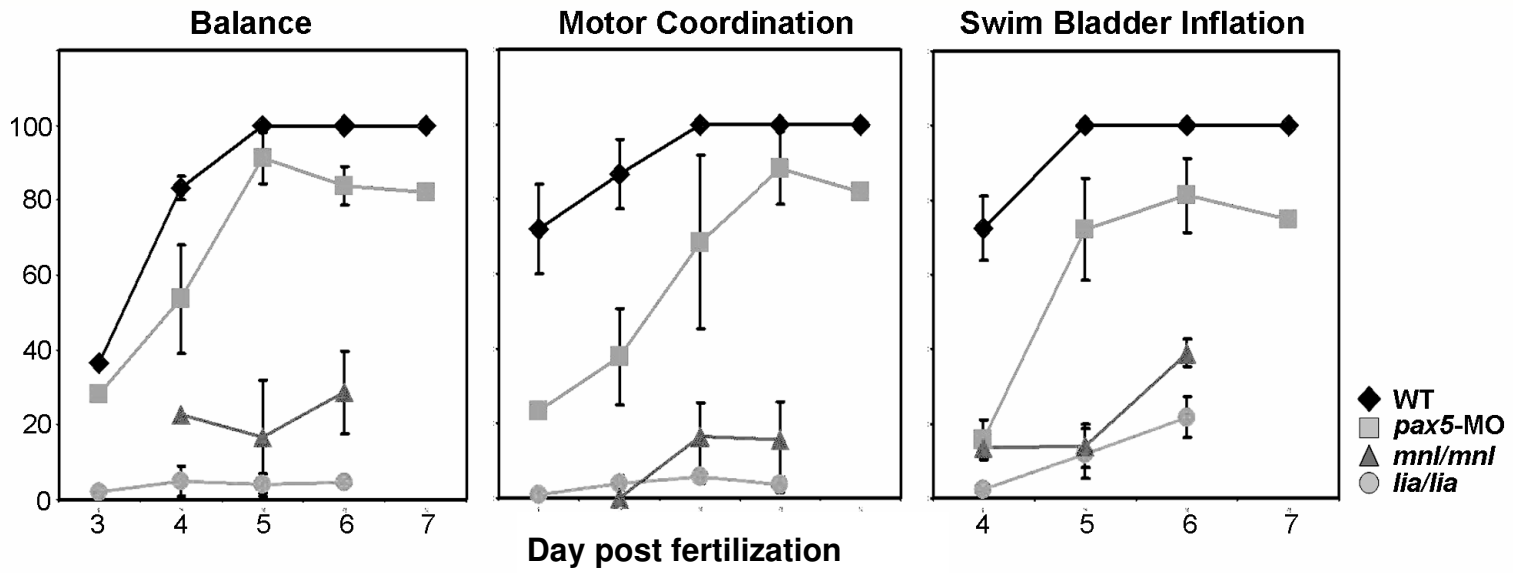


**Fig. 23.** Assessment of vestibular function. Development of balance, motor coordination and swim bladder inflation were assayed in wild-type, *pax5*-morphant, *lia/lia* and *mnl/mnl* at 3-7 dpf. The mean and standard error of two independent experiments is shown. Wild-type, n=173; *pax5*-MO, n=330; *lia/lia*, n=110; *mnl/mnl*, n=238.

suggesting that antero-posterior patterning is normal in *pax5* morphants (Fig. 24C, D). Patterning of dorso-ventral and medio-lateral axes also appear normal as demonstrated by expression of a dorso-medial marker, *dlx3b*, and a ventro-lateral marker, *otx1* (Fig. 24E, F, G, H). Next, I examined the development of vestibular endorgans. Utricular and saccular maculae appear morphologically normal and display normal temporal and spatial expression of *fgf8* (Fig. 24I, J). Semicircular canals and sensory cristae also develop normally (Fig. 24K, L; data not shown). Because *pax5* is expressed earlier in the hindbrain, I examined expression of *fgf3*, which is expressed in the hindbrain and known to regulate otic vesicle patterning (Kwak et al., 2002). Consistent with findings that otic vesicle patterning appears normal, hindbrain expression of *fgf3* is normal (Fig. 24M, N). Similarly, another marker of hindbrain patterning, *krox20*, is also normal (Fig. 24O, P). In summary, hindbrain patterning and general features of otic vesicle patterning and morphogenesis appear normal in *pax5* morphants. I therefore, considered the possibility that the vestibular defects in *pax5* morphants result from subtler defects in the SAG neurons and/or the utricular macula.

**The formation of SAG neurons in *pax5* morphants**

In early stages of SAG development, SAG neuroblasts are specified in the ventral region of the otic vesicle. Neuroblasts delaminate from the otic vesicle and migrate to a position between the antero-medial wall of the otic vesicle and hindbrain. *neurogenin1*(*ngn1*) is a bHLH transcription factor expressed in all cranial ganglia neuroblasts including those of SAG and is required for their differentiation. Based on

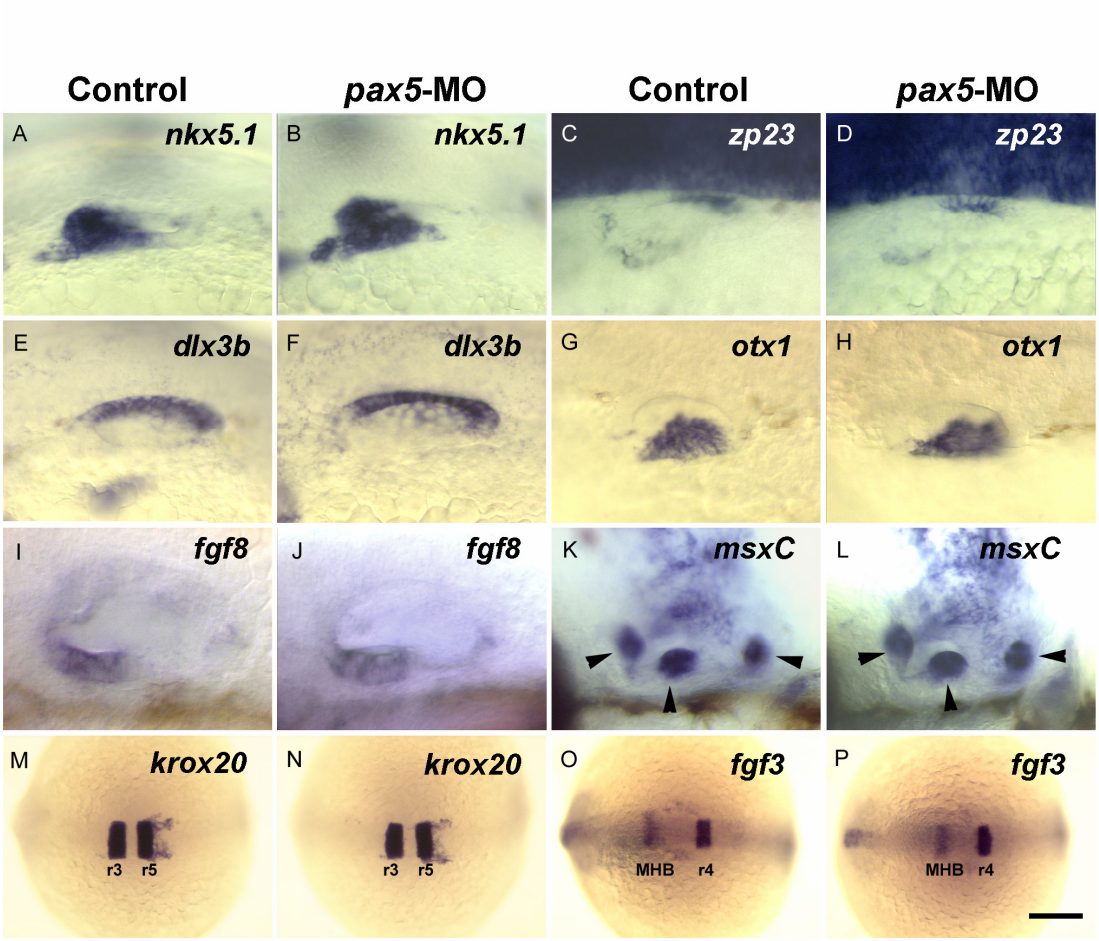


**Fig. 24.** Inner ear and hindbrain patterning in *pax5* morphants. Otic vesicles at 24 hpf (A-H), 48 hpf (I, J) and 72 hpf (K, L). Expression of *nkx5.1*, *zp23*, *dlx3b* and *otx1* in uninjected control embryos (A, C, E, G) and *pax5*-morphants (B, D, F, H) respectively. (I, J) Macular expression of *fgf8* in control (I) and *pax5*-morphants (J). (K, L) Expression of *msxC* in the cristae in control (K) and *pax5*-morphants (L). (M-P) *krox20* and *fgf3* expression at 9-somite stage in uninjected control embryos (M, O) and *pax5* morphants (N, P), respectively. Images show dorsolateral (A-F), lateral (I-L) and dorsal (G-H, M-P) views with anterior to the left. MHB, midbrain-hindbrain border; r3, rhombomere 3; r4, rhombomere 4. Scale bar, 55 µm (A-J), 65 µm (K, L), 210 µm (M-P).

the expression of *ngn1* (Andermann et al., 2002), the specification of neuroblasts begins by18 hpf as the otic vesicle forms, just after the onset of *pax5* expression in the ear. Since the regions of *pax5* expression and *ngn1* expression overlap, it is possible that the depletion of Pax5 could affect the development of SAG neuroblasts directly. *ngn1* expression in the otic vesicle shows a normal pattern in *pax5* morphants (Fig. 25A, B), and as described above expression of *nkx5.1* in the SAG is normal (Fig. 24A, B). In addition, the number and position of SAG neuroblasts is normal at 30 hpf (Fig. 25C, D). Therefore, depletion of *pax5* does not overtly alter SAG development.

**Neuronal targeting of SAG neurons in *pax5* morphants**

SAG neurons are bipolar neurons, sending processes into the hindbrain and sensory patches of the ear. Axonal processes to the hindbrain were visualized by injecting a lipophilic tracer, DiI, into utricular maculae after day 3. Utricular SAG neurons initially extend their axons to the hindbrain in a dorso-posterior direction bundling all axons together. This axonal bundle splits into two main branches in the hindbrain, one ascending and the other descending (Fig. 25E). In about half of control larvae, there are several additional thin branches projecting in parallel to the main branches (Fig. 25F). These patterns of projections are also detected in *isl3:GFP(zc7)* larvae, a transgenic line labeling all cranial ganglia, confirming that observed processes are those of SAG afferent neurons and not of efferent neurons. Minor branches persist through at least day 7 but their development does not appear to be correlated with the onset of vestibular function. Indeed, virtually identical patterns are observed in *mnl* mutants, which are null

**Fig. 25.** Development of the statoacoustic ganglion (SAG) in *pax5* knockdown embryos. (A-B) Expression of *ngn1* in the otic vesicle at 24 hpf in controls (A) and *pax5*-morphants (B). Arrows indicate SAG neuroblasts. (C, D) Isl1 expression at 30 hpf. Dotted region indicates accumulated SAG neuroblasts. In control embryos (C) an average of 16.5±4.2 neuroblasts were detected and comparable numbers were detected in *pax5* morphants (D, 15.7±3.5). Black arrows mark otoliths. (E, F) Axonal processes of the SAG to the hindbrain, visualized by DiI labeling, in wild-type embryos at 72 hpf showing two main branches (E, type 1) and additional branches (F, type 2), indicated by arrows. Inset (in E) shows a cartoon representing the site of DiI injection (orange arrow) and the position of the projections relative to the ear. **Table 1.** Combined data for the pattern of SAG projections to the hindbrain in wild type (n=193), *mnl/mnl* (n=142), *pax5* morphants (n=76) and *lia/lia* (n=89) embryos (3-6 dpf), depicting type 1 and type 2 patterns. $p>0.05$ (G-K) Utricular maculae stained with anti-acetylated tubulin at 48 hpf in control embryos (G, H) and *pax5* morphants (I-K). (G, H) Control embryos stained with anti-acetylated tubulin (green) (G) and double-stained with anti-Pax2 (red) to show hair cell nuclei (H) at 48 hpf. One axonal process innervates one hair cell (white arrows) and dense staining (yellow arrows) is observed in the basal region of the hair cell. (I) An aberrant projection (arrow) extending diagonally in the macula while other processes are relatively normal. (J) One thick process (arrow) extends to the luminal surface while other processes are not clearly visible. (K) *pax5* morphants double-stained with anti-acetylated tubulin and anti-Pax2. Misplaced hair cells (arrowhead) in *pax5* morphants are usually associated with aberrant projections (arrow). Images show dorsolateral (A-B, E-F), dorsal (C, D) and lateral (G-K) views, with anterior to the left. Scale bar, 50 µm (A, B, E, F), 30 µm (C, D), 12.5 µm (G-K).

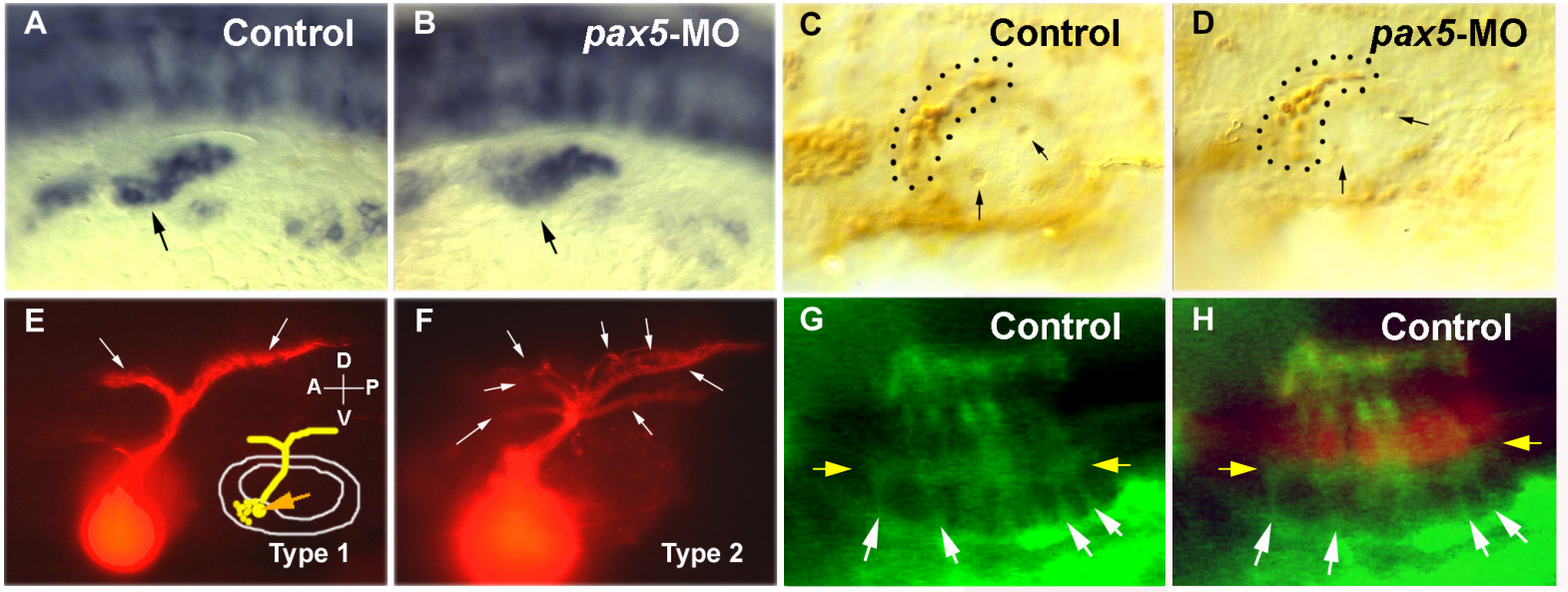


**Table 1**

| | Type 1 | Type 2 |
|---|---|---|
| WT | 40.0 % | 60.0 % (sd=22.5) |
| *pax5*-MO | 25.0 % | 75.0 % (sd=19.7) |
| *mnl/mnl* | 35.0 % | 65.0 % (sd=24.5) |
| *lia/lia* | 42.0 % | 58.0 % (sd=22.4) |

for vestibular function (Fig. 25-Table 1). Thus, formation of the main branches of the SAG function does not require vestibular function, and the status of vestibular signaling does not influence the variable minor branches. Projections of SAG neurons in *pax5* morphants are normal, though the existence of minor branches is seen more frequently than in control embryos (Fig. 25-Table 1). At present, I cannot explain the significance of the ratio of the two different projection patterns. Nevertheless, vestibular deficits in *pax5* morphants do not appear to be caused by the aberrant projection of SAG neurons to the hindbrain.

SAG processes also innervate hair cells in the ear and can be observed by several neuronal markers. Acetylated tubulin is localized in the cortex and cilia of hair cells, as well as axonal processes of SAG neurons (Fig. 25G, H, I, J). In the basal part of hair cells where SAG neurons synapse, dense acetylated tubulin staining is observed, which may be associated with the buton of the hair cell (Fig. 25G). Utricular hair cells in *pax5* morphants often lack this dense staining, and the number of SAG processes is reduced in some specimens (Fig. 25H, I, J). Occasionally, a few axons project aberrantly, failing to innervate hair cells, whereas other axons in the same macula show normal innervation (Fig. 25H). About 20% of observed maculae show very thick dendrites reaching almost to the luminal surface of maculae without contacting any hair cells (Fig. 25I, J). Anti–NCAM labeling, another neuronal marker, demonstrates similar patters of SAG axonal processes (data not shown). To identify whether this targeting problem is specific to the utricular macula or is common in other sensory patches, I examined innervation patterns in other sensory epithelia. Innervation in the saccular macula is hard to detect because

of its close proximity to the bright hindbrain staining in both control embryos and *pax5* morphants. However, SAG innervation to hair cells in cristae is normal in *pax5* morphants (data not shown). These data suggest that deficits in innervation of utricular hair cells could contribute to the observed vestibular deficits in *pax5* morphants.

**Formation of hair cells in the absence of *pax5* function**

Since *pax5* is expressed strongly in hair cells, I hypothesized that *pax5* may regulate normal hair cell development, a function that could also influence SAG neuronal targeting to the hair cell. To test this idea, I analyzed hair cell formation in *pax5* morphants by staining with anti-Pax2 polyclonal antibody, which labels nuclei of mature hair cells (Riley et al., 1999). In *pax5* morphants, hair cells are produced normally in the utricular and saccular maculae at 24 hpf, but subsequently the rate of hair cell production is slower than normal in the utricle (Fig. 26A, B, C). The number of utricular hair cells is consistently reduced by 20-30% relative to uninjected control embryos ($p<0.05$). In contrast, the number of saccular hair cells is not significantly different from control embryos through at least 72 hpf (Fig. 26C). To confirm numbers of hair cells, I used two other markers to stain hair cell cilia, anti-acetylated tubulin and phalloidin. First I used these markers to count hair cells in control embryos to compare with data based on Pax2-staining. Consistent numbers of hair cells are detected by all markers at 30 hpf. At later times, however, the number of saccular hair cells detected by acetylated tubulin or phalloidin-staining greatly exceeds the number of Pax2-postitive cells. At 72 hpf, for example, there are only 2-4 Pax2-positive cells in the saccule, whereas 28 ± 4.8 hair

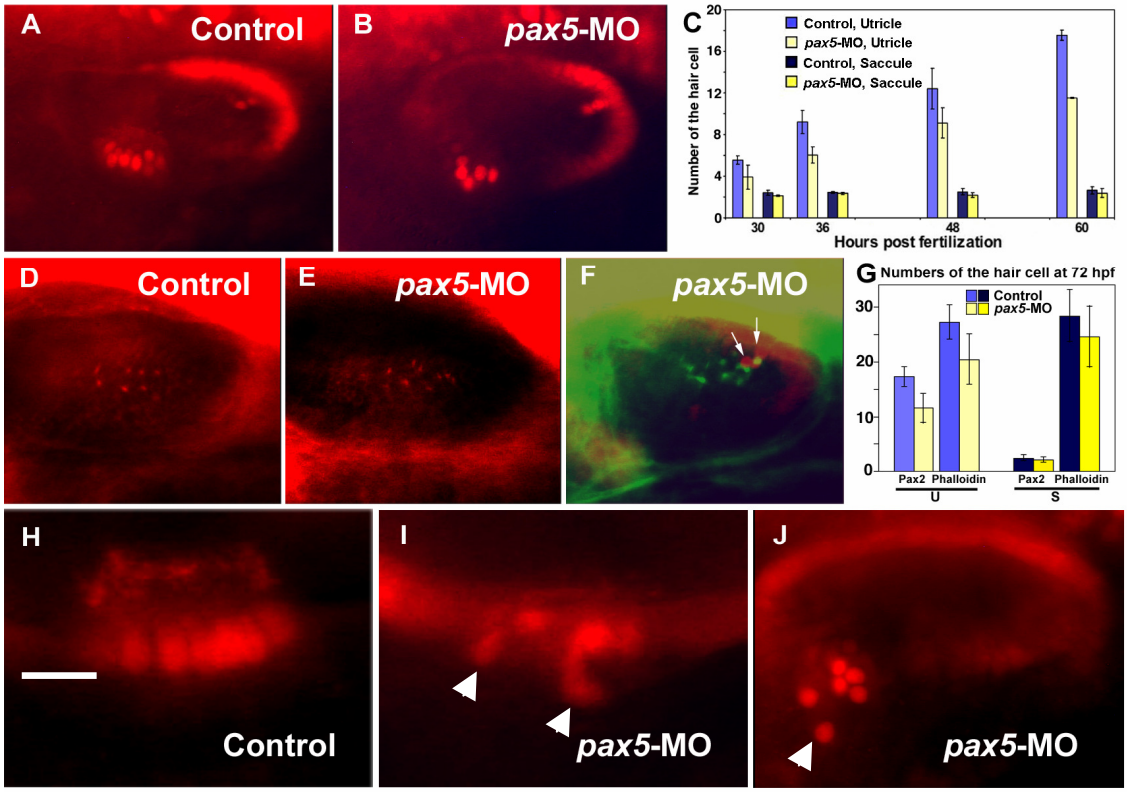


**Fig. 26**. Assessment of hair cell development. (A, B) Anti-Pax2 staining in the otic vesicle at 48 hpf in controls (A) and *pax5* morphants (B). (C) Time course of hair cell production in the utricle and the saccule visualized by anti-Pax2 staining. Error bars represent standard error of means. P-values for the comparison of control hair cell numbers and hair cell numbers in *pax5* morphants are: utricle, p=0.042 (30 hpf), p=0.009 (36 hpf), p=0.0007 (48 hpf), p=0.017 (60 hpf), saccule, p=0.136 (30 hpf), p=0.138 (36 hpf), p=0.05 (48 hpf), p=0.28 (60 hpf). (D, E) Rhodamine-phalloidin staining in the saccular macula of control embryos (D) and *pax5* morphants (E) at 48 hpf. 21.5±5.0 hair cells were observed in the utricular macula and 17.8±9.7 in the saccular macula of controls. In contrast, the number of hair cells in *pax5* morphants decreased significantly in the utricle (16.8±4.5), but not in the saccule (14.78±7.5). (F) Saccular maculae double stained with anti-acetylated tubulin (green) and anti-Pax2 (red) in *pax5* morphant at 48 hpf. (G) Comparison of hair cell numbers in the utricle (U) and saccule (S) observed by anti-Pax2 and phalloidin staining, in *pax5* morphants and uninjected controls. (H-J) Enlarged view of utricular macula stained with anti-Pax2 at 48 hpf in uninjected control (H) and morphant (I). Otic vesicle of *pax5* morphant stained with anti-Pax2 at 36 hpf (J). Arrowheads mark misplaced hair cells. Images show dorsolateral (A, B, D-F, J) and lateral (H, I) views with anterior to the left. Scale bar, 40 µm (A, B, D-F), 12.5 µm (H, I), 25 µm (J).

cells are detected by phalloidin-staining. In the utricle, all three markers showed a similar rate of accumulation of hair cells, although the number of Pax2-positive cells lagged slightly behind the other makers. I do not know the functional significance of the small number of Pax2-positive hair cells in the saccule but note that the pattern of Pax2-staining is similar to the pattern of *pax5* expression. I next used these cilia markers to reexamine hair cell numbers in *pax5* morphants. This confirmed that *pax5* morphants show a 20-30% decrease in hair cells in the utricle but show no significant differences in the saccule (Fig. 26D-G).

Anti-Pax2 staining also demonstrates that *pax5* morphants have irregular arrangements of hair cells in utricular macula. In a fraction of *pax5* morphants ($22.9 \pm 8.3\%$), one or two hair cell nuclei are localized in the basal layer or even outside of the otic vesicle. In some cases, nuclei of misplaced cells show severely deformed shapes and weakened Pax2 staining, suggesting these cells may be sick or dying (Fig. 26I, J). Interestingly, misplaced hair cells are usually accompanied by the appearance of abnormal processes of SAG neurons (Fig. 25J). Ejection of hair cells undergoing apoptosis has been described in previous studies. In mouse and guinea pig, for example, apoptotic hair cells sink to the basal layer within the sensory epithelium (Sobkowicz et al., 1992, Sobkowicz et al., 1997, and Quint et al., 1998). In zebrafish *mind bomb* (*mib*) mutants, supernumerary hair cells formed by loss of lateral inhibition die after 36 hpf and are extruded from sensory epithelia to the underlying mesenchyme (Haddon et al., 1998a). Therefore, the reduced number and misplaced position of hair cells led me to examine the pattern of cell death in utricular maculae of *pax5* morphants.

**Pax5 is required for the survival of hair cells**

To examine the pattern of cell death, embryos were stained with the vital dye, acridine orange (AO). In control embryos, AO positive cells are mostly detected in the medioanterior region of the otic vesicle, which could be the vesicle wall, or outside the vesicle, possibly SAG neurons, and sparsely in other regions at 48 hpf (Fig. 27G). About 5.4 to 7.7% of control embryos (depending on the stage) show single AO positive cells in the utricle, but there is never more than one labeled cell in the macula at any time examined between 30 hpf and 72 hpf. In contrast, the amount of cell death in *pax5* morphants is increased specifically in the utricular macula but not elsewhere in the vesicle (Fig. 27G). 31.2 to 37.1% of *pax5* morphants showed labeled cells in the utricular macula (30 hpf – 48 hpf). Furthermore, *pax5* morphants often contain multiple dying cells in the utricular macula. The saccular macula shows no detectable cell death in either uninjected embryos or *pax5* morphants (Fig. 27A, D). At 72 hpf, the fraction of *pax5* morphants showing cell death is slightly reduced ($21.9 \pm 2.7\%$). Similar results were obtained with wholemount TUNEL assays, which show that 40% of *pax5* morphants have apoptotic cells in utricle at 48 hpf (Fig. 27B, E). I hypothesized that these dying cells correspond to misplaced hair cells. To test this, AO- stained embryos were photographed to record positions of dying cells, then fixed and stained for Pax2. *pax5* morphants with no cell death show normal hair cell arrangements (n=14). In contrast, misplaced hair cells were detected in the corresponding position where AO positive cells had been detected (12 out of 19 embryos, Fig. 27C, F). The remainder of *pax5* morphants (7 out of 19 embryos) showed normal patterns of hair cells. Dying

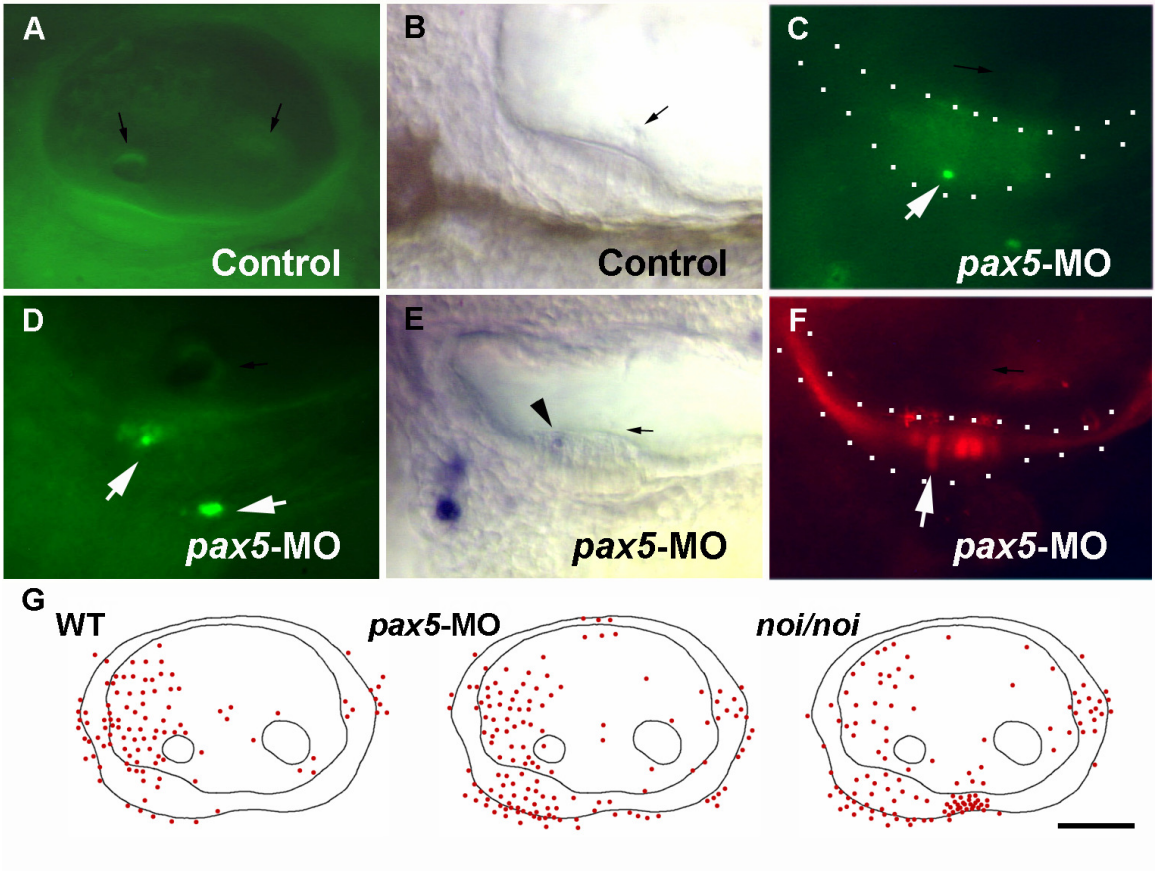


**Fig. 27.** Analysis of cell death in *pax5* morphants. Acridine orange staining and TUNEL assay in uninjected controls (A, B) and *pax5* morphants (D, E), respectively. White arrows indicate AO positive cells (D) and arrowhead shows a TUNEL-positive cell (E). Otic vesicle (A) and utricular maculae (B-F) at 48 hpf. (C, F) *pax5*-MO injected embryos stained with acridine orange at 48 hpf (C), and subsequently immunostained with anti-Pax2 (F) show that cells undergoing apoptosis are ejected from the macula. Utricular macula is indicated by the dotted line. Black arrows mark the otoliths and white arrows indicate a AO positive cell and a misplaced hair cell respectively. (G) Cumulative data (n=30) representing frequency and distribution of acridine orange labeled cells in the otic vesicle of wild-type, *pax5* morphant and *noi/noi,* at 48 hpf. The positions of labeled cells (red spots) were projected onto otic vesicle maps. All images show lateral views, with anterior to the left. Scale bar, 40 µm (A), 25 µm (B, E, D), 30 µm (C, F), 47 µm (G).

cells in these embryos may correspond to other cell types, normally positioned hair cells in early stages of apoptosis, or displaced hair cells that have lost Pax2 as they die. These data suggest that utricular hair cells in *pax5* morphants undergo a higher rate of apoptosis and that dying hair cells are ejected from the utricular macula.

### *pax5* mRNAs rescue defects in *pax5* morphants

I wanted to verify that deficits in *pax5* morphants are due to reduced function of *pax5* and not due to nonspecific morpholino toxicity. Therefore, I injected *pax5* variant 1 and variant 2 mRNAs to try to rescue *pax5* morphants. In the majority of injected embryos, misexpression of *pax5* has no effect on morphology. Nevertheless, *pax5* mRNA restores hair cell numbers in *pax5* morphants to normal at 32 hpf ($p=0.47$, wild-type vs. rescued embryos, Table 3). The fraction of embryos showing cell death in the utricular macula was reduced (21.7%) to half of the level otherwise seen in *pax5* morphants, a significant difference ($p<0.05$). At 48 hpf, the effects of *pax5* mRNAs are less evident (Table 3). This is probably because injected RNAs rarely persist beyond 24 to 30 hpf, whereas morpholinos often continue to function past 3 days. Although the ability to rescue vestibular function could not be properly evaluated due to the limited stability of mRNA, *pax5* mRNAs clearly rescues early defects in the *pax5* morphants. This validates the specificity of *pax5* morpholinos to knock down *pax5* function.

**Table 3.** Rescue of *pax5* morphants by mRNA injection. *pax5* mRNAs (*pax5*-v1,10 pg + *pax5*-v2, 10 pg) were coinjected with *pax5* morpholinos. *pax5* mRNAs and *pax5* morpholinos were injected separately in to the same batch of wild-type embryos as a control. The average number of hair cells was determined by anti-Pax2 labeling (italicized). Percentages represent hair cell numbers normalized by the numbers in wild-type. Cell death was assessed by acridine orange staining at 32 hpf and 48 hpf. Values represent the fraction of embryos showing cell death in the utricular macula. Statistical significance is shown as p value, $^{++}$= wild-type vs *pax5*-MO; *= wild-type vs *pax5*-MO+*pax5* RNA; **= wild-type vs *pax5* RNA; ‡= *pax5*-MO vs *pax5*-MO+*pax5* RNA; ‡‡= *pax5*-MO+*pax5* RNA vs *pax5* RNA.

| | | **WT** | ***pax5*-MO** | ***pax5*-MO +*pax5* RNA** | ***pax5* RNA** |
|---|---|---|---|---|---|
| **Number of hair cells in the utricular macula** | 32 hpf | **100** % *6.8 ± 0.8* | **79.5** % *5.4 ± 0.4* ++p=0.008 | **101.5** % *6.9 ± 0.7* *p=0.474 ‡p=0.013 | **107.4** % *7.3 ± 0.67* **p=0.254 ‡ ‡p=0.297 |
| | 48 hpf | **100** % *14.6 ± 1.1* | **70.5** % *10.3 ± 0.7* ++p=0.023 | **79.5** % *11.6 ± 0.8* *p=0.045 ‡p=0.118 | **nd** |
| **Number of hair cells in the saccular macula** | 32 hpf | **100** % *2.3 ± 0.3* | **100** % *2.3 ± 0.2* ++p=0.492 | **100** % *2.3 ± 0.1* *p=0.434 ‡p=0.422 | **100** % *2.3 ± 0.3* **p=0.493 ‡ ‡p=0.428 |
| | 48 hpf | **100** % *2.1 ± 0.1* | **104.8** % *2.2 ± 0.3* ++p=0.386 | **95.2** % *2.0 ± 0.2* *p=0.242 ‡p=0.242 | **nd** |
| **Cell death** | 32 hpf | **5.42** % *± 1.77* | **37.1** % *± 4.91* | **21.7** % *± 10.9* ‡p=0.032 | **4.00** % |
| | 48 hpf | **7.69** % | **31.2** % *± 11.4* | **26.2** % *± 4.5* ‡p=0.268 | **nd** |

**Mutant study for upstream regulators, *pax2a* and *fgf3***

Previous studies have identified two potential upstream regulators of *pax5*, *pax2a* and *fgf3*. Knocking down *fgf3* function by morpholino injection diminishes the expression of *pax5* in the ear (Kwak et al., 2002). Similarly, *noi* (*pax2a*) mutants show a complete loss of *pax5* expression in the ear (Pfeffer et al., 1998; and Fig.28A). Therefore, I speculated that these mutants might display defects similar to those of *pax5* morphants. *noi* mutants initially produce more hair cells than normal due to weakened lateral inhibition (Riley et al 1999). Thus, *noi* mutants produce an average of $6.0 \pm 0.8$ utricular hair cells by 30 hpf, compared to $4.9 \pm 0.8$ in the wild-type. However, *noi* mutants subsequently show a deficit of hair cells, forming $16 \pm 3.4$ utricular hair cells at 48 hpf compared to $22 \pm 2.7$ in the wild-type (Fig. 28E, F). I hypothesized that this apparent loss of hair cells results from apoptosis. Increased cell death in the ear of *noi* mutants was observed in the utricular macula, and putative regions for posterior and lateral cristae (Fig. 27G) and mutants with dying cells in the utricular macula constituted about 35% of all examined *noi* mutants at 48 hpf (Fig. 28C). The fraction of *noi* mutants showing cell death declines by 72 hpf (13.3%). TUNEL assay revealed similar results (Fig. 28D). Misplaced nuclei of hair cells cannot be visualized in *noi* mutants due to the absence of Pax2a. Nevertheless, acetylated tubulin staining in the hair cell cortex suggests a disorganized pattern of hair cells. Whereas the cortex staining of hair cells with anti-acetylated tubulin is readily visible, SAG projections to the utricular macula are barely detectable. When present, they show disorganized patterns (data not shown). Not only projections to the macula, but projections to the hindbrain are also significantly

distorted (Fig. 28B). This likely reflects aberrant hindbrain development in *noi* mutants. Since morphology of *noi* mutants is severely altered and embryos begin to die by day 3, vestibular function cannot be tested.

Recently an *fgf3* null mutant, *lim absent* (*lia*) was identified (Wiebke et al., 2004). Consistent with the result of *fgf3* morpholino injection, *lia* mutants display decreased *pax5* expression in the otic vesicle (Fig. 28I) and in rare cases, *pax5* transcripts are almost ablated (Fig. 28J). *lia* mutants produce fewer hair cells ($2.6 \pm 0.5$, 30 hpf) in the utricular macula than wild-type ($5 \pm 0.6$, 30 hpf) (Fig. 27G and H). Projections of SAG neurons to the hindbrain are normal, though minor secondary branches were more common than in the wild-type (Fig. 25-Table1). Nonetheless, *lia* mutants do not show increased cell death in the utricular macula (Fig. 28K, L) or misplaced hair cells (data not shown), and show normal projections of SAG neurons to hair cells by 72 hpf. These data suggest that the residual level of Pax5 is sufficient to maintain hair cells in the utricular macula, and thus, the reduced number of hair cells is not because of hair cell death. Fgf3 is implicated in hair cell formation and hence, its loss may be sufficient to explain the deficiency of hair cells. The vestibular function of *lia* mutants is more severely impaired than *pax5* morphants (Fig. 23). However, I note that by day 2 utricular and saccular otoliths fuse in *lia* mutants. Combined with the reduced number of utricular hair cells and abnormal hindbrain patterning, these late stage otolith defects are likely to contribute to the severe vestibular deficits in *lia* mutants.

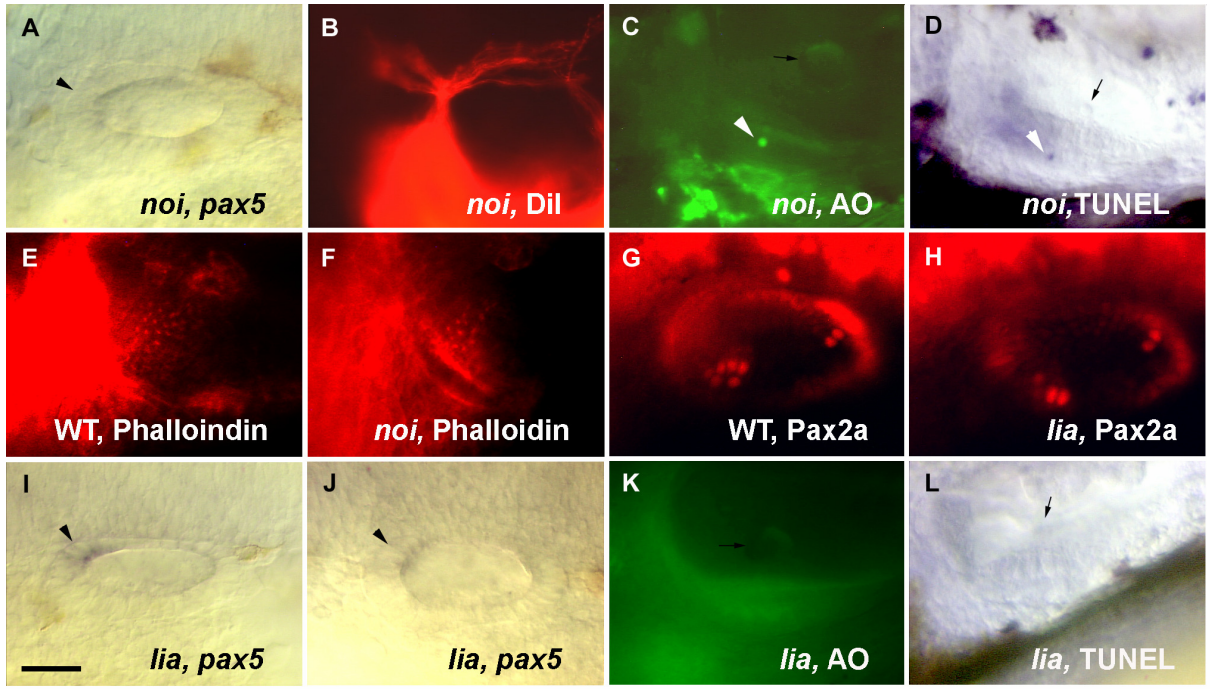


**Fig. 28.** Otic development in *noi* (*pax2a*) and *lia* (*fgf3*) mutants. Otic expression of *pax5* in *noi* (A) and *lia* (I, J) homozygous mutants at 24 hpf (indicated by black arrowhead). Neuronal projections of the SAG to the hindbrain, labeled with DiI, in *noi* mutants at 72 hpf (B). Acridine orange staining (C, K) and TUNEL analysis (D, L) in *noi* and *lia* mutants, respectively. White arrowheads indicate apoptotic cells and arrows mark the anterior otolith. (E, F) Rhodamine-phalloidin labeling in the utricular macula, at 48 hpf, of wild-type (E) and *noi* homozygous mutants (F). An average of 16.3±3.3 hair cells were seen in the utricle of *noi* compared to 22.3±2.7 hair cells in wild-type. The average number of hair cells in the saccule was 15.6±2.1 and 9.3±2.3 at 48 hpf in wild-type and *noi/noi*, respectively. (G, H) Otic vesicle immunolabeled with anti-Pax2 at 30 hpf in wild-type (G) and *lia* mutants (H). *lia* showed a reduction in the average number of utricular hair cells (2.4±0.5) compared to wild-type (5±0.6). However, numbers of saccular hair cells were similar in wild-type (2.6±0.5) and *lia* mutants (2.4±0.5). Images show dorsolateral (A, B, E-H, I, J) and lateral (C, D, K, L) views, with anterior to the left. Scale bar, 30 µm (A, I, J, G, H), 50 µm (B), 25 µm (C-F, K, L).

# DISCUSSION

## Sensory patch specific maintenance of hair cells

In this report, I demonstrated the impairment of utricular hair cell development in the absence of *pax5* function. In *pax5* knockdown embryos, utricular hair cells form but later begin to die. I do not see wholesale loss of hair cells in the utricle, probably because of ongoing developmental expansion of the macula and regeneration of lost hair cells. Globally misexpressing *pax5* in wild-type embryos did not affect the formation of hair cells in the utricular macula or in any other sensory patches. Nevertheless, misexpressed *pax5* rescues cell death in the utricular macula of *pax5* morphants, resulting in restoration of utricular hair cell numbers. Together, these data suggest that *pax5* regulates the maintenance rather than the formation of hair cells, and its function specifically affects the utricular macula. Previously, some genes have been reported for their function in hair cell maintenance. In the mouse, *Brn-3c* is required for the survival of hair cells in all auditory and vestibular sensory patches although auditory hair cells are affected more severely (Xiang et al., 1998). In a gene expression profiling experiment, *Gfi1* was identified as a downstream target of *Brn-3c* (Hertzano et al., 2004). Although *Gfi1* is expressed in all vestibular and auditory hair cells, ablation of this gene function causes cell death only in cochlear hair cells (Wallis et al., 2003). The cochlear phenotype of $Gfi1^{-/-}$ mutants is very similar to that of $Brn\text{-}3c^{-/-}$ mutants implying that *Brn-3c* regulates maintenance of cochlear hair cells through *Gfi1* function. The fact that *Gfi1* seems dispensable for hair cell survival in other sensory region suggests that

each sensory region is maintained by a specific combination of maintenance factors. I have shown that Pax5 is a maintenance factor required specifically by utricular hair cells which may compose a specific utricular combinatory code for hair cell maintenance.

**Pax2 function in hair cell survival**

I showed that *pax2a* is also preferentially expressed in utricular hair cells after 30 hpf although some hair cells in other sensory patches, the saccular macula and three cristae express *pax2a* as well. It was previously shown that *pax2a* is required for normal *delta* expression in the newly forming hair cells which in turn regulates lateral inhibition (Riley et al., 1999). Even after initial hair cell formation and lateral inhibition, *pax2a* expression persists in the hair cell suggesting a later role in maintenance of the hair cell. In fact, *noi* (*pax2a*) mutants show increased cell death in the utricular macula as well as in other sensory patches. In the utricular macula, *pax2a* appears to regulate the survival of hair cells through its down stream regulator *pax5,* since the cell death rate in *pax5* morphants and *noi* mutants are comparable in the utricular macula. In the mouse and chick, the expression and function of *Pax2* have been described most extensively in the cochlea. Recently, its expression was re-examined and was found in hair cells of all sensory epithelia (Lawoko-Kerali et al., 2002; Burton et al., 2004; Sanchez-Calderon et al., 2005). However, its role in hair cell maintenance per se cannot be addressed in *Pax2* null mice because of severe agenesis of the cochlea. The sensory epithelia that do form (utricular macula and cristae) have not been examined in sufficient detail to determine whether there are defects in hair cell patterning or survival.

Mouse ears express two *Pax* genes, *Pax2* and *Pax8* whereas there are 4 *pax* genes, *pax2a*, *pax2b*, *pax5* and *pax8* expressed in the zebrafish ear. Despite these differences, it is likely that many of the same processes are regulated by different sets of *pax* genes in fish versus mouse. It is still unclear whether the role of *pax5* has been conserved. In *Xenopus*, *Pax5* expression in the otic vesicle has been reported (Heller and Brandli, 1999) and recent gene expression profiling data for the chick utricle and the cochlea indicate *Pax5* expression in the ear (http://hg.wustl.edu/lovett/projects/nohr/inner_ear_ratio.html). *Pax5* is not detected in the mouse ear during embryonic development. It is possible that mouse represents a derived state where in *Pax5* is no longer utilized in otic development. Alternatively, it is possible that a subtle role during post embryonic development has been overlooked. Although *Pax5* null mice have no hearing defects, they show abnormal limb reflex (Urbanek et al., 1994). This defect has been attributed to defects in brain development, but the possibility remains that vestibular sensory epithelia are also compromised.

**The pattern of utricular SAG projections**

I demonstrated two patterns of the central projection of utricular SAG neurons, one with limited anterior and posterior projections and the other with multiple parallel projections. These patterns were independent of stage and did not require vestibular activity. Among the examined mutants, only *noi* showed severely distorted projection patterns. Since this mutant does not have midbrain hindbrain boundary and *pax2a* is expressed in the spiral ganglia throughout the hindbrain, SAG projection defects is presumably because of

impaired hindbrain development. Another possibility is that general deteriorations in *noi* embryo bodies around 3 dpf, indirectly affect SAG central projections.

Although the central projection of the SAG is relatively normal, these neurons often show aberrant innervations in the utricle of *pax5* knockdown embryos. Axonal processes sometimes reach to the luminal surface of the macula. In addition, thick bundles of processes were observed in the vicinity of dying hair cells. Since *pax5* is strongly expressed in the hair cell but not in the SAG, this defect is likely a consequence of the hair cell death in the utricular macula. Absence or displacement of target hair cells probably contributes to disorganization of processes in the macula. Similar defects were observed in *Brn-3c* mutants, which show hair cell death in all sensory epithelia (Xiang et al., 2003). Axons of the spiral ganglion are disorganized and later retracted from the outer hair cell layers where the hair cell death is the most severe among the sensory epithelia. In the inner hair cell layers, axons show aberrant aggregations and sometimes bypass inner hair cells invading to the outer hair cell layers.

**Upstream regulator of *pax5* expression**

In my previous study, I demonstrated that knocking down of *fgf3* function by injecting morpholinos caused reduction in *pax5* expression (Kwak et al., 2002). A null mutant for *fgf3, lia,* also showed a range of reduction confirming that *fgf3* is required for a normal level of *pax5* expression (Fig. 28I, J). In contrast, completely ablated *pax5* expression in *noi* mutants implies that *pax2a* is absolutely necessary for *pax5* induction (Pfeffer et al., 1998; Fig. 28A). Although initial *pax2a* expression in the otic placode is regulated by

Fgf signaling (Phillips et al., 2001; Leger and Brand, 2002), *pax2a* expression in the otic vesicle is independent of Fgf signaling (Leger and Brand, 2002). Therefore, it appears that *fgf3* and *pax2a* control *pax5* expression via parallel pathways. While *noi* mutants show comparable defects in hair cell survival to those of *pax5* knockdown embryos, *lia* mutants display little or no hair cell death. This is likely because that residual expression of *pax5* in *lia* is sufficient for maintaining utricular hair cells and *pax5* morpholinos blocked *pax5* function to the level below that in *lia* mutants.

# CHAPTER V

# SUMMARY OF EXPERIMENTS AND DISCUSSION

## SUMMARY OF FINDINGS

This study investigates the function of *pax2/5/8* genes in various stages of inner ear development, and their genetic interaction with Fgfs, the main otic regulatory signaling molecules. Previous studies demonstrated that Fgf3 and Fgf8 are expressed in the hindbrain, and they are necessary and sufficient to induce otic cells and *pax2/8* gene expression in the presumptive otic region (Phillips et al., 2001; Leger and Brand, 2002; Maroon et al., 2002; Phillips et al., 2004). These data suggested the involvement of *pax2/8* genes in Fgf signaling to induce otic cells, but the functions of *pax2/8* genes had not been identified. Therefore, I investigated the function of *pax2/8* genes in early otic development as presented in chapter II. Initially, *pax8* function is required for normal otic induction, and subsequently *pax8*, *pax2a,* and *pax2b* act redundantly to maintain otic fate. After otic cells are induced, Fgf3 is continuously expressed in the hindbrain. This led me to postulate a later role for Fgf3 in otic development. In chapter III, I showed that Fgf3 from the hindbrain specifies anterior fates in the otic vesicle, regulating expression of several genes and promoting hair cell formation in the otic vesicle. *pax5* is one of the genes controlled by later Fgf3 function in the otic vesicle. In chapter IV, I

demonstrated that *pax5* is a survival factor required for utricular hair cells. In summary, this study has expanded our understanding of the molecular mechanisms of otic development, and how *Pax* genes function at multiple stages of organogenesis.

## GENOMIC STRUCTURE AND SPLICE VARIANTS OF *pax2/5/8* GENES

In this study, the sequences of zebrafish *pax8* and *pax5,* which were partially identified previously (Pfeffer et al., 1998), were completed, and their various splice variants were cloned. Vertebrate *Pax2/5/8* genes are composed of 10 exons encoding conserved functional domains and one or two additional gene specific exons (Fig. 29).

Among *pax2/5/8* gene family members in zebrafish, *pax8* shows the most divergent gene structure compared to other vertebrate *pax8* genes. Exon 3 of *pax8,* which encodes the C-terminal half of the paired domain, is subdivided into two exons (exon 3 and exon 4) in zebrafish *pax8*. Furthermore, two additional exons (exon 1a and exon 1b) for 5' UTRs were identified. These two exons and a conventional exon 1 (exon 1c) are subject to alternative splicing yielding to two alternative translation start sites, in exon 1c and exon 2, respectively. In combination with splicing in the 5'end region, extensive splicing in the 3'end region (transactivation and inhibitory domain) produces at least 10 different splice variants of zebrafish *pax8*.

Among them, *pax8* variant 1.1 is the predominant splice variant by 24 hpf. Since exon 1c with the conventional start site is spliced out, *pax8*-v1.1 appears to use a methionine at position 10 of the paired domain (exon 2) for its translation. Thus, this protein has a partial paired domain with altered DNA binding properties (Kozmik et al., 1997). The second prevalent splice form is *pax8*-v2.1 which has the conventional Pax8 protein structure. Since splice variant specific RNA probes or antibodies are not available, it is not clear whether different forms are expressed in the otic region. However, knocking down *pax8*-v2 variants together with *pax8*-v3 variants or *pax8*-v1 variants alone results in formation of small otic vesicles, and knocking down all 10 variants causes much greater reduction in otic vesicles. These findings suggest that splice variants with a whole paired domain and with a partial paired domain function together in otic induction. Interestingly, knocking down the function of *pax8*-v2 and *pax8*-v3 variants induces smaller otic vesicles than those in *pax8*-v1 variant knockdown embryos. In addition, *pax8*-v1 variant depleted embryos show otolith formation defects, which were not seen after knockdown of *pax8*-v2 and *pax8*-v3 variants. These data suggest that each splice variant has some unique function although these functions are as yet unknown.

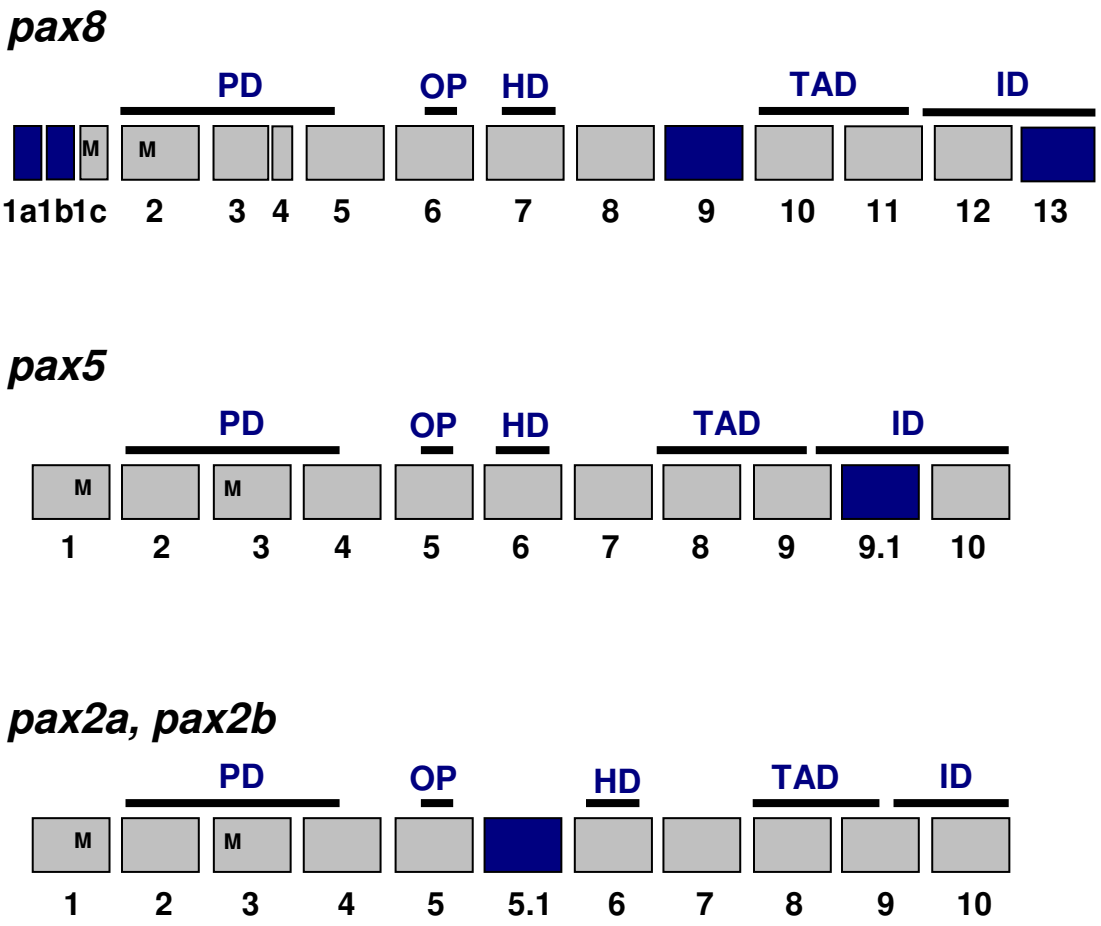


**Fig. 29.** Gene structures of *pax2/5/8*. Schematic diagrams to show exonic structures and domain organization of *pax8*, *pax5*, *pax2a,* and *pax2b*. Gray boxes represent conserved common exons among *pax2/5/8* genes ,and blue boxes represent gene specific exons. Black lines indicate locations of each functional domain. M: translation start site, PD: paired domain, OP: octapeptide domain, HD: homeobox domain, TAD: trans-activation domain, ID: inhibitory domain.

I cloned the full sequence of zebrafish *pax5* and found that all exon–intron boundaries are conserved among vertebrate *pax5* genes. In addition, two splice variants of zebrafish *pax5,* *pax5*-v1, and *pax5*-v2, which are homologous to mouse variants *Pax-5a* and *Pax-5b,* were identified. These findings suggest that the pattern of splicing as well as the genomic structure is conserved among vertebrate *pax5* genes.

11 exons compose *Pax2* genes in all vertebrates. In zebrafish, 12 *pax2a* splice variants have been identified (Lun and Brand, 1998). Although no data about *pax2b* splice variants are available, premature *pax2b* mRNA must be processed by various alternative splicing. It is interesting to note that extensive splicing events occur in the paired domain, the transactivation domain, and the inhibitory domain in all *Pax2/5/8* genes suggesting that the regulation of this gene family function is finely tuned by changing DNA and protein binding specificity.

## *pax2/5/8* GENE FUNCTIONS IN OTIC DEVELOPMENT; SPECIFICITY AND REDUNDANCY

In developmental processes, many genes play specific roles, but at the same time, they show functional redundancy with their homologous genes. This study identified specific and redundant functions among *pax2/5/8* genes in zebrafish inner ear development. In *pax8* depleted embryos, a reduced number of otic cells are induced in the preotic region

indicating that *pax8* function is required for normal otic induction. Depletion of *pax8* function together with *pax2a* and/or *pax2b* exposed another *pax8* function in the maintenance of otic cells. This experiment also revealed the requirement of *pax2a* and *pax2b* function in maintaining otic cells. The fact that any single *pax* gene knockdown does not show this maintenance problem indicates that these three *pax* genes play a redundant role to maintain otic fate and any one gene loss can be compensated for by the others. These findings suggest that all *pax2/5/8* genes have a common potential to regulate the same processes. This idea is further supported by the fact that they can bind to the same DNA sequence (Phelps and Dressler, 1996) and in the mouse, *Pax5* knocked into the *Pax2* locus can substitute for *Pax2* function (Bouchard et al., 2000).

In spite of the conserved structure and function, each *pax2/5/8* gene has specific functions even though they are co-expressed. The expression pattern of *pax2a* and *pax2b* are very similar in the otic placode and the otic vesicle, and their expression overlaps that of *pax5* in the utricular macula. However, downregulation of any one gene function impairs hair cell differentiation in different ways. *pax2a* null mutations initially cause overproduction of hair cells due to weakened lateral inhibition, (Riley et al., 1999) whereas injection of *pax2b* morpholinos impairs hair cell specification (Whitfield et al., 2002). This study demonstrated that *pax5* regulates hair cell survival in the utricular macula under the control of *pax2a.* These observations suggest that *pax2a*, *pax2b,* and *pax5* play different roles in the utricular macula at the same time. This specificity must be controlled by different binding affinities to target DNAs and cofactors which are optimized for the specific function of each gene.

## GENETIC INTERACTIONS IN OTIC INDUCTION

There are many transcription factors identified in the otic region besides *pax2/5/8* genes. By examining *pax2/5/8* gene interactions with other otic genes, I demonstrated that *pax2/5/8* genes function in genetic network under the control of Fgfs. Based on my findings and data from previous studies, two phases for otic induction are hypothesized: initial otic induction and maintenance (Fig. 30).

In the initial induction phase, *foxi1*, *pax8, dlx3b, dlx4b*, *sox9a,* and *sox9b* appear to function together to induce a certain number of otic cells (Liu et al., 2003; Solomon et al., 2004). A fork head domain transcription factor, *foxi1* is initially expressed in the anteroventral region of embryos from early gastrula stages. In late gastrula stages, *foxi1* expression increases in the region lateral to the hindbrain, which encompasses the preotic domain, and decreases in other ventral regions. Ablation of Foxi1 function blocks *pax8* expression completely, implicating Foxi1 as an upstream regulator of *pax8* expression (Solomon et al., 2003). Furthermore, *pax2a*, *dlx3b* and *dlx4b* require Foxi1 function for their normal otic expression. Anteroventral expression of *foxi1* is similar to the expression of Bmp ligands, and Bmp signaling mutants lacks *foxi1* expression (Riley and Phillips, 2003). Thus, Bmp signaling appears to be a regulator of *foxi1*. Whether Fgf3 and Fgf8 affect the otic expression of *foxi1* is ambiguous, for knocking down Fgf function does not affect *foxi1* expression but misexpressed Fgf does induce ectopic *foxi1* expression. Therefore *foxi1* is likely just a weak ventralizing factor modifying the response to localized Fgf signal. Otic expression of *dlx3b, dlx4b*, *sox9a,* and *sox9b*

appears after *pax8* expression begins (Solomon and Fritz, 2002; Liu et al., 2003). *dlx3b* and *dlx4b* are already expressed in a common preplacodal region from late gastrula stages before *pax8* otic expression. This early expression of *dlx3b* and *dlx4b* is independent of Fgf signaling and probably reflects an interaction of Bmp and dorsal factors. After *pax8* expression, they are upregulated in the otic region (Solomon and Fritz, 2002). Thus, together with Foxi1, amplified Fgf signal, through *pax8* function, controls this upregulation as well as *sox9a* and *sox9b* otic expression. Moreover, *dlx3b/4b* and *sox9a/b* crossregulate each other's expression and synergistically function to regulate *pax2a* expression (Solomon and Fritz, 2002; Liu et al., 2003). Because loss of any one of the above gene functions does not ablate the otic placode, each gene seems to contribute in parallel to the initial induction.

In the maintenance phase, *pax8*, *pax2a,* and later *pax2b* cooperate to maintain induced otic gene expressions and otic cells. When any one of these *pax* genes is down-regulated in either Fgf3 or Fgf8 compromised mutant, the number of otic cells diminishes gradually. It is likely that downregulation of Fgfs reduces expression levels of *pax2a*, *pax2b,* and *pax8* genes, and the reduction of these *pax* gene functions results in the failure of otic maintenance. *pax8* and *dlx3b* double knockdown mutants form very tiny otic vesicles though they induce reduced but significant numbers of otic cells at 12 hpf. I didn't clarify whether this minute otic vesicle formation is due to proliferation defects or maintenance defects. However, depletion of Pax8 function and reduced *pax2a*

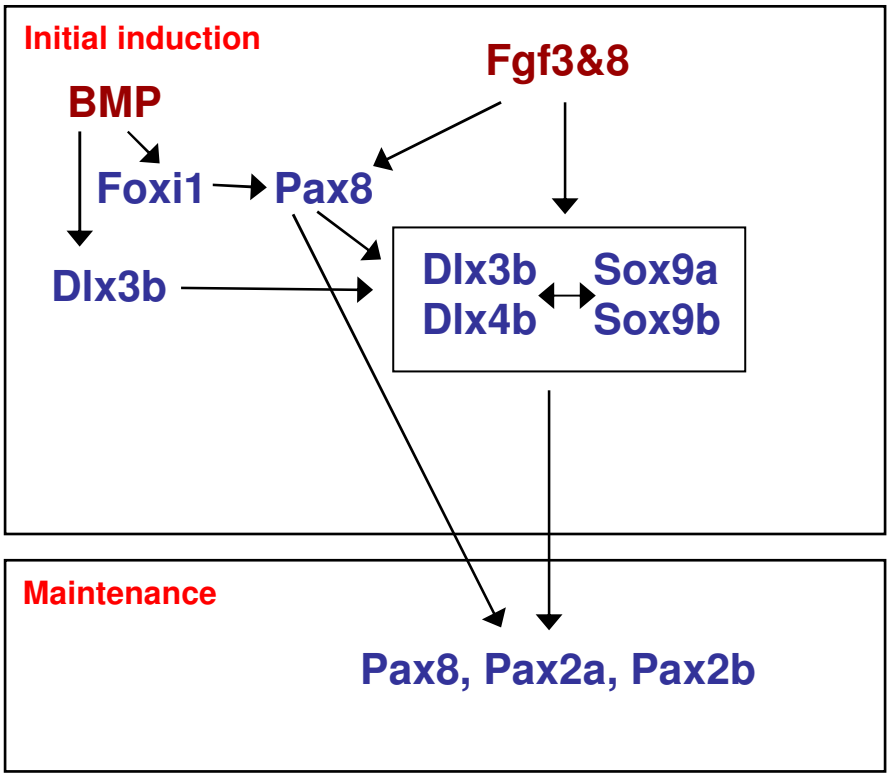


**Fig. 30.** Summary of genetic interactions in otic induction.

expression caused by depletion of Pax8 and Dlx3b function may impair the otic cell maintenance.

## GENETIC INTERACTIONS FOR *pax5* OTIC EXPRESSION

After otic induction, Fgf3 is maintained in the hindbrain in rhombomere 4 as the placode develops, and induces *pax5* in the anterior end of the nascent otic vesicle. *valentino* mutants, in which the *fgf3* expression domain in the hindbrain is expanded, show an enlarged domain of *pax5* expression, and this expanded domain of *pax5* is suppressed by knocking down Fgf3 activity. Furthermore, *pax5* expression in the anterior otic vesicle is significantly downregulated in *fgf3* knockdown embryos and *fgf3*$^{-/-}$ (*lia*) mutants. However, loss of *fgf3* does not ablate *pax5* expression completely, suggesting that other regulatory factors work in conjunction with Fgf3. Fgf8 is a promising candidate for this additional regulatory factor. When *pax5* is expressed in the otic vesicle, *fgf8* is no longer expressed in the hindbrain but appears in the same domain of the otic vesicle as that of *pax5* expression. In addition, an *fgf8* mutant, *ace,* shows slightly reduced *pax5* expression in the otic vesicle but depletion of *pax5* does not alter *fgf8* expression in the otic vesicle (Leger and Brand, 2002). These data suggest that Fgf8 is an upstream regulator of *pax5* expression even though its contribution is weaker than that of Fgf3.

Pfeffer and colleagues found that Pax2a is another regulatory factor of *pax5* otic expression (Pfeffer et al., 1998). *pax2a* is continuously expressed in the otic placode and later becomes restricted to the ventro-medial wall of the otic vesicle, overlapping with the *pax5* expression domain. Ablation of Pax2a function completely blocks *pax5* expression in the otic vesicle (Pfeffer et al., 1998). However, not all *pax2a* expressing cells also express *pax5*. Therefore, Pax2a is necessary but not sufficient to induce *pax5* expression.

As shown previously, *pax2a* is initially induced by Fgf signaling in the preotic region. However, an Fgf signaling inhibitor applied after formation of the placode does not block *pax2a* expression in the otic vesicle (Leger and Brand, 2002). Therefore, *pax2a* expression in the ventro-medial wall of the otic vesicle appears independent of Fgf signaling although the regulatory mechanism is still unclear. Taken all findings together, I hypothesize that *pax2a* provides a competence for *pax5* expression, and Fgf signal instructs *pax5* expression in the localized anterior region of the otic vesicle.

## HINDBRAIN SIGNALING AND OTIC VESICLE PATTERNING

The otic vesicle is formed adjacent to the hindbrain segments rhombomere 4-6. Each hindbrain segment has its own segmental identity and thus it has been postulated that each segment could provide positional cues along the anterior-posterior axis of the otic

vesicle. I showed that Fgf3 from rhombomere 4 specifies anterior fates in the otic vesicle by inducing the expression of anterior markers and suppressing expressions of posterior markers in the otic vesicle. *pax5* expands into posterior territory, and the posterior marker *zp23* is lost entirely in *fgf3* mutants. These expressions affect only medial cells in the otic vesicle, as shown by expression of *nkx5.1*. This gene is normally expressed in the anterior in both medial and lateral walls, but posterior expansion is seen only in the medial wall. Hence, the effect of Fgf3 seems restricted in the medial vesicle wall and therefore, other regulatory factors might regulate A-P axis patterning in the lateral wall of the otic vesicle.

A recent study with chick embryos examined hindbrain effects on otic vesicle axis patterning. Rotation of the hindbrain to reverse the A-P axis did not alter the expression of *Lunatic fringe* (*Lfng*) and *NeuroD* which are in the anterior otic vesicle, suggesting that the hindbrain may not affect A-P axial patterning in the ear (Bok et al., 2005). This result conflicts with my data, which show that hindbrain r4 signaling contributes to A-P axis specification in the zebrafish otic vesicle. However, it is notable that only two anterior makers were examined to make the conclusion in chick embryos. In many cases, genes in the comparable otic vesicle region show different responses to signals from surrounding tissues (Kwak et al., 2002; Hammond et al, 2003). Thus examination of additional A-P axis markers is required to confirm hindbrain effects in chick otic vesicle patterning. It is also possible that A-P axis patterning is already specified before the stage of the hindbrain rotation since the A-P axis is established much earlier than D-V and M-L axes (Harrion, 1936; Wu et al., 1998). Hence, how

manipulation of the hindbrain in earlier stages affects axis patterning in the otic vesicle needs to be investigated further. If the hindbrain affects A-P axis specification in the otic vesicle, unidentified factors in the hindbrain must to be involved in chick embryos. To affect A-P axis of the otic vesicle along hindbrain r4-6 region, signals from the hindbrain need to be restricted to either r4 or r6 region. There are no known signaling molecules restricted in either of these regions in chick embryos. Even *Fgf3*, which was identified as an anterior specifier in the zebrafish otic vesicle, is expressed in the rhombomeres 4-6 abutting most of the medial vesicle wall in chick embryos (Mahmood et al., 1996). Regardless of whether the hindbrain effect on A-P axis patterning is conserved among vertebrates, findings from both chick embryos and zebrafish embryos suggest that signals from other tissues are implicated in the A-P axis specification of the otic vesicle. Considering relative positions, signals from the pharyngeal endoderm could be candidate factors.

## *pax5* AND MAINTENANCE OF HAIR CELLS

Our functional analysis showed that *pax5* is a regulatory factor for hair cell survival and its function is required only for utricular hair cells. There are several hair cell survival factors that have been identified in mouse. All of them are expressed in hair cells of all sensory patches, but their onset of expression and the time of hair cell death in each

mutant are different. Among them, *Brn-3c* is expressed in hair cells from the initiation of hair cell formation (Xiang et al., 1998) and it is known to regulate the transcription of *Gfi1*, another hair cell survival factor (Hertzano et al., 2004). Hair cells in *Brn-3c*$^{-/-}$ mutants and *Gfi1*$^{-/-}$ mutants show defects in differentiation (Xiang et al., 1998; Wallis et al., 2003). Moreover, all cochlear hair cells in both mutants die in early postnatal days whereas vestibular hair cells show slower degeneration than cochlear hair cells. *Barhl1* is expressed in hair cells 2 days after *Brn-3c* expression and hair cell degeneration in *Barhl1* knockout mice begins after postnatal day 6 (Li et al., 2002). These data suggest that there are at least two phases for hair cell maintenance. *Brn3c* and *Gfi1* regulate the early phase as well as hair cell differentiation, and *Barhl1* regulates the later phase of hair cell survival. *pax5* is expressed in the otic vesicle from the time when the first hair cells start to form. In addition, utricular hair cell death is observed at least from 30 hpf and sometimes, cilia markers of the hair cell, anti-acetylated tubulin and phalloidin poorly stain hair cell cilia in *pax5* depleted embryos. Hence, *pax5* seems implicated in the early phase of hair cell maintenance.

There are some questions remaining to understand *pax5* function in hair cells: how does *pax5* maintain utricular hair cells, why do other hair cells not require *pax5* and how is *pax5* related to the function of other known hair cell survival factors, which affect other hair cells as well as utricular hair cells? It has been reported that Pax5 represses *p53* transcription which induces apoptosis in the cell (Stuart et al., 1995). Thus, it is possible that this interaction is conserved in hair cells and *pax5* controls apoptosis by inhibiting *p53*. Another possibility is that *pax5* may regulate hair cell differentiation and

the failure of hair cell differentiation induces hair cell death indirectly. The identification of Pax5 target genes and examination of detail hair cell morphology in *pax5* depleted embryos will provide a better idea how *pax5* functions in hair cells.

The existence of Pax5, a regional factor and commmon factors such as Brn-3c and Gfi1 suggest that each sensory patch maintains its hair cells by a specific combination of maintenance factors. Similarly to *pax5* expression in the utricular macula, *msxC* and *Bmp4* are expressed in cristae from the beginning of cristae formation (Mowbay et al, 2001) suggesting them as candidate survival factors of hair cells in cristae. Unfortunately, downregulation of these gene functions causes early defects, which interfere with their functional study in cristae. Therefore, conditional knockout mutants of these genes in cristae and searching for more genes expressed in a specific sensory patch will facilitate the study of region specific hair cell maintenance. Furthermore, genetic interaction studies between common factors and local factors are also required to understand the mechanism of hair cell survival and maintenance.

## REFERENCES

**Adam, J., Myat, A., Le Roux, I., Eddison, M., Henrique, D., Ish-horowicz, D and Lewis, J.** (1998) Cell fate choices and the expression of Notch, Delta, and Serrate homologues in the chick inner ear: parallels with *Drosophila* sense-organ development. *Development* **125**, 4645–4654.

**Adamska, M., Leger, S., Brand, M, Hadrys, T., Braun, T. and Bober, E.** (2000). Inner ear and lateral line expression o f a zebrafish *nkx5-1* gene and its downregulation in the ears of *fgf8* mutant, *ace*. *Mech. Dev*. **97**, 161-165.

**Akimenko, M.A., Ekker, M., Wegner, J., Lin, W. and Westerfield, M.** (1994). Combinatorial expression of three zebrafish genes related to distal-less: part of a homeobox gene code for the head. *J. Neurosci.* **14**, 3475-3486.

**Alvarez, Y., Alonso, M.T., Vendrell, V., Zelarayan, L.C., Chamero, P., Theil, T., Bosl, M.R., Kato, S., Maconochie, M., Riethmacher, D. and Schimmang, T.** (2003). Requirements for Fgf3 and Fgf10 during inner ear formation. *Development* **130**, 6329-6338.

**Andermann, P., Ungos, J., and Raible, D.W.** (2002) Neurogenin1 defines zebrafish cranial sensory ganglia precursors. *Dev. Biol*. **251**, 45-58.

**Appel, B. and Eisen, J.S.** (1998). Regulation of neuronal specification in the zebrafish spinal cord by *delta* function. *Development* **125**, 371-380.

**Baker, C.V. and Bronner-Fraser, M.** (2001). Vertebrate cranial placodes I. Embryonic induction. *Dev. Biol.* **232**, 1-61.

**Barber, T.D., Barber, M.C., Cloutier, T.E. and Friedman, T.B.** (1999). *Pax3* gene structure, alternative splicing and evolution. *Gene* **237**, 311-319.

**Barr, F.G., Fitzgerald, J.C., Ginsberg, J.P., Vanella, M.L., Davis, R.J. and Bennicelli, J.L.** (1999). Predominant expression of alternative Pax3 and Pax7 forms in myogenic and neural tumor cell lines. *Cancer Res.* **59**, 5443-5448.

**Bever, M.M. and Fekete, D.M.** (2002). Atlas of the developing inner ear in zebrafish. *Dev. Dyn*. **223**, 536-543.

**Bok, J., Bronner-Fraser, M., and Wu, D.K.** (2005) Role of the hindbrain in dorsoventral but not anteroposterior axial specification of the inner ear. *Development* **132,** 2115-2124.

**Bouchard, M., Pfeffer, P. and Busslinger, M.** (2000). Functional equivalence of the transcription factors Pax2 and Pax5 in mouse development. *Development* **127**, 3703-3713.

**Bouchard, M., Souabni, A., Mandler, M., Neubuser, A. and Busslinger, M.** (2002). Nephric lineage specification by Pax2 and Pax8. *Genes Dev.* **16**, 2958-2970.

**Brand, M. Heisenberg, C.-P., Jiang, Y.-L., Beuchle, D., Lun, K., Furutani-Seiki, M., Granato, M., Hafter, P., Hammerschmidt, M., Kane, D., Kelsh, R., Mullins, M., Odenthal, J., van Eeden, F. J. M. and Nüsslein-Volhard, C.** (1996). Mutations in zebrafish genes affecting the formation of the boundary between the midbrain and hindbrain. *Development* **123**, 179-190.

**Brigande, J.V., Keirnan, A.E. Gao, X., Iten, L.E. and Fekete, D.M.** (2000). Molecular genetics of pattern formation in the inner ear: Do compartment boundaries play a role? *Proc. Natl. Acad. Sci. USA* **97**, 11700-11706.

**Burton, Q., Cole, L.K., Mulheisen, M., Chang, W. and Wu, D.K.** (2004). The role of Pax2 in mouse inner ear development. *Dev. Biol.* **272**, 161-175.

**Chi, N. and Epstein, J.A.** (2002). Getting your Pax straight: Pax proteins in development and disease. *Trends Genet.* **18**, 41-47.

**Cordes, S.P. and Barsh, G.S.** (1994). The mouse segmentation gene *kr* encodes a novel basic domain-leucine zipper transcription factor. *Cell* **79**, 1025-1034.

**Cvekl, A., Kashanchi, F., Brady, J.N. and Piatigorsky, J.** (1999) Pax6 interactions with TATA-box-binding protein and retinoblastoma protein. *Invest. Ophthalmol. Vis. Sci.* **40**, 1343-1350.

**Czerny, T., Bouchard, M., Kozmik, Z. and Busslinger, M.** (1997). The characterization of novel *Pax* genes of the sea urchin and *Drosophila* reveal an ancient evolutionary origin of the Pax2/5/8 subfamily. *Mech. Dev.* **67**, 179-192.

**Dahl, E., Koseki, H. and Balling, R.** (1997). *Pax* genes and organogenesis. *Bioessays* **19**, 755-765.

**David, R., Ahrens, K., Wedlich, D. and Schlosser, G** (2001) *Xenopus* Eya1 demarcates all neurogenic placodes as well as migrating hypaxial muscle precursors. *Mech. Dev.* **103**, 180–192.

**Deol, M. S.** (1964). The abnormalities of the inner ear in *kreisler* mice. *J. Embryol. Exp. Morph.* **12**, 475-490.

**Depew, M.J., Liu, J.K., Long, J.E., Presley, R., Meneses, J.J., Pedersen, R.A. and Rubenstein, J.L.R.** (1999). *Dlx5* regulates regional development of the branchial arches and sensory capsules. *Development* **126**, 3831-3846.

**Desplan, C.** (1997) Eye development: governed by a dictator or a junta? *Cell.* 91, 861-864.

**Dorfler, P. and Busslinger, M.** (1996). C-terminal activating and inhibitory domains determine the transactivation potential of BSAP (Pax5), Pax2 and Pax8. *Embo J* **15**, 1971-1982.

**Draper, B.W., Morcos, P.A. and Kimmel, C.B.** (2001). Inhibition of zebrafish *fgf8* pre-mRNA splicing with morpholino oligos: a quantifiable method for gene knockdown. *Genesis* **30**, 154-156.

**Dudley, A.T., Lyons, K.M. and Robertson, E.J.** (1995) A requirement for bone morphogenetic protein-7 during development of the mammalian kidney and eye. *Genes Dev.* **9**, 2795-2807.

**Dupe, V., Ghyselinck, N.B., Wendling, O., Chambon, P. and Mark, M.** (1999) Key roles of retinoic acid receptors alpha and beta in the patterning of the caudal hindbrain, pharyngeal arches and otocyst in the mouse. *Development* **126,** 5051-5059.

**Eberhard, D. and Busslinger, M.** (1999) The partial homeodomain of the transcription factor Pax5 (BSAP) is an interaction motif for the retinoblastoma and TATA-binding proteins. *Cancer Res.* **59**(7 Suppl), 1716s-1724s.

**Eberhard, D., Jimenez, G., Heavey, B. and Busslinger, M.** (2000) Transcriptional repression by Pax5 (BSAP) through interaction with corepressors of the Groucho family. *EMBO J*. **19**, 2292-2303.

**Ekker, M., Akimenko, M.A., Bremiller, R. and Westerfield, M.** (1992a). Regional expression of three homeobox transcripts in the inner ear of zebrafish embryos. *Neuron* **9**, 27-35.

**Ekker, S.C., von Kessler, D.P. and Beachy, P.A.** (1992b). Differential DNA sequence recognition is a determinant of specificity in homeotic gene action. *Embo J* . **11**, 4059-4072.

**Ellies, D.L., Stock, D.W., Hatch, G., Giroux, G., Weiss, K.M. and Ekker, M.** (1997). Relationship between the genomic organization and the overlapping embryonic expression patterns of the zebrafish *dlx* genes. *Genomics* **45**, 580-590.

**Enfors, P.,Van de Water, T., Loring, J. and Jaenisch, R.** (1995) Complementary roles of BDNF and NT-3 in vestibular and auditory development. *Neuron* **12**, 1153–1164.

**Epstein, J.A., Glaser, T., Cai, J., Jepeal, L., Walton, D.S. and Maas, R.L.** (1994). Two independent and interactive DNA-binding subdomains of the Pax6 paired domain are regulated by alternative splicing. *Genes Dev.* **8**, 2022-2034.

**Farinas, I., Jones, K.R., Backus, C., Wang, X.-Y. and Reichardt, L.F.** (1994) Severe sensory and sympathetic deficits in mice lacking neurotrophin-3. *Nature* 369, 658–661.

**Favor, J., Sandulache, R., Neuhauser-Klaus, A., Pretsch, W., Chatterjee, B., Senft, E., Wurst, W., Blanquet, V., Grimes, P., Sporle, R. and Schughart, K.** (1996). The mouse *Pax2(1Neu)* mutation is identical to a human Pax2 mutation in a family with renal-coloboma syndrome and results in developmental defects of the brain, ear, eye, and kidney. *Proc. Natl. Acad. Sci.USA* **93**, 13870-13875.

**Fekete, D.M., Muthukumar, S. and Karagogeos.** (1998). Hair cells and supporting cells share a common progenitor in the avian inner ear. *Neuron* **18**, 7811–7821.

**Fitzsimmons, D., Hodsdon, W., Wheat, W., Maira, S.M., Wasylyk, B. and Hagman, J.** (1996) Pax5 (BSAP) recruits Ets proto-oncogene family proteins to form functional ternary complexes on a B-cell-specific promoter. *Genes Dev.* **10**, 2198-2211.

**Frascella, E., Toffolatti, L. and Rosolen, A.** (1998) Normal and rearranged Pax3 expression in human rhabdomyosarcoma. *Cancer Genet. Cytogenet.*. **102,** 104-109.

**Fritzsch, B., Beisel, K.W., Jones, K., Farinas, I., Maklad, A., Lee, J. and Reichardt, L.F.** (2002) Development and evolution of inner ear sensory epithelia and their innervation. *J Neurobiol.* **53**, 143-156.

**Fritzsch, B., Pirvola, U. and Ylikoski, J.** (1999) Making and breaking the innervation of the ear: neurotrophic support during ear development and its clinical implications. *Cell Tissue Res.* **295**, 369-382.

**Fürthauer, M., Reifers, F., Brand, M., Thisse, B. and Thisse, C.** (2001) *sprouty4* acts in vivo as a feedback-induced antagonist of Fgf signaling in zebrafish. *Development* **128**:2175-2186.

**Gallagher, B.C., Henry, J.J. and Grainger, R.M.** (1996). Inductive processes leading to inner ear formation during *Xenopus* development. *Dev. Biol.* **175**, 95-107.

**Gnarra, J.R. and Dressler, G.R.** (1995) Expression of Pax2 in human renal cell carcinoma and growth inhibition by antisense oligonucleotides. *Cancer Res.* 55, 4092-4098.

**Groves, A.K. and Bronner-Fraser, M.** (2000). Competence, specification and commitment in otic placode induction. *Development* **127**, 3489-3499.

**Haddon, C. and Lewis, J.** (1996). Early ear development in the embryo of the zebrafish, *Danio rerio. J. Comp. Neurol*. **365**, 113-128.

**Haddon, C., Jiang, Y.J., Smithers, L. and Lewis, J.** (1998a) Delta-Notch signalling and the patterning of sensory cell differentiation in the zebrafish ear: evidence from the *mind bomb* mutant. *Development* **125,** 4637-4644.

**Haddon, C., Smithers, L., Schneider-Maunoury, S., Coche, T., Henrique, D. and Lewis, J.** (1998b). Multiple *delta* genes and lateral inhibition in zebrafish primary neurogenesis. *Development* **125**, 359-370.

**Haddon, C., Mowbray, C., Whitfield, T., Jones, D., Gschmeissner, S. and Lewis, J.** (1999) Hair cells without supporting cells: further studies in the ear of the zebrafish *mind bomb* mutant. *J. Neurocytol*. **28**, 837-850.

**Hammond, K., Hill, R., Whitfield, T.T. and Currie, P.** (2002) Isolation of three zebrafish dachshund homologues and their expression in sensory organs, the central nervous system and pectoral fin buds. *Mech. Dev.* **112,** 183–189.

**Hammond, K.L., Loynes, H.E., Folarin, A.A., Smith, J. and Whitfield, T.T.** (2003) Hedgehog signalling is required for correct anteroposterior patterning of the zebrafish otic vesicle. *Development.* **130**, 1403-1417.

**Hans, S., Liu, D. and Westerfield, M.** (2004). Pax8 and Pax2a function synergistically in otic specification, downstream of the Foxi1 and Dlx3b transcription factors. *Development* **131**, 5091-5102.

**Harrison, R.G.** (1935). Factors concerned in the development of the ear in *Ablystoma punctatum*. *Anat. Rec.* **64** (suppl. 1), 38-39.

**Harrison, R.G.** (1936). Relations of symmetry in the developing ear of *Ablystoma punctatum*. *Proc. Natl. Acad. Sci.* **22**, 238-247.

**Hauptmann, G. and Gerster, T.** (2000). Combined expression of zebrafish *Brn-1*- and *Brn-2*-related POU genes in the embryonic brain, pronephric primordium, and pharyngeal arches. *Dev. Dyn*. **218**, 345-358.

**Heanue, T.A., Davis, R.J., Rowitch, D.H., Kispert, A., McMahon, A.P., Mardon, G and Tabin, C.J.** (2002) Dach1, a vertebrate homologue of *Drosophila dachsund*, is

expressed in the developing eye and ear of both chick and mouse and is regulated independently of Pax and Eya genes. *Mech. Dev.* **111**, 75-87.

**Heanue, T.A., Reshef, R., Davis, R.J., Mardon, G., Oliver, G., Tomarev, S., Lassar, A.B. and Tabin, C.J.** (1999) Synergistic regulation of vertebrate muscle development by Dach2, Eya2, and Six1, homologs of genes required for *Drosophila* eye formation. *Genes Dev*. **13**, 3231–3243.

**Heller, N. and Brandli, A.W.** (1999) *Xenopus* Pax-2/5/8 orthologues: novel insights into *Pax* gene evolution and identification of Pax-8 as the earliest marker for otic and pronephric cell lineages. *Dev. Genet*. **24**, 208-219.

**Hertzano, R., Montcouquiol, M., Rashi-Elkeles, S., Elkon, R., Yucel, R., Frankel, W.N., Rechavi, G., Moroy, T., Friedman, T.B., Kelley, M.W. and Avraham, K.B.** (2004) Transcription profiling of inner ears from Pou4f3(ddl/ddl) identifies Gfi1 as a target of the Pou4f3 deafness gene. *Hum. Mol. Genet.* **13**, 2143-2153.

**Herzog, W., Sonntag, C., Walderich, B., Odenthal, J., Maischein, H.M. and Hammerschmidt, M.** (2004) Genetic analysis of adenohypophysis formation in zebrafish. *Mol. Endocrinol.* **18**, 1185-1195.

**Hewitt, S.M., Hamada, S., Monarres, A., Kottical, L.V., Saunders, G.F. and McDonnell , T.J.** (1997) Transcriptional activation of the Bcl-2 apoptosis suppressor gene by the paired box transcription factor Pax8. *Anticancer Res.* **17,** 3211-3215.

**Hutson, M.R., Lewis, J.E., Nguyen-Luu, D., Lindberg, K.H. and Barald, K.F.** (1999). Expression of Pax2 and patterning of the chick inner ear. *J. Neurocytol.* **28**, 795-807.

**Itoh, M., Kim, C.-H., Palardy, G., Oda, T., Jiang, Y.-J., Maust, D., Yeo, S.-Y., Lorick, K., Wright, S.M., Ariza-McNaughton, L., Chandrasekharappa, S.C., Chitnis, A.B.,** (2003) Mind Bomb is a ubiquitin ligase that is essential for efficient activation of Notch signaling by Delta. Dev. Cell 4, 67-82.

**Jacobson, A.G.** (1963) The determination and positioning of the nose, lens, and ear. I. Interactions within the ectoderm, and between the ectoderm and underlying tissue. *J. Exp. Zool.* **154**, 273-283.

**Jowett, T.** (1996) Double fluorescent in situ hybridization to zebrafish embryos. *Trends Genet.* **12**, 387-389.

**Kiefer, P., Mathieu, M., Mason, I. and Dickson, C.** (1996a) Secretion and mitogenic activity of zebrafish Fgf3 reveal intermediate properties relative to mouse and *Xenopus* homologues. *Oncogene* **12**, 1503-1511.

**Kiefer, P. Strahle, U. and Dickson, C.** (1996b). The zebrafish *fgf3* gene: cDNA sequence, transcript structure and genomic organization. *Gene* **168**, 211-215.

**Kim W.-Y., Fritzsch, B., Seris, A., Bakel, L.A., Huang, E.J., Reichardt, L.F., Barth D.S. and Lee, J.E.** (2001) NeuroD-null mice are deaf due to a severe loss of the inner ear sensory neurons during development. *Development* 128, 417–426.

**Kimmel, C.B., Ballard, W.W., Kimmel, S.R., Ullmann, B. and Schilling, T.F.** (1995). Stages of embryonic development of the zebrafish. *Dev. Dyn.* **203**, 253-310.

**Kozmik, Z., Czerny, T. and Busslinger, M.** (1997). Alternatively spliced insertions in the paired domain restrict the DNA sequence specificity of Pax6 and Pax8. *Embo J.* **16**, 6793-6803.

**Kozmik, Z., Kurzbauer, R., Dorfler, P. and Busslinger, M.** (1993). Alternative splicing of *Pax8* gene transcripts is developmentally regulated and generates isoforms with different transactivation properties. *Mol. Cell. Biol.* **13**, 6024-6035.

**Krauss, P. and Lufkin, T.** (1999). Mammalian *Dlx* homeobox gene control of craniofacial and inner ear morphogenesis. *J. Cell. Biochem*. **Suppl. 32/33**, 133-140.

**Krauss, S., Johansen, T., Korzh, V., Moens, U., Ericson, J. U. and Fjose, A.** (1991b). Zebrafish *pax[zf-a]*: a paired box-containing gene expressed in the neural tube. *Embo J.* **10**, 3609-3619.

**Krelova, J., Holland, L. Z., Schubert, M., Burgtorf, C., Benes, V. and Kozmik, Z.** (2002). Functional equivalency of amphioxus and vertebrate Pax2/5/8 transcription factors suggests that the activation of mid-hindbrain specific genes in vertebrates occurs via the recruitment of Pax regulatory elements. *Gene* **282**, 143-150.

**Kwak, S.J., Phillips, B.T., Heck, R. and Riley, B.B**. (2002) An expanded domain of *fgf3* expression in the hindbrain of zebrafish *valentino* mutants results in mispatterning of the otic vesicle. *Development* **129**, 5279-5287.

**Ladher, R.K., Anakwe, K.U., Gurney, A.L., Schoenwolf, G.C. and Francis-West, A.L.** (2000). Identification of synergistic signals initiating inner ear development. *Science* **290**, 1965-1967.

**Ladher, R.K., Wright, T.J., Moon, A.M., Mansour, S.L. and Schoenwolf, G.C.** (2005) Fgf8 initiates inner ear induction in chick and mouse. *Genes Dev.* **19**, 603-613.

**Lawoko-Kerali, G., Rivolta, M.N. and Holley, M.** (2002) Expression of the transcription factors GATA3 and Pax2 during development of the mammalian inner ear. *J. Comp Neurol.* **442**, 378-391.

**Leger, S. and Brand, M.** (2002). Fgf8 and Fgf3 are required for zebrafish ear placode induction, maintenance and inner ear patterning. *Mech. Dev.* **119**, 91-108.

**Lewis, A.K., Frantz, G.D. Carpenter, D.A., de Sauvage, F.J. and Gao, W.-Q.** (1998) Distinct expression patterns of notch family receptors and ligands during development of the mammalian inner ear. *Mech. Dev.* **78**, 159–163.

**Lewis, E.R., Leverenz, E.L. and Bialek, W.S.** (1985). "The vertebrate inner ear" (CRC Press, Boca Raton, FL).

**Li, S., Price, S.M., Cahill, H., Ryugo, D.K., Shen, M.M. and Xiang, M.** (2002) Hearing loss caused by progressive degeneration of cochlear hair cells in mice deficient for the Barhl1 homeobox gene. *Development* **129**, 3523-3532.

**Li, Y., Allende, M.L., Finkelstein, R. and Weinberg, E.S.** (1994). Expression of two zebrafish *orthodenticle*-related genes in the embryonic brain. *Mech. Dev*. **48**, 229-244.

**Linderson, Y., Eberhard, D., Malin, S., Johansson, A., Busslinger, M. and Pettersson, S.** (2004) Corecruitment of the Grg4 repressor by PU.1 is critical for Pax5-mediated repression of B-cell-specific genes. *EMBO Rep.* **5**, 291-296.

**Liu, D., Chu, H., Maves, L., Yan, Y.L., Morcos, P.A., Postlethwait, J.H. and Westerfield, M.** (2003). Fgf3 and Fgf8 dependent and independent transcription factors are required for otic placode specification. *Development* **130**, 2213-2224.

**Lombardo, A. and Slack, J.M.W.** (1998). Postgastrulation effects of fibroblast growth factor on *Xenopus* development. *Dev. Dyn.* **212**, 75-85.

**Lombardo, A., Isaacs, H.V. and Slack, J.M.W.** (1998). Expression and functions of *Fgf3* in *Xenopus* development. *Int. J. Dev. Biol*. **42**, 1101-1107.

**Lui, W.O., Foukakis, T., Liden, J., Thoppe, S.R., Dwight, T., Hoog, A., Zedenius, J., Wallin, G., Reimers, M. and Larsson, C.** (2005) Expression profiling reveals a distinct transcription signature in follicular thyroid carcinomas with a Pax8-PPAR(gamma) fusion oncogene. *Oncogene.* **24**, 1467-1476.

**Lun, K. and Brand, M.** (1998) A series of *no isthmus* (*noi*) alleles of the zebrafish *pax2.1* gene reveals multiple signaling events in development of the midbrain-hindbrain boundary. *Development* **125**, 3049-3062.

**Luo, G., Hofmann, C., Bronckers, A.L., Sohocki, M., Bradley, A. and Karsenty, G.** (1995) Bmp7 is an inducer of nephrogenesis, and is also required for eye development and skeletal patterning. *Genes Dev*. **9**, 2808-2820.

**Ma, Q., Anderson D.J. and Fritzsch, B.** (2000) Neurogenin 1 null mutant ears develop fewer, morphologically normal hair cells in smaller sensory epithelia devoid of innervation. *J. Assoc. Res. Otolaryngol.*, **1**, 129–143.

**Macchia, P.E., Lapi, P., Krude, H., Pirro, M.T., Missero, C., Chiovato, L., Souabni, A., Baserga, M., Tassi, V., Pinchera, A., Fenzi, G., Gruters, A., Busslinger, M., and Di Lauro,R.** (1998) *Pax8* mutations associated with congenital hypothyroidism caused by thyroid dysgenesis. *Nature Genet.* **19**, 83-86.

**Mackereth, M.D., Kwak, S.J., Fritz, A., Riley, B.B.** (2005) Zebrafish *pax8* is required for otic placode induction and plays a redundant role with *pax2* genes in the maintenance of the otic placode. *Development* **132**, 371-382.

**Mahmood, R., Kiefer, P., Guthrie, S., Dickson, C. and Mason, I.** (1995). Multiple roles for Fgf3 during cranial neural development in the chicken. *Development* **121**, 1399-1410**.**

**Mahmood, R., Mason, I.J. and Morrisskay, G.M.** (1996). Expression of *Fgf3* in relation to hindbrain segmentation, otic pit position and pharyngeal arch morphology in normal and retinoic acid exposed mouse embryos. *Anat. & Embryol.* **194**, 13-22

**Mansour, S.L., Goddard, J.M. and Capecchi, M.R.** (1993). Mice homozygous for a targeted disruption of the proto-oncogene *int-2* have developmental defects in the tail and inner ear. *Development* **117**, 13-28.

**Mansouri, A., Chowdhury, K. and Gruss, P.** (1998). Follicular cells of the thyroid gland require *Pax8* gene function. *Nat. Genet.* **19**, 87-90.

**Mansouri, A., Hallonet, M. and Gruss, P.** (1996) *Pax* genes and their roles in cell differentiation and development. *Curr. Opin. Cell Biol*. **6**, 851-857.

**Maroon, H., Walshe, J., Mahmood, R., Keifer, P., Dickson, C and Mason, I.** (2002). Fgf3 and Fgf8 are required together for formation of the otic placode and vesicle. *Development* **129**, 2099-2108.

**Mazan, S., Jailard, D, Baratte, B. and Janvier, P.** (2001). *Otx1* gene-controlled morphogenesis of the horizontal semicircular canal and the origin of the gnathostome characteristics. *Evol & Dev*. **2**, 186-193.

**McKay, I.J., Lewis, J. and Lumsden, A.** (1996). The role of *Fgf3* in early inner ear development: an analysis in normal and *kreisler* mutant mice. *Dev. Biol.* **174**, 370-378.

**Mendonsa, E.S. and Riley, B.B.** (1999). Genetic analysis of tissue interactions required for otic placode induction in the zebrafish. *Dev. Biol.* **206**, 100-112.

**Milili, M., Gauthier, L., Veran, J., Mattei, M.G. and Schiff, C.** (2002) A new Groucho TLE4 protein may regulate the repressive activity of Pax5 in human B lymphocytes. *Immunology* **106**, 447-455.

**Moens, C.B., Cordes, S.P., Giorgianni, M.W., Barsh, G.S. and Kimmel, C.B.** (1998). Equivalence in the genetic control of hindbrain segmentation in fish and mouse. *Development* **125**, 381-391.

**Moens, C.B., Yan, Y-L., Appel, B., Force, A.G. and Kimmel, C.B.** (1996). *valentino*: a zebrafish gene required for normal hindbrain segmentation. *Development* **122**, 3981-3990.

**Morsli, H., Choo, D., Ruyan, A., Johnson, R. and Wu, D.K.** (1998) Development of the ear and origin of its sensory organs. *J. Neurosci.* **18**, 2235–3327.

**Morsli, H., Tuorto, F., Choo, D., Postiglione, M.P., Simeone, A. and Wu, D.K.** (1999). *Otx1* and *Otx2* activities are required for the normal development of the mouse inner ear. *Development* **Suppl.126**, 2333-2343.

**Mowbray, C., Hammersschmidt, M., Whitfield, T.T.** (2001) Expression of Bmp signaling pathway members in the developing zebrafish inner ear and lateral line. *Mech. Dev.* **108**, 179-184.

**Nasevicius, A. and Ekker, S.C.** (2000). Effective targeted gene 'knockdown' in zebrafish. *Nat. Genet.* **26**, 216-220.

**Niederreither, K., Vermot, J., Schuhbaur, B., Chambon, P. and Dollé, P.** (2000) Retinoic acid synthesis and hindbrain patterning in the mouse embryo. *Development* **127**, 75–85.

**Nissen, R.M., Yan, J., Amsterdam, A., Hopkins, N. and Burgess, S.M.** (2003). Zebrafish foxi one modulates cellular responses to Fgf signaling required for the integrity of ear and jaw patterning. *Development* **130**, 2543-2554.

**Noramly, S. and Grainger, R.M.** (2002). Determination of the embryonic inner ear. *J. Neurobiol.* **53**, 100-128.

**Nornes, S., Mikkola, I., Krauss, S., Delghandi, M., Perander, M. and Johansen, T.** (1996). Zebrafish *pax9* encodes two proteins with distinct C-terminal transactivating domains of different potency negatively regulated by adjacent N-terminal sequences. *J. Biol. Chem.* **271**, 26914-26923.

**Ohno, H., Ueda, C. and Akasaka, T.** (2000) The t(9;14)(p13;q32) translocation in B-cell non-Hodgkin's lymphoma*. Leuk. Lymphoma.* **36**, 435-445.

**Oxtoby, E. and Jowett, T.** (1993). Cloning of the zebrafish *krox20* gene (*krx20*) and its expression during hindbrain development. *Nucleic Acids Res.* **21**, 1087-1095.

**Pfeffer, P.L., Gerster, T., Lun, K., Brand, M. and Busslinger, M.** (1998). Characterization of three novel members of the zebrafish Pax2/5/8 family: dependency of Pax5 and Pax8 expression on the Pax2.1 (*noi*) function. *Development* **125**, 3063-3074.

**Phelps, D.E. and Dressler, G.R.** (1996) Identification of novel Pax2 binding sites by chromatin precipitation. *J. Biol. Chem.* **271**, 7978-7985.

**Phillips, B.T., Bolding, K. and Riley, B.B.** (2001). Zebrafish *fgf3* and *fgf8* encode redundant functions required for otic placode induction. *Dev. Biol.* **235**, 351-365.

**Phillips, B.T., Storch, E.M., Lekven, A.C. and Riley, B.B.** (2004). A direct role for Fgf but not Wnt in otic placode induction. *Development* **131**, 923-931.

**Pirvola, U., Spencer-Dene, B., Xing-Qun, L., Kettunen, P., Thesleff, I., Fritzsch, B. and Dickson, C.** (2000). Fgf/Fgfr-2 (IIIb) signaling is essential for inner ear morphogenesis. *J. Neurosci.* **20**, 6125-6134.

**Pirvola, U., Ylikoski, J., Trokovic, R., Hébert, J.M., McConnell, S.K., and Partanen J.** (2002) Fgfr1 is required for the development of the auditory sensory epithelium. *Neuron* **35**, 671-680.

**Plachov, D., Chowdhury, K., Walther, C., Simon, D., Guenet, J. L. and Gruss, P.** (1990). Pax8, a murine paired box gene expressed in the developing excretory system and thyroid gland. *Development* **110**, 643-651.

**Plaza, S., Prince, F., Jaeger, J., Kloter, U., Flister, S., Benassayag, C., Cribbs, D. and Gehring, W.J.** (2001) Molecular basis for the inhibition of *Drosophila* eye development by Antennapedia. *EMBO J.* **20**, 802-811.

**Prince, V.E., Moens, C.B., Kimmel. C.B. and Ho, R.K.** (1998). Zebrafish *hox* genes: expression in the hindbrain region of the wild-type and mutants of the segmentation gene, *valentino*. *Development* **125**, 393-406.

**Puschel, A.W., Gruss, P. and Westerfield, M.** (1992). Sequence and expression pattern of *Pax6* are highly conserved between zebrafish and mice. *Development* **114**, 643-651.

**Quint, E., Furness, D.N. and Hackney, C.M.** (1998) The effect of explantation and neomycin on hair cells and supporting cells in organotypic cultures of the adult guinea-pig utricle. *Hear. Res.***118**, 157-167.

**Raible, F. and Brand, M.** (2001). Tight transcriptional control of the ETS domain factors Erm and Pea3 by Fgf signaling during early zebrafish development. *Mech. Dev.* **107**:105-117.

**Reifers, F., Bohli, H., Walsh, E.C., Crossley, P.H. and Stainier, D.Y.R.** (1998). *fgf8* is mutated in zebrafish *acerebellar* (*ace*) mutants and is required for maintenance of midbrain-hindbrain boundary and somitogenesis. *Development* **125**, 2381-2395.

**Represa, J., Leon, Y., Miner, C. and Giraldez, F.** (1991). The *int-2* proto-oncogene is responsible for induction of the inner ear. *Nature* **353**, 561-563.

**Riccomangno, M.M., Martinu, L., Mulheisen, M., Wu, D.K., and Epstein, D.J.** (2002) Specification of the mammalian cochlea is dependent on sonic hedgehog. *Genes Dev.* **16**, 2365–2378.

**Riley, B.B. Chiang, M.-Y., Farmer, L. and Heck, R.** (1999). The *deltaA* gene of zebrafish mediates lateral inhibition of hair cells in the inner ear and is regulated by *pax2.1*. *Development* **126**, 5669-5678.

**Riley, B.B. and Grunwald D.J.** (1996) A mutation in zebrafish affecting a localized cellular function required for normal ear development. *Dev. Biol.* **179**, 427-435.

**Riley, B.B. and Moorman, S.J.** (2000) Development of utricular otoliths, but not saccular otoliths, is necessary for vestibular function and survival in zebrafish. *J. Neurobiol.* **43**, 329-337.

**Riley, B.B. and Phillips, B.T.** (2003). Ringing in the new ear: resolution of cell interactions in otic development. *Dev. Biol* **261**, 289-312.

**Riley, B.B., Zhu, C., Janetopoulos, C. and Aufderheide, K.J.** (1997). A critical period of ear development controlled by distinct populations of ciliated cells in the zebrafish. *Dev. Biol*. **191**, 191-201.

**Robledo, R.F., Rajan, L., Li, X. and Lufkin, T.** (2002) The *Dlx5* and *Dlx6* homeobox genes are essential for craniofacial, axial, and appendicular skeletal development. *Genes Dev.* **16,** 1089–1101.

**Robson, E.J., He, S.J. and Eccles, M.R.** (2006) A PANorama of *Pax* genes in cancer and development. *Nat. Rev. Cancer.* **6**, 52-62.

**Roehl, H. and Nüsslein-Volhard, C.** (2001). Zebrafish *pea3* and *erm* are general targets of Fgf8 signalling. *Curr. Biol.* **11**:503-507.

**Rolink, A.G., Nutt, S.L., Melchers, F. and Busslinger, M.** (1999) Long-term *in vivo* reconstitution of T-cell development by Pax5-deficient B-cell progenitors. *Nature* **401**, 603-606.

**Rothenpieler, U.W. and Dressler, G.R.** (1993) Pax2 is required for mesenchyme-to-epithelium conversion during kidney development. *Development* **119**, 711-720.

**Sahly, I., Andermann, P. and Petit, C.** (1999) The zebrafish *eya1* gene and its expression pattern during embryogenesis. *Dev. Genes Evol.* **209**, 399–410.

**Sanchez-Calderon, H., Martin-Partido, G. and Hidalgo-Sanchez, M.** (2005) Pax2 expression patterns in the developing chick inner ear. *Gene Expr. Patterns.* **5**, 763-773.

**Schaniel, C., Bruno, L., Melchers, F. and Rolink, A.G.** (2002) Multiple hematopoietic cell lineages develop in vivo from transplanted Pax5-deficient pre-B I-cell clones. *Blood.* **99**, 472-478.

**Schimmang, T., Alvarez-Bolado, G.,`Minichiello, L., Vazquez, E., Giraldez, F., Klein, F. and Represa, J.** (1997) Survival of inner ear sensory neurons in trk mutants. *Mech. Dev.* **64**, 77–85.

**Seo, H.C., Saetre, B.O., Havik, B., Ellingsen, S. and Fjose, A.** (1998). The zebrafish Pax3 and Pax7 homologues are highly conserved, encode multiple isoforms and show dynamic segment-like expression in the developing brain. *Mech. Dev.* **70**, 49-63.

**Sobkowicz, H.M., August, B.K. and Slapnick, S.M.** (1992) Epithelial repair following mechanical injury of the developing organ of Corti in culture: an electron microscopic and autoradiographic study. *Exp Neurol.* **115**, 44-49.

**Sobkowicz, H.M., August, B.K. and Slapnick, S.M.** (1997) Cellular interactions as a response to injury in the organ of Corti in culture. *Int. J. Dev. Neurosci.***15**, 463-485.

**Solomon, K.S. and Fritz, A.** (2002). Concerted action of two *dlx* paralogs in sensory placode formation. *Development* **129**, 3127-3136.

**Solomon, K.S., Kudoh, T., Dawid, I.B. and Fritz, A.** (2003). Zebrafish Foxi1 mediates otic placode formation and jaw development. *Development* **130**, 929-940.

**Solomon, K.S., Kwak, S.J. and Fritz, A.** (2004). Genetic interactions underlying otic placode induction and formation. *Dev. Dyn.* **230**, 419-433.

**Sorensen, P.H., Lynch, J.C., Qualman, S.J., Tirabosco, R., Lim, J.F., Maurer, H.M., Bridge, J.A., Crist, W.M., Triche, T.J. and Barr, F.G.** (2002) Pax3-FKHR and *Pax7*-FKHR gene fusions are prognostic indicators in alveolar rhabdomyosarcoma: a report from the children's oncology group. *J. Clin. Oncol.* **20**, 2672-2679.

**Stachel, S.E., Grunwald, D.J. and Meyers, P.Z.** (1993). Lithium perturbations and *goosecoid* expression identify a dorsal specification pathway in the pregastrula zebrafish. *Development* **117**, 1261-1274.

**Stone, L.S.** (1931). Induction of the ear by the medulla and its relation to experiments on the lateralis system in amphibia. *Science* **74**, 577.

**Streit, A.** (2002) Extensive cell movements accompany formation of the otic placode. *Dev. Biol.* **249**, 237–254.

**Stuart, E.T., Haffner, R., Oren, M. and Gruss, P.** (1995) Loss of *p53* function through Pax-mediated transcriptional repression. *EMBO J.* **14**, 5638-5645.

**Stuart, E.T., Kioussi, C. and Gruss, P.** (1994). Mammalian *Pax* genes. *Annu. Rev. Genet.* **28**, 219-236.

**Tavassoli, K., Ruger, W. and Horst, J.** (1997) Alternative splicing in *Pax2* generates a new reading frame and an extended conserved coding region at the carboxy terminus. *Hum. Genet.* **101**, 371-375.

**Torres, M. and Giraldez, F.** (1998) The development of the vertebrate inner ear. *Mech. Dev.* **71**, 5-21.

**Torres, M., Gomez-Pardo, E. and Gruss, P.** (1996) Pax2 contributes to inner ear patterning and optic nerve trajectory. *Development* **122**, 3381-3391.

**Torres, M., Gómez-Pardo, E., Dressler, G.R., and Gruss, P.** (1995) Pax2 controls multiple steps of urogenital development. *Development* **121**, 4057-4065.

**Treisman, J., Harris, E. and Desplan, C.** (1991) The paired box encodes a second DNA-binding domain in the paired homeo domain protein. *Genes Dev.* **5**, 594-604.

**Underhill, D.A. and Gros, P.** (1997) The paired domain regulates DNA binding by the homeodomain within the intact Pax3 protein. *J. Biol. Chem.* **272**, 14175-14182.

**Urbanek, P., Wang, Z.Q., Fetka, I., Wagner, E.F. and Busslinger, M.** (1994) Complete block of early B cell differentiation and altered patterning of the posterior midbrain in mice lacking Pax5/BSAP. *Cell* **79**, 901-912.

**Vendrell, V. Carnicero, E., Giraldez, F., Alonso, M. T. and Schimmang, T.** (2000) Induction of inner ear fate by Fgf3. *Development* **127**, 155-165.

**Vendrell, V., Gimnopoulos, D., Beckler, T. and Schimmang, T.** (2001) Functional analysis of Fgf3 during zebrafish inner ear development. *Int. J. Dev.Biol.* **45 (S1)**, S105-S106.

**Vogan, K.J., Underhill, D.A. and Gros, P.** (1996) An alternative splicing event in the Pax3 paired domain identifies the linker region as a key determinant of paired domain DNA-binding activity. *Mol. Cell Biol.* **16**, 6677-6686.

**Waddington, C.H.** (1937). The determination of the auditory placode in the chick. *J. Exp. Bio.* **14**, 232-239.

**Wallis, D., Hamblen, M., Zhou, Y., Venken, K.J., Schumacher, A., Grimes, H.L., Zoghbi, H.Y., Orkin, S.H., Bellen, H.J.** (2003) The zinc finger transcription factor Gfi1, implicated in lymphomagenesis, is required for inner ear hair cell differentiation and survival. *Development* **130**, 221-232.

**Walther, C., Guenet, J.L., Simon, D., Deutsch, U., Jostes, B., Goulding, M.D., Plachov, D., Balling, R. and Gruss, P.** (1991). Pax: a murine multigene family of paired box-containing genes. *Genomics* **11**, 424-434.

**Wawersik, S. and Maas, R.L.** (2000) Vertebrate eye development as modeled in *Drosophila*. *Hum. Mol. Genet.* **9**, 917-925.

**White, J.C., Highland, M., Kaiser, M. and Clagett-Dame, M.** (2000) Vitamin A deficiency results in the dose-dependent acquisition of anterior character and shortening of the caudal hindbrain of the rat embryo. *Dev. Biol.* **220**, 263-284.

**Whitfield, T.T., Riley, B.B., Chiang, M.Y. and Phillips, B.** (2002). Development of the zebrafish inner ear. *Dev. Dyn.* **223**, 427-458.

**Wiellette, E.L. and Sive, H.** (2004). Early requirement for Fgf8 function during hindbrain pattern formation in zebrafish. *Dev. Dyn.* **229**, 393-399.

**Wilson, D., Sheng, G., Lecuit, T., Dostatni, N. and Desplan, C.** (1993) Cooperative dimerization of paired class homeo domains on DNA. *Genes Dev*. **7**, 2120-2134.

**Woo, K., and Fraser, S.E.** (1998). Specification of the hindbrain fate in the zebrafish. *Dev. Biol.* **197**, 283-296.

**Woods, C., Montcouquiol, M. and Kelley, M.W.** (2004) Math1 regulates development of the sensory epithelium in the mammalian cochlea. *Nat. Neurosci.* **7**, 1310-1318.

**Wright, T.J. and Mansour, S.L.** (2003) Fgf3 and Fgf10 are required for mouse otic placode induction. *Development* **130**, 3379-3390.

**Wu, D.K., Nunes, F.D. and Choo, D.** (1998) Axial specification for sensory organs versus non-sensory structures of the chicken inner ear. *Development* **125**, 11-20.

**Xiang, M., Gao, W.Q., Hasson, T. and Shin, J.J.** (1998) Requirement for Brn-3c in maturation and survival, but not in fate determination of inner ear hair cells. *Development* **125**, 3935-3946.

**Xiang, M., Maklad, A., Pirvola, U. and Fritzsch, B.** (2003) Brn-3c null mutant mice show long-term, incomplete retention of some afferent inner ear innervation. *BMC Neurosci.* **4**, 2.

**Xu, W., Rould, M.A., Jun, S., Desplan, C. and Pabo, C.O.** (1995). Crystal structure of a paired domain-DNA complex at 2.5 A resolution reveals structural basis for Pax developmental mutations. *Cell* **80**, 639-650.

**Yntema, C.L.** (1933). Experiments on the *determination* of the ear ectoderm in the embryo of *Ablystoma punctatum*. *J. Exp. Zool.* **65**, 317-352.

**Zebrafish Information Network (ZFIN),** Structure description: ear, the Zebrafish International Resource Center, University of Oregon, Eugene, available http://zfin.org/zf_info/anatomy/dict/ear/ear.html., accessed Jan. 2006.

**Zwollo, P., Arrieta, H., Ede, K., Molinder, K., Desiderio, S. and Pollock, R.** (1997). The *Pax5* gene is alternatively spliced during B-cell development. *J. Biol. Chem.* **272**, 10160-10168.

# VITA

Su Jin Kwak
1100 Hensel Dr. Z1I
College Station, TX 77840
E-mail: skwak@mail.bio.tamu.edu

## EDUCATION

1997 B.S. KAIST, Republic of Korea, Department of Biological Sciences
1999 M.S. Seoul National University, Republic of Korea, Department of Molecular Biology
2006 Ph.D. Texas A&M University, USA, Department of Biology

## WORKING EXPERIENCE

Teaching Assistant, Introductory Biology, Seoul National University, Republic of Korea, 1998
Internship, Plant genetic engineering laboratory, Seoul National University, Republic of Korea, 1999-2000
Teaching Assistant, Introductory Biology/Embryology Lab, Texas A&M University, Fall 2000, Spring 2001, Fall 2002, Spring 2002, Spring 2003
Graduate research assistant, Texas A&M University, 2002-2005

## PEER-REVIEWED PUBLICATIONS

**Pepper A.E., Seong-Kim, M., Hebst, S.M., Ivey, K.N, Kwak, S.J., Broyles, D.E.** (2001) shl, a New set of Arabidopsis mutants with exaggerated developmental responses to available red, far-red, and blue light. *Plant Physiol.* **127**, 295-304.

**Kwak, S.J., Phillips, B.T., Heck, B., and Riley, B.B.** (2002) An expanded domain of *fgf3* expression in the hindbrain of zebrafish *valentino* mutants results in mis-patterning of the otic vesicle. *Development.* **129**, 5279-5287.

**Solomon,K.S., Kwak, S.J., and Fritz, A.** (2004) Genetic interactions underlying otic placode induction and formation. *Dev Dyn.* **230**, 419-433.

**Mackereth M.D.*, Kwak, S-J.*, Fritz A., and Riley, B.B.** (2005) Zebrafish Pax8 is required for otic placode induction and plays a redundant role with *pax2* genes in the maintenance of the otic placode. *Development*. **132**, 371-382.
* These authors contribute equally.